Organisation and transcriptional regulation of the polyphenol oxidase (PPO) multigene family of the moss *Physcomitrella patens* (Hedw.) B.S.G. and functional gene knockout of *PpPPO1*

Dissertation zur Erlangung des Doktorgrades
- Dr. rer. nat. -
im Department Biologie
der Fakultät Mathematik, Informatik und Naturwissenschaften
an der Universität Hamburg

von Hanna Richter

Hamburg, Januar 2009

Genehmigt vom Department Biologie
der Fakultät für Mathematik, Informatik und Naturwissenschaften
an der Universität Hamburg
auf Antrag von Professor Dr. R. LIEBEREI
Weiterer Gutachter der Dissertation:
Herr Priv.-Doz. Dr. K. von SCHWARTZENBERG
Tag der Disputation: 23. Januar 2009

Hamburg, den 09. Januar 2009

Professor Dr. Jörg Ganzhorn
Leiter des Departments Biologie

TABLE OF CONTENTS

SUMMARY

Polyphenol oxidases (PPOs) are copper-binding enzymes of the plant secondary metabolism that oxidise polyphenols to quinones in the presence of molecular oxygen. Characterisation of seed plant PPOs suggested these enzymes to be involved in different processes, for example, in pest and pathogen defence mechanisms, in strong light stress response, in flower colouration, and in retardation of *postmortem* proteolysis. PPO-mediated promotion (re-oxidation) of enzymes involved in cytokinin degradation has further been hypothesised; yet, the *in planta* relevance of this involvement in hormonal regulation is unclear. A general function cannot be attributed to plant PPOs.

This work aimed to analyse PPOs in the basal land plant *Physcomitrella patens* (Hedw.) B.S.G. It was demonstrated, that the bryophyte *Physcomitrella* exhibits PPO activity, and that part of the overall PPO protein is secreted to the culture medium. The *Physcomitrella PPO* gene family comprising twelve paralogues (*PpPPO1* to *PpPPO12*) was identified and characterised. PpPPOs cluster in five groups with 2-3 PPOs each, and exhibit similarities but also differences to seed plant PPOs. Phylogenetic analyses revealed that *PPO* gene duplications within the monophyletic *Physcomitrella* gene family have occurred after separation from the seed plant lineage, and suggested that PPOs have evolved with the conquest of land, possibly with bacterial tyrosinases as ancestors. *Physcomitrella* PPO functionality was demonstrated for the example of recombinant PPO11, which showed *o*-diphenol oxidase activity, after expression in *E. coli* and subsequent polarographic enzyme assays using 4-methyl catechol as a substrate.

The expression of the *PPO* gene family members, analysed by real-time RT-PCR, was shown to be differentially regulated under standard *in vitro* conditions and changed during the time course of a culture. Three *PPO* genes were not expressed in protonema tissue under standard conditions. The expression pattern of the *PPO* gene family changed drastically after strong light exposure (~1000 µmol $m^{-2}s^{-1}$), and the gene family members reacted differently to the irradiation. *PPO4* and *PPO12* gene expression was strongly upregulated, while expression of *PPO1, -2, and -3* was decreased. Moreover, the *PPO* expression pattern also changed after incubation with the putative PPO substrate caffeic acid, revealing that the expression of most *PPO* genes was downregulated, whereas *PPO1* and *PPO8* expression was upregulated.

Targeted *Physcomitrella PPO1* knockout (*PPO1*_ko) plants were generated, and plants lacking *PPO1* exhibited a ~60 % reduced extracellular PPO activity compared to wild type. Expression levels of the remaining *PPO* gene family members were shown to be regulated to a great extent independently from *PPO1* under standard conditions as well as under strong light exposure, as *PPO1*_ko plants exhibited only slight changes in *PPO2* to *PPO12* expression. *PPO1*_ko lines were less tolerant towards externally applied 4-methyl catechol compared to wild type. Furthermore, abnormal protonema growth with shorter and roundly shaped chloronema cells was observed, and *PPO1*_ko plants produced significantly more gametophores than wild type. As gametophore formation is induced by cytokinins, *in vivo* cytokinin metabolism was monitored. *PPO1*_ko plants exhibited a reduced depletion of the applied tritiated cytokinin ^{3}H-isopentenyladenine, suggesting a reduction of cytokinin breakdown catalysed by cytokinin oxidase/dehyrdogenase.

HPLC-analysis of putative PPO substrates from tissue and culture medium revealed that *Physcomitrella* produced only little amounts of phenolic compounds under standard *in vitro* conditions. However, production of phenolic compounds and their secretion was induced by supplementing the culture medium with D-glucose.

From the obtained experimental data it was concluded, that the different members of the *Physcomitrella* PPO family are likely to possess different functions. PPO1 and possibly PPO8 might be involved in the establishment of appropriate extracellular conditions, like the removal of inhibitory extracellular phenolic compounds. PPO1 might further be involved in tuning of differentiation processes by promoting cytokinin degradation. Other PPOs might be involved in strong light response. Finally, the characterisation of a bryophyte *PPO* gene family opens new possibilities towards the understanding of PPO functions during the evolution of land plants.

ZUSAMMENFASSUNG

Polyphenoloxidasen (PPOs) sind kupferhaltige Enzyme des pflanzlichen Sekundärstoffwechsels, die die Oxidation von Polyphenolen zu Chinonen katalysieren. Studien an Samenpflanzen zeigten, dass PPOs an verschiedenen Prozessen beteiligt sein können, z.B. bei der Pathogenabwehr, bei Mechanismen zum Schutz vor Starklichtschäden, bei der Bildung von Blütenfarben sowie bei der Hemmung der *postmortem*-Proteolyse. Darüber hinaus wurde angenommen, dass PPOs Cytokinin-abbauende Enzyme aktivieren können und somit indirekt auch an Differenzierungsprozessen beteiligt sein könnten, wobei die Relevanz dieses Prozesses *in planta* allerdings noch unklar ist. Eine generelle PPO-Funktion in Pflanzen ist nicht bekannt.

Ziel dieser Arbeit war die Charakterisierung von PPOs in der basalen Landpflanze *Physcomitrella patens* (Hedw.) B.S.G. Es wurde gezeigt, dass *Physcomitrella* PPO-Aktivität besitzt und dass ein Teil der Gesamt-PPO-Aktivität in das Kulturmedium sekretiert wird. Mittels bioinformatischer Genomanalysen wurde die *PPO*-Genfamilie aus *Physcomitrella* identifiziert und charakterisiert. *In silico*-Analysen ergaben, dass sich die *PPO*-Genfamilie aus zwölf paralogen Genen (*PpPPO1* bis *PpPPO12*) zusammensetzt, die in fünf Gruppen mit jeweils mit 2-3 *PPOs* angeordnet sind und sowohl Ähnlichkeiten als auch wesentliche Unterschiede zu PPOs aus Samenpflanzen besitzen. Phylogenetische Analysen zeigten, dass *PPO*-Genduplikationen innerhalb der monophyletischen *Physcomitrella PPO*-Genfamilie nach Abspaltung von der Abstammungslinie der Samenpflanzen stattgefunden haben. Außerdem lassen Metagenomanalysen vermuten, dass sich PPOs mit der Besiedlung des Landes entwickelt haben und möglicherweise aus bakteriellen Tyrosinasen hervorgegangen sind. Der funktionelle Nachweis für *Physcomitrella*-PPOs wurde am Beispiel von rekombinanter PPO11 erbracht, die nach Expression in *E. coli* und polarographischen Enzym-aktivitätsmessungen *o*-Diphenoloxidaseaktivität zeigte.

Die Expression der *PPO*-Genfamilie in Protonemagewebe wurde mittels *real-time* RT-PCR untersucht. Die Expression der *PPO*-Gene war differenziell reguliert und veränderte sich im Verlauf einer Kultur. Drei *PPO*-Gene wurden unter Standardbedingungen nicht exprimiert. Unter Stark-lichtbestrahlung (~1000 µmol $m^{-2}s^{-1}$) veränderte sich das Expressionsmuster der *PPO*-Genfamilie drastisch, und die verschiedenen *PPOs* reagierten unterschiedlich auf die Bestrahlung. *PPO4* und *PPO12* wurden deutlich stärker exprimiert, während die Expression von *PPO1, -2* und *-3* stark vermindert wurde. Weiterhin veränderte sich das *PPO*-Expressionsmuster auch nach Inkubation mit dem putativen PPO-Substrat Kaffeesäure. Die Expression der meisten *PPO*-Gene wurde hierdurch herunterreguliert, wohingegen die *PPO1*- und *PPO8*-Expression gesteigert wurde.

Physcomitrella PPO1-knockout-Pflanzen (*PPO1*_ko), die eine Reduktion der extrazellulären PPO-Aktivität um ~60 % im Vergleich zum Wildtyp aufwiesen, wurden hergestellt. Die Expression der übrigen *PPO*-Gene war unter Standard- und Starklichtbedingungen in hohem Maße unabhängig von *PPO1,* da *PPO1*_ko-Pflanzen im Vergleich zum Wildtyp nur geringfügige Unterschiede im Expressionsmuster von *PPO2* bis *PPO12* aufzeigten. *PPO1*_ko-Pflanzen besaßen im Vergleich zum Wildtyp eine geringere Toleranz gegenüber dem PPO-Substrat 4-Methylcatechol. Weiterhin wurde bei *PPO1*_ko-Pflanzen ein abweichendes Protonemawachstum mit kürzeren und rundlichen Chloronema-zellen beobachtet. *PPO1*_ko-Pflanzen produzierten darüber hinaus deutlich mehr Gametophoren als der Wildtyp. Da Cytokinine die Gametophorenbildung bei Laubmoosen induzieren, wurde der *in vivo* Cytokinin-Metabolismus untersucht. *PPO1*_ko-Pflanzen zeigten einen niedrigeren Verbrauch von exogen appliziertem, radioaktiv markiertem Cytokinin ^{3}H-Isopentenyladenin, der möglicherweise auf eine reduzierte Aktivität des Cytokinin-abbauenden Enzyms Cytokininoxidase/dehyrdogenase zurückzuführen ist.

HPLC-Analysen von putativen PPO-Substraten in Gewebe und Kulturmedium ergaben, dass *Physcomitrella* unter Standardbedingungen nur geringe Menge phenolischer Substanzen anreichert. Allerdings konnte die Produktion und Sekretion von phenolischen Substanzen durch den Zusatz von D-Glucose zum Kulturmedium induziert werden.

Die Ergebnisse dieser Arbeit deuten darauf hin, dass die verschiedenen *Physcomitrella PPOs* unterschiedliche Funktionen besitzen. PPO1 und möglicherweise PPO8 könnten an der Erhaltung von

geeigneten extrazellulären Bedingungen durch die Metabolisierung von inhibierenden phenolischen Substanzen beteiligt sein. Weiterhin könnte PPO1 durch eine Förderung des Cytokininabbaus indirekt Einfluss auf Differenzierungsprozesse haben. Andere *Physcomitrella* PPOs könnten in Starklicht-Reaktionen involviert sein.

Aufgrund der phylogenetischen Schlüsselposition von Bryophyten, eröffnet die Charakterisierung der *Physcomitrella PPO*-Genfamilie neue Möglichkeiten, PPOs im Hinblick auf die Evolution der Landpflanzen zu untersuchen.

1. INTRODUCTION

1.1. Polyphenol oxidases

Reaction mechanism and classification

Polyphenol oxidases are copper-binding enzymes that oxidise polyphenols and their derivatives to the corresponding quinones in the presence of molecular oxygen.

The extended group of polyphenol oxidases is divided into three subgroups based on their substrates: *o*-diphenol oxidases (PPO, EC 1.10.3.1) oxidising *o*-diphenols to *o*-diquinones, laccases (LAC, EC. 1.10.3.2) oxidising *p*-diphenols, and tyrosinases (TYR, EC 1.14.18.1), which are catechol oxidases with an additional function for hydroxylation of monophenols to *o*-diphenols prior to the diphenol oxidation.

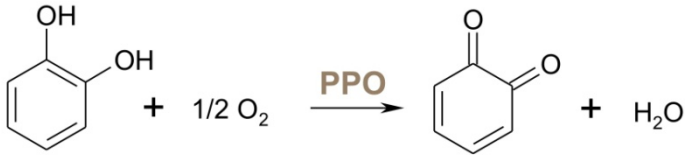

Fig. 1.1 Reaction mechanism of *o*-diphenol oxidases (PPO, EC 1.10.3.1): Oxidation of a simple *o*-diphenol to an *o*-diquinone in the presence of molecular oxygen.

Occurrence

The extended group of polyphenol oxidases is widespread among all groups of organisms. Whereas TYRs are mostly present in microorganisms and animals, plants only possess PPOs and LACs. PPOs are nearly ubiquitous in the plant kingdom, although for *Arabidopsis thaliana* no *o*-diphenol oxidase encoding genes have been found in the genome (Sullivan *et al.*, 2004). For *Arabidopsis*, only the presence of a large laccase encoding gene family was reported (McCaig *et al.*, 2005).

The following sections will mainly focus only on *o*-diphenol oxidases (PPO); LAC and TYR will only be mentioned when necessary.

PPO *genes and* PPO *gene families*

PPOs are nuclear encoded proteins (Lax *et al.*, 1984). *PPO* genes and cDNAs have been identified, isolated and characterised for numerous seed plant species, for example from *Solanum tuberosum* (Hunt *et al.*, 1993; Thygesen *et al.*, 1995), *Lycopersicon esculentum* (Newman *et al.*, 1993), *Prunus armeniaca* (Chevalier *et al.*, 1999), *Vitis vinifera* (Dry and Robinson, 1994), *Musa cavendishii*

(AAA group, Cavendish subgroup) cv. Williams (Gooding *et al.*, 2001) and *Triticum aestivum* (Demeke and Morris, 2002).

In most plant species, PPOs are encoded by multigene families, e.g. from *Lycopersicon esculentum* seven *PPO* genes (Newman *et al.*, 1993), from *Vicia faba* three (Cary *et al.*, 1992), from *Trifolium pratense* three (Sullivan *et al.*, 2004) and from *Solanum tuberosum* six *PPO* genes (Thygesen *et al.*, 1995) have been identified. *Vitis vinifera* has been described to possess only one *PPO* gene (Dry and Robinson, 1994), although, genome analysis revealed *Vitis vinifera* to possess more *PPO* genes than previously reported (Thipyapong *et al.*, 2007).

PPO genes from dicotyledonous plants usually do not possess introns (e.g. Newman *et al.*, 1993; Dry and Robinson, 1994; Thygesen *et al.*, 1995). However, for *PPO* genes from monocotyledonous plants, small introns in the coding sequences have been reported. For example, pineapple (Zhou *et al.*, 2003) and banana *PPO* genes (Gooding *et al.*, 2001) possess one intron; wheat *PPO* genes possess two small introns (Sun *et al.*, 2005). Due to these findings, Massa *et al.* (2007) concluded that the insertion of introns in *PPO* genes occurred after divergence of monocots and dicots.

PPO *expression pattern*

PPO transcript levels are generally highest in young tissue and in meristematic regions but decline during further development (e.g. Thygesen *et al.*, 1995; Dry and Robinson, 1994). Often no PPO expression can be detected in late stages of plant development as demonstrated for *PPO* genes from *Prunus armeniaca* (e.g. Chevalier *et al.*, 1999).

Moreover, *PPO* gene family members from seed plants exhibit temporal and spatial gene expression patterns with different expression levels in different vegetative and reproductive organs, e.g. as described for the tomato *PPO* gene family (Thipyapong *et al.*, 1997). Also in *Trifolium pratense PPO* genes are differently expressed, each being predominant in a certain stage, e.g. *TpPPO1* in young leaves, *TpPPO2* in flowers and petioles (Sullivan *et al.*, 2004). For potato, different *PPO* cDNAs were isolated from different tissue types such as from leaves and tubers (Thygesen *et al.*, 1995).

In addition to these findings, *PPO* transcript levels were found to be induced by several biotic stress factors. In hybrid poplar, *PPO* gene expression was induced especially in young leaves by tissue wounding, methyl jasmonate spraying, and by forest tent caterpillars feeding on the plants

(Constabel *et al.*, 2000). Promoter::GUS fusions revealed the transcription of the tomato *PPO* gene *F* being induced in young leaves in response to wounding and upon infection by *Alternaria solani* and *Pseudomonas syringae,* presumably to protect juvenile tissues from subsequent attack by pathogens and pests (Thipyapong and Steffens, 1997).

So far, only little information exists on transcriptional changes in *PPO* expression upon abiotic stress conditions such as strong (UV) light exposure, drought, cold and osmotic changes. Hind *et al.* (1995) concluded that a spinach *PPO* gene is light regulated, as the authors could not detect *PPO*-mRNA in etiolated cotyledons and heavily shaded shoot tissue. However, this is the only description of light induction of *PPO* transcript.

Aside from these findings, *PPO* genes *B* and *D* of the tomato gene family are transcriptionally upregulated in response to water stress, suggesting that these *PPO* genes may facilitate apoptosis during water stress (Thipyapong *et al.*, 2004b). Moreover, *PPO* genes *B* and *F* were ethylene-inducible in tomato, but expression of the *PPO F* is absent during water stress (Thipyapong *et al.*, 2004b; Thipyapong and Steffens, 1997).

PPO activity

Enzyme activity of PPOs is normally highest in young tissues and decreases during further development, e.g., during fruit ripening as described for *Prunus armeniaca* (Chevalier *et al.*, 1999).

One characteristic property of PPO is latency, which means that PPOs are bound to thylakoid membranes in an inactive form and become active after membrane disintegration (Steffens *et al.*, 1994). PPOs also possess certain persistence. Often the protein is very stable throughout growth and development. For example, the apricot PPO protein is still present and active at an advanced stage of fruit development, whereas its mRNA is not detected (Chevalier *et al.*, 1999). In contrast, Thipyapong *et al.* (1997) suggested PPO protein accumulation being primarily controlled by mRNA levels, as in tomato plants they observed that PPO accumulation pattern reflects that of *PPO* transcripts.

PPO protein structure

PPO proteins have been isolated and characterised from a broad spectrum of seed plants, e.g., from *Vicia faba* (Flurkey, 1989), *Vitis vinifera* (Dry and Robinson, 1994), *Prunus armeniaca* (Chevalier *et al.*, 1999) and *Coffea arabica* (Mazaferra and Robinson, 2000).

The amino acid sequence of all known PPOs contains two highly conserved copper-binding domains CuA and CuB (Fig. 1.2A), responsible for the copper coordination and interaction with molecular oxygen and the phenolic substrate. Each copper-binding domain possesses three histidines that bind one copper atom; hence, one PPO molecule has six histidines binding two copper atoms in total (Steffens *et al.*, 1994). The above mentioned classification of the extended group of polyphenol oxidases into three subgroups is also reflected in the structure of the copper-binding domains: *o*-diphenol oxidases (PPO) and tyrosinases (TYR) are type-3 copper proteins, whereas laccases (LAC) possess a combination of type-2 and type-3 copper centres (reviewed by Gerdemann *et al.*, 2002).

Elucidation of the crystal structure of the active form of a catechol oxidase from *Ipomoea batatas* revealed that the secondary structure is dominated by α-helical regions (Fig. 1.2B). The catalytic copper centre is located within four α-helices in a hydrophobic pocket near the enzyme surface (Klabunde *et al.*, 1998). Moreover, the structure of a *Vitis vinifera* PPO, which was solved in March 2007 (PDB ID: 2P3X) (Reyes-Grajeda *et al.*, unpublished), possesses high similarities to the PPO structure of *Ipomoea batatas*.

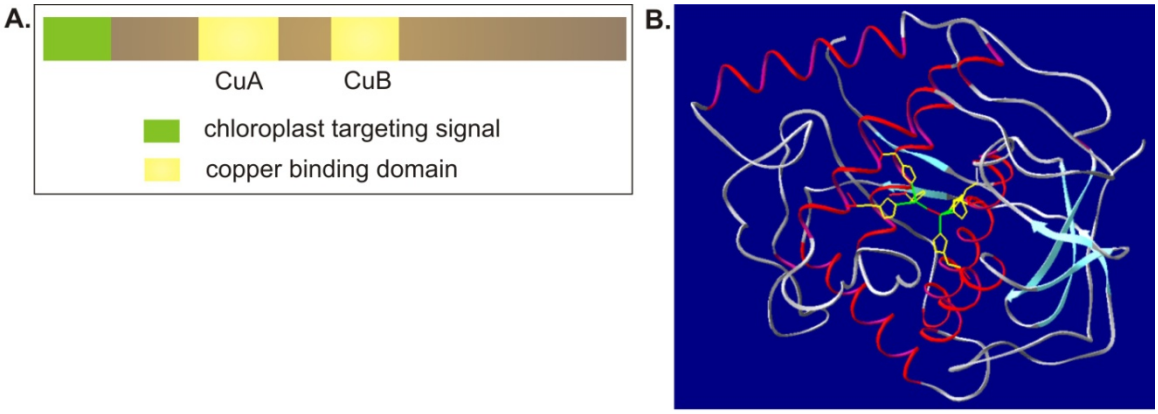

Fig. 1.2 Main structural features of seed plant PPOs. (A.) simplified structure of plants PPOs with two copper-binding domains CuA and CuB as catalytic sites and an N-terminal transit peptide for chloroplast targeting. (B.) crystal structure of the PPO from *Ipomoea batatas* (according to Klabunde *et al.*, 1998; modelled with the Swiss-Pdb viewer 4.0), six histidines (displayed in yellow) derived from the two copper-binding domains CuA and CuB coordinate two copper atoms in total (displayed in green). α-helices are displayed in red; β-sheets are displayed in blue.

Plant PPOs from different organisms exhibit sequence identities of 40 to 60 %. High sequence homologies were observed within one plant family; for example PPOs of different species from *Rosaceae* possess 85 – 97 % identity in their core amino acid sequence (Thipyapong *et al.*, 2007); PPOs from *Lycopersicon esculentum* and *Solanum tuberosum*, both belonging to the *Solanaceae*, possess 61 - 92 % identity in their overall amino acid sequence.

PPO localisation

Seed plant PPOs are predominantly located in plastids, mostly associated to the thylakoid membrane (Steffens *et al.*, 1994; Mayer, 2006).

The 5´ termini of *PPO* genes from higher plants contain leader sequences encoding for two-domain transit peptides of approximately 60 to 100 amino acids, which are responsible for the transport of the PPO to its destination (Newman *et al.*, 1993; Chevalier *et al.*, 1999). The two step transport of the thylakoid lumen localised PPO B was described in detail for *Lycopersicon esculentum* using an *in vitro* system and pea chloroplasts (Sommer *et al.*, 1994). In an ATP-dependent process, the precursor protein, having a molecular mass of 67 kDa, is transported into the stroma of the chloroplast. The resulting intermediate 62 kDa PPO protein is subsequently transported into the thylakoid lumen by a light dependent process, leading to the mature protein with a molecular mass of 59 kDa.

Nakayama *et al.* (2000) reported on a PPO homolog from *Antirrhinum majus*, an aureusidin synthase, which is involved in flavonoid synthesis, thus providing yellow flower colouration. Sequence analysis revealed that the copper containing protein belongs to the family of polyphenol oxidases and shares high sequence similarity with *o*-diphenol oxidases. However, the aureusidin synthase possesses no plastid transit peptide, but was found to be glycosylated and localised in the vacuole lumen of petal cells (Ono *et al.*, 2006).

Proteolytic processing of PPO

The reported molecular weights of plant PPOs are very diverse and variable. In *Vitis vinifera* proteolytic cleavage of a 67 kDa latent PPO results in a ca. 40 kDa active form (Dry and Robison, 1994). As reviewed by Flurkey and Inlow (2008), not only the N-terminal transit peptide (ca. 8 - 10 kDa) is cleaved off from plant PPOs after transport to the plastids, but a peptide at the C-terminus (ca. 15 kDa) with unknown function is also removed. Hence, seed plant PPOs are generally synthesised as precursor proteins of > 60 kDa, which are subsequently processed to mature forms with a molecular mass of ca. 40 kDa. So far, no protein responsible for C-terminal cleavage could be identified, and function and control of the cleavage remains unclear. The C-terminal processing might occur due to purification methods or may result from *in vivo* proteolysis. It has been proposed, that larger PPO forms still possessing the C-terminus are inactive forms, in which the C-terminal domain covers the active site of the enzyme (reviewed by Flurkey and Inlow, 2008).

PPO functions in seed plants

Due to their chloroplast association in seed plants (Steffens *et al.*, 1994), PPOs were suggested to be involved in the Mehler reaction removing an excess of electrons and O_2 produced by the photosynthetic light reaction (Vaughn *et al.*, 1988). However, as other redox candidates have been identified, this hypothesis has become less pronounced during the last years.

As the polyphenols are stored in the vacuoles, PPO enzymes usually react with their substrates after loss of cell integrity. The products of the PPO-catalysed oxidation of phenolic compounds, the electrophilic quinones, are very reactive and therefore able to undergo secondary reactions. They polymerise and form melanins or covalent bonds with nucleophilic residues on proteins or free amino acids. Through this so called "quinone tanning" dark coloured reaction products are formed (Steffens *et al.*, 1994).

Although no general function could be attributed to PPO, in recent literature, different functions were proposed for seed plant PPOs and PPO-mediated reactions:

- Involvement in plant pest and pathogen defence

  After disruption of the cell by wounding or infection, PPO enzymes react with their substrates, and the PPO-mediated insoluble reaction products can serve as wound protection layers (Waterman and Mole, 1994). Constabel *et al.* (2000) demonstrated that PPO activity and expression in hybrid poplar increased after wounding, methyl jasmonate spraying or attacks by forest tent caterpillars, and the authors therefore suggested PPOs as important components in defence mechanisms against leaf-eating insects. Overexpression studies in tomato (Li and Steffens, 2002) and in poplar (Wang and Constabel, 2004) confirmed a protective role of PPOs by showing an enhanced resistance of *PPO* overexpressing plants to *Pseudomonas syringae* and forest tent caterpillar, respectively. In contrast, *PPO* antisense downregulation in tomato led to enhanced disease susceptibility (Thipyapong *et al.*, 2004a).

- Involvement in light protection

  An increased PPO activity in birch seedlings exposed to UV-B radiation (Lavola *et al.*, 2000) as well as in leafs and roots of UV-B and UV-C treated *Capsicum annuum* tissue (Mahdavian *et al.*, 2008) was reported, and the authors proposed PPO to be involved in scavenging of free radicals produced under stress conditions. However, Balakumar *et al.* (1997) observed decreased PPO activities in leafs of UV-B treated tomato plants and suggested that through a

reduction of PPO activity the maintenance of high levels of phenolic compounds acting as antioxidants was ensured.

- Involvement in flower coloration

  A copper containing glycoprotein, aureusidin synthase, belonging to the family of plant polyphenol oxidases but localised in the vacuoles of *Antirrhinum major*, was found to be involved in aurone synthesis, providing yellow flower colouration (Nakayama *et al.*, 2000; Ono *et al.*, 2006).

- Involvement in inhibition of *postmortem* proteolysis

  Another role of PPOs is seen in retarding proteolysis. Sullivan *et al.* (2004) demonstrated that overexpression of red clover *PPO* in alfalfa resulted in a reduction of proteolysis in leaf extracts. This effect could be important in forest ecosystems as reduced nitrogen is transiently fixed in tanned protein complexes in leaf litter and soil (Waterman and Mole, 1994).

- Involvement in generation of electron acceptors for re-oxidation of cytokinin oxidase (CKX):

  Frébortová *et al.* (2004) and Galuzska *et al.* (2005) demonstrated that laccase derived quinones can function as electron acceptors *in vitro* to re-oxidise the enzyme cytokinin oxidase/dehydrogenase (CKX) catalysing in cytokinin breakdown. The authors hypothesised that PPO-mediated processes are indirectly involved in the modulation of cytokinin activities and can thereby influence developmental and differentiation processes. The *in planta* significance of this mechanism remains to be shown.

1.2. Phenolic compounds

Phenolic compounds are secondary plant metabolites, which are widely distributed among the plant kingdom. Some phenolics, such as chlorogenic acid, are nearly ubiquitous, whereas others exclusively occur in restricted and specific plant families or genera (Boudet, 2007).

Phenolic compounds consist of very heterogeneous structures, all exhibiting at least one aromatic benzene ring substituted with one or more hydroxyl groups. They are synthesised primarily from phenylalanine produced in the shikimate pathway, thus, at the gateway from the primary to the secondary metabolism. Phenylalanine ammonia-lyase (PAL; EC 4.3.1.24) catalyses the deamination of L-phenylalanine to *trans*-cinnamic acid. The products of the phenylpropanoid pathway serve as precursors for biosynthesis of further phenolics, such as benzoic derivatives, coumarins, stilbenes, flavonoids, lignins, and suberins.

Phenolic compounds possess several diverse roles in seed plant: They are involved in defence mechanisms against herbivores and pathogens, UV light protection, blossom pigmentation, and possess antibiotic effects against bacteria and fungi. Complexes, such as suberin and lignins, serve as polymeric elements to support surface and cell structure. Hence, synthesis of phenolic compounds is modulated and increased by several external stimuli, for example, in response to herbivoral attacks and mechanical wounding, pathogen infections, and irradiation with UV light (reviewed by Hahlbrock and Scheel, 1989; Waterman and Mole, 1994).

Regarding human nutrition, the interest on phenolic compounds has grown enormously in the last years, because they have antioxidative properties as radical scavengers (Rice-Evans *et al.*, 1995), and are therefore considered to possess protective effects, e.g., against cancer and cardiovascular diseases. Moreover, during fermentation processes, PPO and polyphenols are involved in flavour generating processes, for example, in fermentation of wine, tea, coffee, and cocoa. In contrast, during production of vegetable products (e.g., potato chips, noodles) PPO-mediated browning is undesirable and is aimed to be prevented.

1.3. The model plant *Physcomitrella patens*

The moss *Physcomitrella patens* (Hedw.) B.S.G. belongs to the family of the *Funariaceae*. It is a monoecious, self-fertile bryophyte widely distributed in the northern hemisphere, which naturally grows in open, unshaded, and nutrient-rich habitats.

Development

Physcomitrella exhibits a heteromorphic, heterophasic alternation of generations, the haploid phase being predominant in the life cycle (reviewed by Cove, 2000; Cove, 2005; Reski, 1998). The diploid sporophyte produces haploid spores by meiosis, that are able to germinate in the presence of light and water and generate filamentous protonema tissue. Protonema consists of chloronema cells with numerous large chloroplasts, and divides by apical growth and branching. Stimulated by auxin (Ashton *et al.*, 1979) thinner and longer caulonema cells with less chloroplasts and diagonal orientated cross walls are formed. Budding on chloronema and caulonema cells occurs in the presence of cytokinins (Bopp and Brandes, 1964; Reski and Abel, 1985), and buds subsequently develop to leafy shoots (gametophores) with phylloids and rhizoids. The gametophores produce male (antheridia) and female (archegonia) gametangia. After fertilisation, the zygote develops to the diploid sporophyte growing directly on the gametophyte (Fig. 1.3).

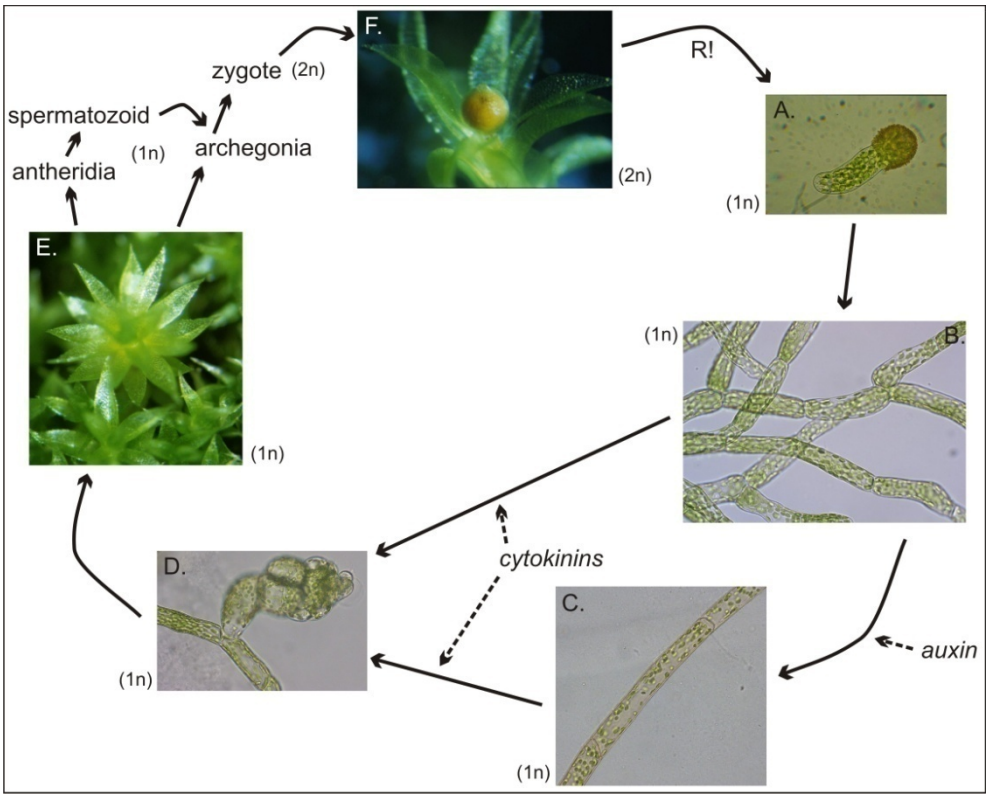

Fig. 1.3 Heteromorphic heterophasic life cycle of *Physcomitrella patens*. A. germinating spore B. chloronema C. caulonema D. bud E. gametophore F. sporophyte on gametophore (images by S. Bringe, H. Richter, K. v. Schwartzenberg, H. Turčinov)**.**

In vitro *cultivation, gene targeting and gene silencing*

Physcomitrella tissue can be cultivated axenically *in vitro* either on solid agar plates or in liquid cultures in a simple mineral medium without growth hormones. Also regeneration of tissue can be performed without the addition of hormones.

Transgenic *Physcomitrella* plants can be generated by PEG-mediate protoplast transformation (Schaefer *et al.*, 1991), by biolistic transformation (Sawahel *et al.*, 1992) or by *Agrobacterium*-mediated transformation (Schaefer, 2002).

High frequencies of integration of foreign DNA sequences preferentially at targeted locations into the nuclear genome can be achieved in *Physcomitrella* (Schaefer and Zryd, 1997). The use of homologous recombination is an important feature and serves as an essential tool to inactivate or modify specific gene targets and generate knockout plants.

Moreover, genes and complete gene families can be downregulated and silenced *via* RNA interference (RNAi) (Bezanilla *et al.*, 2005). Just recently, Khraiwesh *et al.* (2008) published, that genes can also be specifically silenced using artificial microRNAs (amiRNAs) derived from *Arabidopsis* microRNA precursors.

Genomic resources and EST databases

The haploid moss genome consists of 27 chromosomes with a total estimated length of about 510 mega base pairs (Schween *et al.*, 2003).

During the last years, *Physcomitrella* genomic resources have grown enormously. EST collections were generated in different research groups all over the world, and the transcriptome databases are publicly accessible (www.cosmoss.org/; www.nibb.ac.jp/evodevo/titleE.html) (Rensing *et al.*, 2002; Nishiyama *et al.*, 2003).

Through the International Moss Genome Consortium (a collaboration of groups from the USA, United Kingdom, Japan, and Germany), the *Physcomitrella* nuclear genome was sequenced at the Joint Genome Institute, and the draft sequence (V1.1 available on http://genome.jgi-psf.org/cgi-bin/browserLoad/491daf7677bccb9d41c21030) was published in early 2008 (Rensing *et al.*, 2008). About 36,000 protein-encoding genes were predicted from V1.1. However, the adjusted version V1.2 is now available on the *Physcomitrella* server "cosmoss.org" of the University of Freiburg (http://www.cosmoss.org/cgi/gbrowse/physcome/) with 27,949 predicted protein-encoding genes (Lang *et al.*, 2008).

Physcomitrella *genome analysis and abundance of metabolic genes*

Analysis of the collection of the assembled ESTs and the genome revealed that *Physcomitrella* has undergone at least one whole-genome duplication, which occurred 45 million years ago; hence, the haploid moss *Physcomitrella* is a paleopolyploid species (Rensing *et al.*, 2007).

Furthermore, analysis revealed that *Physcomitrella* retained an excess of metabolic genes and possesses a general expansion of gene families that can be associated with the conquest of land and with the acquisition of morphological complexity. Its metabolism was found to be uniquely complex, and alternative metabolic pathways not found in seed plants exist in *Physcomitrella* (Lang. *et al.*, 2005; Rensing *et al.*, 2007; Rensing *et al.*, 2008).

Physcomitrella *and tolerance to abiotic stress*

Physcomitrella is highly tolerant towards abiotic stress and able to survive salt and osmotic stress of up to 300 mM NaCl and 500 mM sorbitol without any phenotypic differences to control plants (Frank *et al.*, 2005). It appears that common mechanisms to cope with severe abiotic stress such as drought, salt and osmotic stress have been evolutionary conserved, as the bryophyte *Physcomitrella* and seed plants, which separated 450 million years ago, share basic mechanisms of

abiotic stress response. However, Frank and co-workers proposed, that *Physcomitrella* possesses further stress-related genes and proteins, not present in seed plants (Kroemer *et al.*, 2004; Frank *et al.*, 2005).

Features of Physcomitrella *as a model organism*

In summary, *Physcomitrella* exhibits numerous properties that make it ideally suited as a model organism, such as:

- simple morphology; predominant haploid phase
- cultivation and regeneration on minimal salt medium without supplementation of hormones; the complete life cycle can be controlled *in vitro*
- high frequencies of homologous recombination enabling gene targeting
- gene silencing *via* RNAi and amiRNAs
- large genomic resources with a fully sequenced genome publicly available as well as sequenced organellar genomes and large EST databases

Despite its simple morphology, *Physcomitrella* exhibits the basic organisational structures of land plants and a similar response to growth factors. Due to the predominant haploid phase, direct detection of recessive mutations is possible without back-crossing experiments. High frequency of homologous recombination allows reverse genetic approaches by direct gene replacement and elimination (Schaefer and Zryd, 1997). Gene targeting has been successfully performed in *Physcomitrella* (e.g., Hofmann *et al.*, 1999; Koprivova *et al.*, 2002; Mittmann *et al.*, 2004), including high throughput studies of functional genomics (Schween *et al.*, 2005b; Reski and Frank, 2005).

As bryophytes are representatives of early diverging embryophytes (having separated about 450 million years ago), they possess a key position in land plant evolution. Hence, *Physcomitrella* occupies an important phylogenetic position to reconstruct evolutionary changes that accompanied the conquest of land. Since the genomic sequence of *Physcomitrella* is available, comparison to sequenced genomes of green algae, diploid higher eukaryotic plants, and the club moss *Selaginella moellendorffii* is possible, elucidating new insights into land plant evolution.

Taken together, *Physcomitrella* has become a well recognised model organism in plant research to study evolutionary subjects of plant development, as well as physiological and metabolic processes.

PPO and phenolic compounds in bryophytes

Very little is known so far on PPOs in bryophytes. In a phylogenetic study performed by Sherman *et al.* (1991), no PPO activity was detected in the genera *Dicranum, Sphagnum and Thuidium*. However, PPO activity was determined in *Funaria hygrometrica* using a photometrical enzyme assay (Kapoor and Bhatla, 1999).

Regarding substrates, no detailed information exists on phenolic compounds and flavonoids in *Physcomitrella* so far (see Asakawa, 1995). However, a multigene family of chalcone synthases (EC 2.3.1.74), catalysing the first step in flavonoid biosynthesis, was identified and characterised for *Physcomitrella*, and functionality was proven for one of the gene family members (Jiang *et al.*, 2006).

1.4. Aim of this research

As described above, several diverse functions for PPOs in seed plants were proposed. In this research work, the large genomic resources of the model organism *Physcomitrella* in combination with the unique feature of gene targeting by homologous recombination will be used for the characterisation and functional analysis of the *Physcomitrella PPO* gene family. The following questions were addressed:

- Are there differences in the organisation of the *Physcomitrella PPO* gene family compared to seed plants?
- Are *Physcomitrella* PPOs functional *o*-diphenol oxidases?
- Are the *PPO* genes differentially regulated under standard conditions and under environmental stress?
- Does a *PPO* knockout of one gene family member affect the expression pattern of the remaining *PPO* genes?
- Are there phenotypical effects in functional *PPO* knockout lines?

The results obtained from this work will be discussed with respect to possible functions of *Physcomitrella* PPOs.

2. MATERIALS AND METHODS

2.1. Chemicals

Chemicals were purchased from Duchefa (Haarlem, NL), Merck (Darmstadt, G), Roth (Karlsruhe, G) and Sigma-Aldrich (Taufkirchen, G) unless separately specified.

All solutions were prepared with MilliQ water (Millipore, Schwalbach, G). Solutions for RNA experiments were prepared using DEPC-treated MilliQ water (0.1% DEPC in H_2O stirred over night and subsequently autoclaved). For sterilisation, media and buffer were autoclaved for 20 minutes at 121 °C and 1.2 bar or filtered through a filter with 0.22 µM pore size (Roth, Karlsruhe, G).

The composition of buffers, media and solutions are described in corresponding sections.

2.2. Plant material and cell culture

2.2.1. Plant material and standard growth conditions

The plant material used in this study was the bryophyte *Physcomitrella patens* (Hedw.) B.S.G (*Bryophyta, Funariales, Funariaceae*). All experiments were carried out using the wild type WTL6, which was the sixth sporophyte generation derived from the "Gransden wild type" (strain 16/14) originally collected in Gransden Wood (Huntingdonshire, UK) by H.L.K. Whitehouse in 1968.

A´BCD(N)TV culture medium, liquid (modified according to Wang *et al.*, 1980)

A´:	59 mg	$Ca(NO_3)_2$
B:	250 mg	$MgSO_4$*7 H_2O
C:	250 mg	KH_2PO_4
D:	1.04 g	KNO_3
N:	920 mg	di-NH_4 tartrate
T:	1 mL	TES (see below)
V:	1 mL	of each vitamin stock solution (see below)
	12.5 mg	$FeSO_4$*7 H_2O

MilliQ-H_2O was added up to 1L; pH was adjusted to 6.5 using KOH. Medium was autoclaved.

ABC(N)TV culture medium, solid (modified according to Knight *et al.*, 1988)

A:	1.18 g	$Ca(NO_3)_2$*4 H_2O
B:	250 mg	$MgSO_4$*7 H_2O
C:	250 mg	KH_2PO_4
N:	920 mg	di-NH_4 tartrate
T:	1 mL	TES (see below)
V:	1 mL	of each vitamin stock solution (see below)
	12.5 mg	$FeSO_4$*7 H_2O
	13 g	plant agar (Duchefa, Haarlem, NL)

MilliQ-H_2O was added up to 1L; pH was adjusted to 6.5 using KOH. Medium was autoclaved.

TES (trace element solution) (1000x stock) (modified according to Ashton and Cove, 1977)			
H_3BO_3	614 mg/L	$Al(SO_4)_3$*18 H_2O	38.6 mg/L
$MnCl_2$*4 H_2O	389 mg/L	KBr	28 mg/L
$NiCl_2$*6 H_2O	59 mg/L	KI	28 mg/L
$CoCl_2$*6 H_2O	55 mg/L	LiCl	28 mg/L
$CuSO_4$*5 H_2O	55 mg/L	$SnCl_2$*2 H_2O	28 mg/L
$ZnSO_4$*7 H_2O	55 mg/L		

Vitamin stock solutions (1000x stocks)	
* **nicotinic acid**	1 g/L
* ***p*-aminobenzoic acid**	0.25 g/L
* **thiamine/HCl**	5 g/L

Moss tissue was cultivated in growth chambers (RUMED Typ 1602+, Rubarth Apparate GmbH, Laatzen, G) at 25±1 °C and white light (fluorescent tubes Philips TLM 18W/840) under long-day conditions (16 h: ~50 µmol $m^{-2}s^{-1}$ light; 8 h: dark). Axenic liquid cultures of *Physcomitrella* were grown in A´BCDNTV media in 500 mL- or 1L-flasks, which were covered with cotton and aluminium caps. Aeration and mixing of the cultures was provided by sterile air (approx. 600 mL/min) pumped into the culture through a flexible silicone tube and a filter (0.2 µm pore size, Roth, Karlsruhe, G). Plant material was disintegrated every 7 to 10 days with an Ultra-Turrax blender T 25 basic, type S 25 N-18 G (IKA, Staufen, G), separated from media by filtration on a nylon sieve with 100 µM pore size (Wilson Sieves, Nottingham, UK), extensively washed with fresh medium and subsequently transferred to fresh A´BCDNTV medium (t0). Under standard conditions, protonema stadium was maintained by supplementation of medium with di-ammonium tartrate (N) as described above.

For cultivation on solid media, tissue from liquid cultures was transferred to ABC(N)TV agar plates and cultivated axenically at 25±1 °C under long-day conditions (16 h: ~50 µmol $m^{-2}s^{-1}$ light; 8 h: dark).

Axenity of the cultures was tested routinely by application of a small amount of the liquid culture on LB agar plates (2.3.10) and subsequent incubation at 22 °C for 3 to 5 days.

2.2.2. Application of phenolic compounds to *Physcomitrella* liquid cultures

Physcomitrella liquid cultures grown in A´BCDNTV were cultivated as described above (2.2.1). An aliquot of the liquid culture (approx. 10 mL) was transferred to a 100 mL flask closed with an air-permeable silicone cap. A sterile filtered stock solution of 4-methyl catechol (4-MC) was added to liquid cultures to a final concentration of 50, 100 or 200 µM and cultures were incubated under standard growth conditions (2.2.1) on a table agitator at 120 rpm until further use.

The polyphenol caffeic acid (CA) was added to solid culture medium (ABCNTV) to a final concentration of 50, 100, 500 or 1000 µM, or to liquid culture medium (A´BCDNTV) to a final concentration of 100 µM. A 10 mM CA stock solution was prepared in sterile 15 % ethanol; thus, medium used for the negative controls were prepared with the appropriate final concentrations of ethanol. *Physcomitrella* protonema tissue applied on solid medium as well as in liquid cultures containing CA was cultivated under standard conditions (2.2.1) until further use.

2.2.3. Irradiation with strong light intensities (sun simulator)

Exposure of moss tissue to a solar-like light radiation was performed as described by Hanelt *et al.* (2006) with a sun simulator (iSiTEC, Bremerhaven, G) equipped with a stabilised 400 W lamp (Philips MSR 400 HR). Light with a sunlight like spectrum was bundled to parallel and intensity was adjusted to ~1000 µmol $m^{-2}s^{-1}$ by filtering through a wire mesh without changing the spectrum. Beakers with samples of moss liquid cultures were placed on a rotating plate (5 rounds per hour) in a water filled glass container. The water in the container was kept at 23 °C; and temperature of the exposed liquid cultures was monitored continuously ensuring a constant temperature of 25 °C during 4 h exposure time.

2.2.4. Application of tritiated isopentenyladenine (^{3}H-iP) to *Physcomitrella* liquid cultures

In order to determine CKX activity *in vivo* of liquid cultured protonema, feeding experiments with tritiated isopentenyladenine (^{3}H-iP) were carried out at 25 °C and constant white light exposure of ~30 µmol $m^{-2}s^{-1}$ (fluorescent tubes Osram L, 15 W). Tissue from 80 mL of a 6 day old standard liquid culture was pored over a nylon mesh with 100 µM pore size (Wilson Sieves, Nottingham, UK) and transferred to a 50 mL conical tube. The tissue, which was not washed with fresh medium, was resuspended in a volume of 5 mL of old culture medium. To this concentrated protonema suspension, 1 mL stock solution of ^{3}H-iP in A´BCDNTV (spec. activity 1.29 Tbq/mmol) was added to a final concentration of 5 pmol (= 2,000,000 dpm) (t0). After 2, 4 and 8 hours, 50 µL samples of the culture medium were taken and stored at -20 °C until determination of overall radioactivity by liquid scintillation counting (2.6) and chromatographic analysis by RP-HPLC-online-LSC (2.7).

2.2.5. Harvest of *Physcomitrella* tissue from liquid culture and weight measurements

Plant material was harvested by filtration on a 100 µm nylon mesh (Wilson Sieves, Nottingham, UK). Tissue weight was determined after removal of residual media using a funnel connected to a

water-jet vacuum pump. Preparation of protein extracts (2.4.1) and extraction of phenolic compounds was carried out directly after tissue harvesting; plant material for RNA extraction (2.3.13) was frozen in liquid nitrogen and stored at -80 °C until further use.

2.2.6. Protoplast isolation from *Physcomitrella* liquid cultures

Plant material was collected from 5 to 6 day old A´BCDNTV liquid cultures using a nylon sieve of 100 µm pore size (Wilson Sieves, Nottingham, UK), washed with 0.5 M mannitol solution and transferred to a 9 cm petri dish. For cell wall digestion, 20 mL of a 0.5 % driselase solution were added, and tissue was incubated for 2 h in the dark at 100 rpm on a table agitator (IKA, Staufen, G). For separation of protoplasts from undigested plant material, the solution was passed through sieves of 100 and 50 µm pore size, respectively and centrifuged at 50 x g (Universal 16 A, Hettich, Tuttlingen, G) for 5 min. The sedimented protoplasts were carefully washed twice with 0.5 M mannitol solution and the protoplast number was determined using a Neubauer counting chamber. Subsequently, the protoplast suspension was adjusted to a density of $1.2*10^6$ protoplasts/mL by application of a third centrifugation step and resuspension in an appropriate volume of 3M medium (2.2.7).

0.5 M mannitol solution	**0.5 % driselase solution (w/v)**
(550 - 560 mOs)	in 0.5 M mannitol.
autoclaved.	prepared directly before use, sterile-filtered.

2.2.7. Transformation of *Physcomitrella*

The transformation of *Physcomitrella* protoplasts was carried out according to Schaefer *et al.* (1991) with slight modifications. For stable transformation 300 µL of protoplasts in 3M medium ($4*10^6$ protoplast, 2.2.6) were incubated with 300 µL PEG solution and 25 µg linear DNA. Transient expression was performed by adding 25 µg of circular plasmid instead. Transformation assays were incubated for 5 min at 45 °C, followed by a 10 min incubation at room temperature. The transformation mix was diluted by adding 1, 2, 3 and 4 mL 3M medium, every 5 min respectively, carefully mixing the suspension after each step. Protoplasts were centrifuged at 50 x g for 5 min, resuspended in 2.5 mL REG medium, transferred to 3 cm petri dishes, and incubated for 24 h at 25 °C in the dark followed by cultivation under standard growth conditions for 10 days. For selection of stable transformants, regenerating protoplasts were transferred to solid ABCNTV medium containing 25 µg G418/mL, covered with sterile cellophane membranes (Schütt, Hamburg, G). After 2.5 to 3 weeks this first round of selection was followed by a two week period on non-selective ABCNTV medium and a subsequent second selection period of two weeks. Plants

that survived the second round of selection without lesions were transferred to ABCNTV plates without cellophane ensuring direct contact of the tissue and the G418-containing culture medium. Plants that survived this third selection were considered to be stable transformants.

3M medium	**PEG solution**	**REG medium**
15 mM MgCl2	40 % PEG 4000	5 % (w/v) glucose
0.1 % MES	0.1 M $Ca(NO_3)_2$	3 % (w/v) mannitol
0.5 M mannitol	dissolved in 3M Medium.	dissolved in ABCTV, liquid
(pH 5.6, 580 - 590 mOs)	**(pH 5.6)**	**(pH 5.8, 540 - 580 mOs)**

for all solutions pH was adjusted with KOH and the solutions were sterile-filtered.

2.3. Molecular biology

2.3.1. *E. coli* strains

For cloning and expression experiments the following strains were used:

BL21(DE3) (Novagen by Merck, Darmstadt, G)
F– ompT gal dcm lon hsdSB(rB- mB-) λ(DE3 [lacI lacUV5-T7 gene 1 ind1 sam7 nin5])

DH5α
F- endA1 glnV44 thi-1 recA1 relA1 gyrA96 deoR nupG Φ80dlacZΔM15 Δ(lacZYA-argF)U169, hsdR17(rK- mK+), λ–

NovaXG (Novagen by Merck, Darmstadt, G)
F- mcrA .(mcrC-mrr) endA1 recA1 φ80dlacZ.M15 .lacX74 araD139 .(araleu) 7697 galU galK rpsL nupG λ- tonA

TOP10 (Invitrogen, Karlsruhe, G)
F- mcrA Δ(mrr-hsdRMS-mcrBC) φ80lacZΔM15 ΔlacX74 deoR nupG recA1 araD139 Δ(ara-leu)7697 galE15 galK16 rpsL(Str^R) endA1 λ^-

XL1-Blue (Stratagene, La Jolla, USA)
recA1 endA1 gyrA96 thi-1 hsdR17 supE44 relA1 lac [F'proAB lacIqZDM15 Tn10 (Tetr)]

2.3.2. DNA vectors

The following plasmids were used for cloning and expression:

Plasmid	*bacterial resistance*	*source*
pBluescriptSK-	ampicillin	Stratagene, La Jolla, USA
pET28a	kanamycin	Novagen by Merck, Darmstadt, G
pMLS46	kanamycin	Sullivan *et al.* (2004)
pHP23	ampicillin	Paszkowski *et al.* (1988)
pTrcHis2_TOPO	ampicillin	Invitrogen, Karlsruhe, G
pTrcHis2_TOPO/*lacZ*	ampicillin	Invitrogen, Karlsruhe, G

2.3.3. Oligonucleotides

Primers with standard purification grade were synthesised by MWG Biotech (Ebersberg, G) or Metabion (Martinsried, G). Annealing temperatures (T_a) used in PCRs were 0 - 3 °C lower than the calculated melting temperatures (T_m) obtained from the online application "OligoAnalyzer" http://eu.idtdna.com/analyzer/Applications/OligoAnalyzer/.

1. Primers for *PpPPO1* (Acc.No. AY904721)

Name	*Sequence 5´-3´*	T_m	*restriction site*
cPPO1_forw	GATCCATGGAGTTTACGTGCGTATTG	53.1	NcoI
cPPO1_rev	GCATGTCGACTTTCTCAAGCTTGATC	57.8	SalI
cPPO1_forw1	TTTCCCCCTCCGCAGTTTAGG	59.4	-
cPPO1_rev1	TTTCTCAAGCTTGATCTTGGTAG	52.7	-
PPO1_1	CGATAACACCTGCGTTGCTT	55.9	-
PPO1_2	TGAGTTGTGTCTGTCAAGCC	56.1	-
PPO1_3	GTTCCAGACAGGTCTGCCGT	60.4	-
PPO1_4	CTACCACCCATGCCTTTCCA	59.4	-
PPO1_5	CTCCATCGTCTCTCGCTGTAA	56.1	-
PPO1_6	CGGACAGAGTGTAGAGGCAA	57.2	-
PPO1_7	TTGCCTCTACACTCTGTCCG	57.2	-

2. Primers for *PpPPO11*

Name	*Sequence 5´-3´*	T_m
cPPO11_forw	ACAACTGGAAAAAGCAGGGC	56.3
cPPO11_rev	CATAGTAACCTCCGGGCTGA	56.1

3. Primerpairs for *PpPPO1 to PpPPO12*, designed with the online application "Primique" (http://cgi-www.daimi.au.dk/cgi-chili/primique/front.py)

	Forward Primer		*Reverse Primer*	
Name	*Sequence 5´-3´*	T_m	*Sequence 5´-3´*	T_m
PPO1exp	AGTCACAAGGTGCTACTC	46.6	ACCATCCGAACCTGTATG	47.2
PPO2exp	ACGGTTGGTTCTTCTTCC	48.1	GTGTACATGAGACGGTTG	46.3
PPO3exp	TCAATTACGTGTCAGGTG	45.7	TTAGCAATGTAGGCATCG	46.7
PPO4exp	ACCTTCCGGATTCTGATC	47.2	CCAATTCCAGAACGGAAG	47.6
PPO5exp	ACAAGCGGAACACCTGTC	50.6	GCAGTACAGACAGTGGAG	47.7
PPO6exp	TCGATCAAGGCACAACACAG	52.9	GGCATGCAACAGTTCTCC	49.2
PPO7exp	ACTCCACACGGCAATGTG	50.8	AACTAGATTCTGCTTCTCG	47.3
PPO8exp	GATGGTCGATCATTCCAAG	47.6	TGGCAAGTACGCCACAGAG	54.1
PPO10exp	CCTGACATATACTGATTGG	43.5	ATGTTAGTGCCATCATGG	44.6
PPO11exp	ATTCCTGTTGTCCACCATC	49.8	CTCGACCAGAGTGAAGCTC	52.3
PPO12exp	CCACCGACACAGTGTCTCC	54.7	TCTACCTCCTGGACGAGCTC	55.0

4. Primers for *35S_nptII*

Name	*Sequence 5´-3´*	T_m
nptII_1	GGGTTTCGCTCATGTGTTGA	56.3
nptII_2	ACTGTCGGCAGAGGCATCTT	58.9
nptII_3	GCTGCATACGCTTGATCC	54.0
nptII_4	GCCACAGTCGATGAATCC	53.3

5. General primers

Name	*Sequence 5´-3´*	T_m	*Reference*
T7prom	TAATACGACTCACTATAGGG	47.5	Novagen, Darmstadt,G
act3_forw	CGGAGAGGAAGTACAGTGTGTGGA_	59.9	Nakamura *et al.*(2005)
act3_rev	ACCAGCCGTTAGAATTGAGCCCAG	61.1	Nakamura *et al.*(2005)

2.3.4. Polymerase chain reaction (PCR)

2.3.4.1. Standard PCR

Standard PCRs were performed in 0.5 mL or 0.2 mL reaction tubes in the Mastercycler 5330 (Eppendorf, Hamburg, G) or the TRIO Thermoblock (Biometra, Göttingen, G). DNA amplification was performed with *Taq* DNA polymerase isolated from *Thermus spec.* (DNA Cloning Service, Hamburg, G). For amplification of precise nucleotide sequences, a mixture of *Taq* DNA polymerase (0.3 U) together with the proof reading *Pfu* DNA polymerase (0.7 U) from *Pyrococcus furiosus* (Fermentas, St.Leon-Rot, G) was used. dNTPs were purchased from Fermentas (St. Leon-Rot, G). Depending on the application, the amount of template varied from 10 pg to 100 ng per 25 µL reaction. For each primer pair a negative control was performed by adding MilliQ-H_2O instead of template.

Reaction mixtures were pipetted on ice in a volume of 25 µL comprising:

2.5 µL 10x PCR buffer
1 µL forward primer (12.5 µM), end concentration 0.5 µM
1 µL reverse primer (12.5 µM), end concentration 0.5 µM
0.25 µL dNTPs (25 mM each), end concentration 0.25 mM each
1 U DNA polymerase (or polymerase mixture)

The standard PCR protocol, in which annealing temperature was adjusted according to the utilised primer pair (2.3.3), was performed as followed:

94 °C	3 min	initial denaturation	
94 °C	30 sec	denaturation	25 - 30 cycles
T_a °C	30 sec	annealing	
72 °C	1 min/kb	elongation	
72 °C	10 min	final elongation	

2.3.4.2. Colony PCR

In order to screen for positive *E. coli* clones after transformation with ligation products (2.3.9 and 2.3.10), colony PCRs were carried out. As a template, part of an *E. coli* colony was transferred with a toothpick from LB agar plates to 5 µL MilliQ-H_2O. PCR mixture was added on ice, and the reaction (standard PCR, 2.3.4.1) was started with an elongated initial denaturation time of 5 min.

2.3.4.3. Real-time PCR

Real-time PCRs were performed in the iCycler iQ (Bio-Rad, München, G) in a volume of 25 µL with the following components:

12.5 µL iQ SYBR® Green Supermix, Bio-Rad, München, G (composed of 100 mM KCl, 40 mM Tris-HCl pH 8.4, 0.4 mM of each dNTP, 50 U/mL iTaq DNA pol., SYBR®-Green I, 20 nM fluorescein)
0.5 µL forward primer (12.5 µM), end concentration 0.25 µM
0.5 µL reverse primer (12.5 µM), end concentration 0.25 µM

For real-time RT-PCRs, 3 µL of a RT reaction (2.3.14) were used as a template. Real-time PCR protocol was performed as followed (T_a was adjusted according to the primer pair utilised (2.3.3)):

95 °C	5 min	initial denaturation and activation of DNA polymerase	
94 °C	30 sec	denaturation	
T_a °C	30 sec	annealing	50 cycles
72 °C	30 sec	elongation	
T_a °C	10 sec	melt curve	85 - 95 cycles / +0.5 °C at each cycles

Accumulation of double stranded PCR product during PCR amplification resulting in an increase of SYBR green fluorescence was monitored during the annealing and elongation steps.

Subsequent to real-time PCR, melt curve analysis was performed in order to check for specific PCR amplification. During melt curve performance, the fluorescence decrease was monitored, which was caused by the release of SYBR green from double stranded DNA melted in this step.

Efficiencies of real-time PCR amplifications with each primer pair (2.3.3) were tested with different concentrations of genomic DNA as a template DNA.

For the comparability of expression levels between different *PPO* gene family members from one cDNA preparation, CT (cycle threshold) values of cDNA amplifications were adjusted for eventual differences in PCR efficiencies with the CT values obtained from PCRs using genomic DNA as a template with the corresponding primer pairs. For this purpose, CT values for the reference gene *PpACT3* (Acc.No. AW698983) were used as anchor to adjust CT values for *PpPPO* genes for slight differences in PCR efficiencies. Concentration of genomic DNA for control PCRs was chosen to result in CT values in the same range (±1-2 CT) as for cDNA CT values, and equal concentrations of genomic DNA were used for *PPO* and *ACT3* amplifications with each different primer pair (2.3.3).

The CT value for *PPOx* amplified from genomic DNA (CT_{gPPOx}) was subtracted from the CT value for the reference gene *PpACT3* amplified from the same genomic DNA (CT_{gACT}). The resulting difference was added to the CT value obtained for the corresponding *PPOx* amplification from a distinct cDNA preparation, e.g., cDNA(A) ($CT_{c(A)PPOx}$), resulting in the corrected CT value for *PPOx* ($cCT_{c(A)PPOx}$) for PCR efficiency (equation 1).

Equation 1: Formula for calculation of CT value correction for PCR efficiency

$$CT_{c(A)PPOx} + (CT_{gACT} - CT_{gPPOx}) = cCT_{c(A)PPOx}$$

[CT_{gACT}: identical for each *PPO* CT correction]

For the comparability of CT values between different cDNA preparations, the CT value obtained for *PPOx* amplification from one cDNA preparation, e.g., cDNA(A) ($CT_{c(A)PPOx}$), was adjusted with the CT values obtained for the constitutively expressed reference gene *ACT3* from the same cDNA(A) ($CT_{c(A)ACT}$).

The lowest CT value for *ACT3* of all compared cDNAs, e.g., cDNA(B) ($CT_{c(B)ACTmin}$), was selected and subtracted from the CT values for *ACT3* amplification from each cDNA, e.g., cDNA(A) ($CT_{c(A)ACT}$). The resulting difference was subtracted from the CT value for *PPOx* amplification from the corresponding cDNA(A) ($CT_{c(A)PPOx}$), resulting in the corrected CT ($c´CT_{c(A)PPOx}$) value for RNA quality and RT efficiency (equation 2).

Equation 2: Formula for calculation of CT value correction for the reference gene

$$CT_{c(A)PPOx} - (CT_{c(A)ACT} - CT_{c(B)ACTmin}) = c´CT_{c(A)PPOx}$$

[$CT_{c(B)ACTmin}$: lowest CT value for *ACT3* and identical for each *PPO* CT correction]

Equation 3 results from a fusion of equation 1 and 2 for the possibility to compare between both, different *PPO* gene family members and different cDNAs, resulting in corrected CT values for PCR efficiencies as well as for RNA qualities and RT efficiencies ($cc´CT_{c(A)PPOx}$).

Equation 3:

$$CT_{c(A)PPOx} + (CT_{gACT} - CT_{gPPOx}) - (CT_{c(A)ACT} - CT_{c(B)ACTmin}) = cc´CT_{c(A)PPOx}$$

[CT_{gACT} identical for each *PPO CT* correction; $CT_{c(B)ACTmin}$: lowest CT value for *ACT3* and identical for each *PPO* CT correction]

In order to obtain relative transcript amounts, the highest corrected CT value (equation 3) corresponding to the lowest expression level for *PPO* amplification from cDNA, e.g., *PPOy*

($cc´CT_{cPPOy}$), was selected, and the difference of all other corrected CT values to this CT was determined. This difference for each *PPO* gene and cDNA was used as the exponent according to equation 4, resulting in the relative expression levels.

Equation 4: $2^{(cc´CT_{cPPOy} - cc´CT_{cPPOx})}$

[$cc´CT_{cPPOy}$: highest corrected CT value, identical for determination of each *PPO* transcript level]

Calculations were modified according to the method described by Livak and Schmittgen, (2001).

2.3.5. Electrophoretic separation of DNA and RNA

Separation of DNA fragments or RNA according to their size was carried out by horizontal gel electrophoresis (wide mini-sub cell GT, Bio-Rad, München, G). 1x TAE gels with 0.9 - 1.2 % agarose and ethidium bromide at a final concentration of 0.5 µg/mL were prepared. DNA samples or RNA were mixed with DNA loading buffer and separated at 70 - 80 V in 1x TAE as running buffer. For molecular weight determination of DNA fragments, Lambda DNA digested with PstI was used as a marker. DNA fragments or RNAs were visualised using a UV transilluminator and gels were documented with BioPrint 96.07 (Vilber Lourmat, Eberhardzell, G).

5x DNA loading buffer		10x TAE buffer	
50 % (v/v)	glycerol	48.4 g/L	Tris base
60 mM	EDTA pH 8.0	20 mL/L	0.5 M EDTA, pH 8.0
0.25 % (w/v)	bromphenol blue	11.42 mL/L	acetic acid

2.3.6. Purification of PCR products and DNA elution from agarose gels

Purification of DNA fragments for cloning was carried out with the Avegene Gel/PCR DNA Fragments Extraction Kit (DNA Cloning Service, Hamburg, G) according to the manufacturer's protocol.

2.3.7. Small- and large-scale preparation of plasmid DNA

Small-scale isolation of plasmid DNA was performed with the Avegene High-Speed Plasmid Mini Kit (DNA Cloning Service, Hamburg, G) according to manufacturer's protocol. DNA was eluted in 50 µL TE buffer or MilliQ-H_2O. For large-scale preparation of plasmid DNA, the Plasmid Maxi Kit (Qiagen, Hilden, G) was used following the manufacturer's instructions. Plasmid DNA was resuspended in 300 - 500 µL sterile MilliQ-H_2O and stored at -20 °C. DNA concentration was determined spectrophotometrically (Ultrospec 3000, Pharmacia Biotech, München, G). The

extinction of diluted DNA was measured at 260 nm, and concentration was calculated by the assumption that 1 OD_{260} corresponds to 50 µg double stranded DNA/mL. Information on purity of DNA was given by the ratio of E_{260}/E_{280}.

2.3.8. Restriction analysis of DNA

Enzymatic cleavage of DNA was performed at 37 °C using restriction endonucleases from Fermentas (St. Leon-Rot, G). For analytic digestion usually 1 µg DNA was digested in a 20 µL reaction volume with 1 U enzyme for 1 hour. Larger amounts of DNA were digested in an increased reaction volume with higher amounts of enzyme and longer incubation times. Efficiency of digestion was verified by agarose gel electrophoresis (0). The enzyme was heat inactivated according to the manufacturer's instructions, and DNA was isolated by precipitation using SureClean (Bioline, Luckenwalde, G).

2.3.9. Klenow reaction, dephosphorylation and ligation of DNA fragments

Insertion of DNA fragments into a vector was carried out by blunt or sticky end ligation using the T4 DNA ligase. Prior to blunt end ligations 5´-overhangs produced by restriction enzymes were filled in using the Klenow fragment. To prevent self circulation of the digested vector DNA, terminal 5´-phosphate groups were removed from DNA by treatment with Calf Intestine Alkaline Phosphatase (CIAP). Klenow fragment, CIAP and T4 DNA ligase were purchased from Fermentas (St. Leon-Rot, G), and all reactions were performed as described by the manufacturer. Each enzymatic reaction was stopped by heat inactivation and elimination of the enzyme using SureClean (Bioline, Luckenwalde, G). After the ligation reaction, DNA was resuspended in sterile MilliQ-H_2O for transformation of electrocompetent cells (2.3.10).

2.3.10. Preparation and transformation of electrocompetent *E. coli* cells

As a starter culture, 2.5 mL LB medium were inoculated with a single colony of the appropriate *E. coli* strain (2.3.1) and grown over night at 37 °C. For the main culture, 400 mL 2YT medium were inoculated with 250 µL of the overnight culture and grown at 22 °C to an OD_{600} of 0.4. Cells were harvested by centrifugation at 4,000 x g and 4 °C for 15 min (Sorvall, Kendro, Hanau, G). The bacterial pellet was carefully resuspended in 400 mL sterile, ice cold MilliQ-H_2O, centrifuged and washed twice with 250 mL and 20 mL MilliQ-H_2O, respectively. After a last centrifugation step, the electrocompetent cells were resuspended in 7 % DMSO, and 50 µL aliquots were frozen in liquid nitrogen and stored at -80 °C until transformation.

Transformation was performed using the Electroporator 2510 and electroporation cuvettes with 1 mm gap width (both Eppendorf, Hamburg, G). A 50 µL aliquot of competent *E.coli* cells was mixed with desalted plasmid DNA (1 - 50 ng), and a voltage of 1250 V was subsequently applied for 3 - 4 milli sec. Immediately, the cells were transferred to a 10 mL culture tube with 300 µL SOC medium and incubated at 37 °C at continuous shaking. After 30 min of regeneration, the cells were plated on LB agar plates containing the appropriate antibiotic for selection, and plates were cultivated over night at 37 °C.

2YT medium	**LB medium**	**SOC medium**
10 g/L yeast extract	5 g/L yeast extract	10 g/L yeast extract
16 g/L peptone	10 g/L peptone	5 g/L peptone
5 g/L NaCl	10 g/L NaCl	10 mM NaCl
	(7.5 g/L Agar)	2.5 mM KCl
		20 mM D-glucose
		20 mM $MgSO_4$
		10 mM $MgCl_2$

pH was adjusted with NaOH to 7.0.
2YT and LB Media were autoclaved. SOC medium was sterile-filtered.

Concentrations of antibiotics ampicillin 100 µg/mL
kanamycin 50 µg/mL

2.3.11. TOPO®-TA cloning and transformation

The pTrcHis2 TOPO® TA Expression Kit (Invitrogen, Karlsruhe, G) was used for cloning PCR products into the pTrcHis2-TOPO® vector. All procedures were carried out according to the manufacturer's protocol.

2.3.12. Isolation of genomic DNA from *Physcomitrella*

A simplified CTAB method was used for isolation of genomic DNA from moss tissue. Part of a young green gametophore was transferred to a 1.5 mL tube containing 400 µL of 2x CTAB buffer and grinded with a small plastic pestle. The homogenate was incubated for one hour at 60 °C in a water bath, subsequently extracted with an equal volume of chloroform:isoamylalcohol (25:1) and centrifuged at 16,000 x g for 10 min (Biofuge pico, Kendro, Hanau, G). The upper aqueous phase was transferred to a new tube, and an equal volume of 2-propanol (approx. 300 - 350 µL) was added followed by a second centrifugation to precipitate the genomic DNA. The supernatant was discarded; the DNA pellet was washed with 70 % ethanol and finally dissolved in 50 µL of TE buffer containing 1 µL of 1 mg/mL RNaseA. For PCRs 0.5 - 2.0 µL DNA were used as a template in a total PCR volume of 25 µL (2.3.4.1).

2x CTAB buffer		TE buffer
2 % (w/v)	CTAB	10 mM Tris-HCl pH 8.0
100 mM	Tris-HCl pH 8.0	1 mM EDTA pH 8.0
1.4 M	NaCl	
20 mM	EDTA pH 8.0	

2.3.13. Isolation of RNA from *Physcomitrella*

Isolation of RNA from *Physcomitrella* was accomplished with the peqGOLD RNAPure solution (peqlab, Erlangen, G) following the manufacturer's instructions with a minor modification in cell disruption. 50 - 100 mg plant tissue were homogenised in 1.5 mL peqGOLD solution with glass beads (Ø 1.7 - 2 mm) for 20 sec at speed 4 (2 cycles) using the FastPrep FP120 homogeniser (MP Biomedicals, Heidelberg, G). Cell debris were removed by centrifugation at 16,000 x g and 4 °C for 5 min (2 MK, Sigma, Taufkirchen, G). The supernatant was used for subsequent steps, performed according to the manufacturer's protocol. RNA was finally resuspended in 25 - 50 µL DEPC treated MilliQ-H_2O.

2.3.14. DNase treatment of RNA and reverse transcription (RT) for cDNA synthesis

Prior to reverse transcription RNA was treated with DNase I (Fermentas, St. Leon-Rot, G) according to the manufacturer's protocol. After heat inactivation of DNase I, RNA was precipitated with ethanol and resuspended in DEPC-treated MilliQ-H_2O. RNA concentration was determined spectrophotometrically (Ultrospec 3000, Pharmacia Biotech, München, G). The extinction of RNA was measured at 260 nm, and the concentration was calculated based on the assumption that 1 OD_{260} corresponds to 40 µg RNA/mL.

Reverse transcription of RNA was performed as followed:

3 µg RNA
1 µL random octamers, 40 µM (MP Biomedicals, Heidelberg, G)
to 10 µL MilliQ-H_2O (DEPC treated)

were mixed and incubated for 5 min at 70°C, subsequently placed on ice.

4 µL 5x buffer
2 µL dNTPs (10 mM each)
to 19 µL MilliQ-H_2O (DEPC treated)

were added and incubated for 5 min at 25 °C. 200 U RevertAid M-MuLV reverse transcriptase (Fermentas, St. Leon-Rot, G) were added, reactions were incubated for 10 min at 25 °C and subsequently for one hour at 42 °C. The reverse transcriptase was inactivated by a terminal incubation step at 70 °C for 10 min. Samples were directly used as a template for PCR or real-time

PCR (2.3.4.1 and 2.3.4.3). In order to test for possible DNA contamination of the RNA samples, "RT minus controls" consisting of RT reactions without reverse transcriptase were performed and used as PCR templates as well.

2.3.15. Sequencing of DNA

Sequencing of plasmid DNA and PCR products was performed by the DNA Cloning Service (Hamburg, G).

2.4. Protein biochemistry

2.4.1. Preparation of protein extracts from *Physcomitrella* tissue

Tissue from *Physcomitrella* liquid cultures (300 - 400 mg) was harvested as described above (2.2.5) and transferred to a 2 mL microcentrifuge tube filled to ¼ with glass beads (Ø 1.7-2 mm). Samples were frozen in liquid nitrogen and homogenised in ice cold phosphate buffer for 20 sec at speed 4 (2 cycles) using the FastPrep FP120 homogeniser (MP Biomedicals, Heidelberg, G). To remove cell debris, the homogenate was centrifuged for 10 min at 16,000 x g and 4 °C (2 MK, Sigma, Taufkirchen, G). The resulting supernatant was re-centrifuged and used as a crude protein extract. Protein content of these tissue extracts was determined using the Bradford assay (2.4.4).

Phosphate buffer, pH 6.4, with KH_2PO_4 and Na_2HPO_4 (67 mM each)
738 mL/L solution A (comprising 9.078 g KH_2PO_4/L)
262 mL/L solution B (comprising 11.876 g Na_2HPO_4*$2H_2O$/L)

2.4.2. Preparation of protein extracts from *Physcomitrella* medium

Culture medium (A´BCDNTV) was separated from tissue on a 50 µM nylon sieve, filtered through a three times folded nylon gaze with 30 µM pore size and freeze-dried by lyophilisation at -20 °C (Alpha I-6 Christ, Osterode, G; pump Duo 5M, Pfeiffer, Asslar, G). All following steps were performed at 4 °C. The lyophilised powder was resuspended in ice cold phosphate buffer (2.4.1) and insoluble compounds were sedimented by centrifugation at 1,000 rpm for 5 min (Universal 16 A, Hettich, Tuttlingen, G). In order to remove salts and low molecular weight compounds, the supernatant was subsequently applied to an illustra NAP 25 column (GE Healthcare, München, G), and the proteins were eluted in ice cold phosphate buffer. Protein content of the desalted solution was determined by NanoOrange® protein quantitation kit (2.4.4).

2.4.3. Preparation of protein extracts from *E. coli* and purification of recombinant PPO

To obtain recombinant PPO from *PPO* expressing *E. coli* clones, 200 mL LB culture (2.3.10) supplemented with the appropriate antibiotic was inoculated with a starter culture. Cultures were grown in 1 L flasks with 200 rpm shaking at room temperature to an OD_{600} of 0.4, and transcription was induced by the addition of 1 mM IPTG. Cultures were further supplemented with 20 µM $CuCl_2$ and grown for additional 6 hours at room temperature. The cells were harvested by centrifugation at 4,000 x g and 4 °C for 15 min (Sorvall, Kendro, Hanau, G) and resuspended in 20 mL phosphate buffer (2.4.1) supplemented with 0.5 % Triton X-100. Lysozyme was added to a final concentration of 100 µg/mL, and the cell suspension was incubated at room temperature for 15 min with gentle agitation. All subsequent steps were performed at 4 °C. The cell suspension was sonicated briefly with a probe-type sonicator (Branson Sonifier B15 with micro tip, Danbury, USA) with 10 short bursts of 10 sec (placed on ice in between) and subsequently centrifuged at 13,000 x g and 4 °C for 30 min in order to remove cell debris. The clear homogenate was adjusted to pH 7 by the addition of NaOH, passed through a filter with 0.45 µm pore size (Roth, Karlsruhe, G), and loaded on a pre-packed His●bind® column (Novagen by Merck, Darmstadt, G). Purification of recombinant His-tagged protein by column chromatography was performed following the manufacturer's instructions, and the recombinant protein was eluted in buffer comprising 400 mM imidazole, 500 mM NaCl and 20 mM Tris-HCl pH 7.9. The purified protein was applied to an illustra NAP 25 column (GE Healthcare, München, G), and finally eluted in phosphate buffer . Protein content was determined with the NanoOrange® kit (2.4.4).

2.4.4. Determination of protein concentrations

Protein contents were determined according to Bradford (1976) using BSA as a standard. 20 to 100 µL of a protein extract were mixed with 1x Bradford reagent (Bio-Rad, München, G), and extinction of the assay was measured spectrophotometrically (Ultrospec 3000, Pharmacia Biotech, München, G) at 595 nm.

For quantification of low concentrated protein extracts, the NanoOrange® protein quantitation kit from Invitrogen (Karlsruhe, G) was used. Assays were performed as described in the manufacturer's instructions using BSA as a standard, and fluorescence was determined with the luminescence spectrometer LS 55 (PerkinElmer, Rodgau-Jügesheim, G).

2.4.5. Polarographical determination of *in vitro* PPO activity

PPO activity was determined polarographically using the Clark electrode system (electrode YSI 5331, chamber YSI 5301, Yellow Springs Instruments, Yellow Springs, USA) by measuring the concomitant oxygen depletion.

Assays were performed at 25 °C in a cuvette in a total volume of 3 mL comprising:

x µL protein extract (prepared as described in 2.4.1, 2.4.2 or 2.4.3)
100 µL 10 % SDS solution (end concentration 0.3 %)
to 2.9 mL phosphate buffer (2.4.1), air saturated, equilibrated to 25 °C

Reactions were started by the addition of 4-methyl catechol as a substrate to a final concentration of 7.5 mM (100 µL of a 225 mM stock solution). Percentage of air consumption after addition of the substrate was documented over a time of 6 min with a chart recorder (Kipp&Zonen, Delft, NL). Autoxidation of 4-methyl catechol was determined from assays without protein extracts and subtracted from the determined values for assays with protein extracts. Enzyme activity was calculated as µmol O_2-consumption per h*mg protein according to the fact that air saturated buffer contains 0.67 µmol oxygen.

In order to attribute substrate specific O_2-depletion to PPO activity, control experiments including the addition of KCN to the reaction assay (final concentration 2 mM) were carried out to specifically inhibit PPO activity, as cyanide forms cyano-complexes with copper coordinated to the PPO copper-binding domains (Kavrayan and Aydemir, 2001). After KCN addition no further O_2-consumption should be measurable.

2.4.6. SDS polyacrylamide gel electrophoresis (PAGE)

Proteins were separated according to their molecular weight by SDS PAGE performed in a Mini-Protean 3 cell (Bio-Rad, München, G). As a standard, a 5 % stacking gel on top of a 12.5 % separating gel was used. Prior to sample loading, protein extracts were denaturated by mixing with SDS loading buffer and incubation at 95 °C for 5 min. For molecular weight determination of the proteins the prestained protein ladder PageRuler (Fermentas, St. Leon-Rot, G) was used. Protein samples were separated at 150 V for 1 hour in 1x SDS running buffer.

5x SDS loading buffer		10x SDS running buffer	
312.5 mM	Tris-HCl pH 6.8	250 mM	Tris base
10 % (w/v)	SDS	1 % (w/v)	SDS
50 % (v/v)	glycerol	1.92 M	glycine
0.5 M	DTT		
0.125 % (w/v)	bromphenol blue		

SDS stacking gel (5 %)	
2.88 mL	MilliQ-H_2O
1.25 mL	stacking buffer (0.5 M Tris-HCl, pH 6.8)
0.624 mL	acrylamide/bisacrylamide 37.5:1 (Rotiphorese® Gel 40, Roth, Karlsruhe, G)
50 µL	SDS solution (10 %)
25 µL	ammonium persulphate solution (10 %)
5 µL	TEMED (AppliChem, Darmstadt, G)

SDS separating gel (12.5 %)	
4.22 mL	MilliQ-H_2O
2.5 mL	separating buffer (1.5 M Tris-HCl, pH 8.8)
3.13 mL	acrylamide/bisacrylamide 37.5:1 (Rotiphorese Gel 40, Roth, Karlsruhe, G)
100 µL	SDS solution (10 %)
50 µL	ammonium persulphate solution (10 %)
5 µL	TEMED (AppliChem, Darmstadt, G)

2.4.7. Coomassie brilliant blue staining

For visualisation of protein bands, SDS gels were incubated in coomassie staining solution by gentle rotation on a table agitator. After 2 to 5 hours gels were transferred to the stop stain solution and further incubated for approx. 2 hours to remove coomassie background.

Coomassie staining solution	Stop stain solution
40 % (v/v) methanol	40 % (v/v) methanol
10 % (v/v) glacial acetic acid	10 % (v/v) glacial acetic acid
0.18 % (w/v) coomassie brilliant blue R250	

2.4.8. Western blot

Prior to transfer of proteins, the SDS gel (2.4.6), a PVDF membrane (Roti-PVDF, Roth, Karlsruhe, G) and six sheets of 3 mm blotting paper (Schleicher&Schuell, Dassel, G) were equilibrated in transfer buffer for 15 min. Subsequently, proteins from the SDS gel were blotted onto the PVDF membrane for 30 min at 20 V using a semi-dry transfer unit (Keutz, Reiskirchen, G). Unused membrane sites were blocked by incubation in 1x PBS solution containing 1 µg polyvinyl alcohol (PVA)/mL for 30 sec and three subsequent washing steps (10 min each) in PBS/Tween/milk solution comprising 1x PBS with 1 % (w/v) skim milk powder and 0.3 % (v/v) Tween 20. Afterwards, the membrane was incubated for 1 hour in the primary antibody solution, followed by three 10 min washes with PBS/Tween/milk solution, and subsequently incubated for 1 hour in the secondary antibody conjugated to alkaline phosphatase. Antibodies were diluted in PBS/Tween/milk; all incubation steps were carried out at room temperature and gentle shaking on a table agitator. To remove residual Tween 20 and milk powder, the membrane was incubated in 1x PBS prior to detection.

Membranes were developed colorimetrically. The NBT/BCIP colour development solution was prepared by adding NBT at a final concentration of 0.3 mg/mL and BCIP at a final concentration of 0.15 mg/mL to the NBT/BCIP buffer. The membrane was immersed in the NBT/BCIP colour development solution and incubated in the dark until colour development was clearly visible (approx. 10 - 20 min).

10x PBS, pH 7.4	**Transfer buffer, pH 8.3**	**NBT/BCIP buffer, pH 9.8**
80 g/L NaCl	48 mM Tris base	0.1 M $NaHCO_3$
2 g/L KCl	39 mM glycine	1 mM $MgCl_2$
26.8 g/L Na_2HPO_4*$7H_2O$	0.0375 % (w/v) SDS	
2.4 g/L KH_2PO_4	20 % (v/v) methanol	

NBT (Nitroblue tetrazolium) solution
75 mg/mL in 70 % N,N-dimethylformamide (DMF)

BCIP (5-Bromo-4-chloro-3-indolyl phosphate) solution
50 mg/mL in 100 % DMF

Antibodies

	primary antibody	*secondary antibody*
Name	anti His-tag® monoclonal antibody (Novagen by Merck, Darmstadt, G)	anti mouse IgG-alkaline phosphatase (Sigma Aldrich, Taufkirchen, G)
Dilution	1: 1000	1: 5000

2.5. Determination of cell vitality

2.5.1. Fluorescein diacetate (FDA) staining

To analyse cell vitality of *Physcomitrella* cultures, 2 µL of a fluorescein diacetate (FDA) stock solution (10 mg/mL in DMSO) were added to 500 µL protonema culture. After a 5 min incubation at room temperature green fluorescence of living cells, resulting from deesterification of FDA to fluorescein by esterase activity in vital cells was examined under blue light excitation using the BH-2 microscope equipped with the filter combination BBY455 (Olympus, Hamburg, G).

2.5.2. PAM fluorometry

The photosynthetic (PS) activity was measured as parameter to determine photoinhibition, thus cell vitality, of *Physcomitrella* tissue irradiated with strong light (2.2.3) or incubated with 4-methyl catechol (2.2.2). PS activity from protonema samples was measured by *in vivo* chlorophyll fluorescence using the pulse-amplitude modulation chlorophyll fluorometer PAM-101, data were acquired with the PAM Data Acquisition System PDA-100 and processed with the WinControl Software (all three Walz, Effeltrich, G). The optimal quantum yield of PSII electron transport,

which is the ratio of variable to maximal fluorescence F_v/F_m, is an indirect method to measure PS activity, but was shown earlier to be consistent with direct PS activity measurements (Hanelt *et al.*, 1995). F_m is defined as the maximal fluorescence (all PS II reaction centres inactive); F_v is defined as $F_v = F_m - F_0$, in which F_0 is the initial fluorescence (all PS II centres open). F_v/F_m was determined from dark adapted protonema stirred in a cuvette in a cuvette holder adjusted to 25 °C by connection to a water bath. In order to oxidise the electron transport chain, far red light (~30 µmol m^{-2} s^{-1}; 720 nm) was applied, followed by 5 min incubation in the dark. F_0 was subsequently measured with a pulsed red light (~0.3 µmol m^{-2} s^{-1}, 650 nm), and F_m was determined with a saturating white light pulse (~5000 µmol m^{-2} s^{-1}). A quantum yield of PSII electron transport [F_v/F_m] of 0.8 corresponds to 100 % photosynthesis activity (Krause and Weis, 1991), thus, indirectly to 100 % cell vitality.

2.6. Quantification of tritiated isopentenyladenine (^{3}H-iP) from culture medium to determine extracellular CKX activity

To quantify the amount of total radioactivity from culture medium, 50 µL samples were taken from protonema liquid cultures incubated with ^{3}H-iP (2.2.4) and mixed with 3 mL liquid scintillation cocktail Optisafe "HiSafe" 2 (two samples of each reaction assay). Subsequently, samples were analysed with the liquid scintillation analyser Tri-Carb 2800 TR (both PerkinElmer, Rodgau-Jügesheim, G) by counting the disintegrations per minutes (dpm) of each sample for 1 min.

In this way, *in vivo* cytokinin oxidase/dehydrogenase (CKX) activity was monitored indirectly by the CKX-mediated degradation of ^{3}H-isopentenyladenine to 3-methyl-2-butenal and ^{3}H-adenine, because the radioactive labelled adenine is taken up by the plant cell. Thus, overall radioactivity is subsequently reduced in the culture medium resulting from CKX activity metabolising ^{3}H-iP (Schwartzenberg *et al.*, 2003).

2.7. Qualitative determination of tritiated isopentenyladenine (^{3}H-iP) by RP-HPLC-online-LSC

For the qualitative analysis of determined total radioactivity (2.6), aliquots of the culture medium samples were analysed directly by reverse phase HPLC equipped with a diode array detector DAD 540+ (Bio-TEK, Kontron, Neufahrn, G) in combination with online liquid scintillation counting. Separation was carried out on a LiChrospher 60, RP-Select B, 5 µm column (Merck, Darmstadt, G) at a flow rate of 0.8 mL/min and approx. 70 bar at room temperature in a gradient of methanol and triethylamine (TEA) as described below. Optical density of the HPLC effluent was monitored at

269 nm; radioactive signals were detected by a scintillation counter (LSC Radiomatic 500 TR Series, Canberra-Packard, Schwadorf, A; Ultima-Flo M scintillation cocktail, PerkinElmer, Rodgau-Jügesheim, G). A gradient of solvent A (10 mM TEA, 10 % methanol (v/v)) and solvent B (100% methanol) was applied as followed:

time [min]	solvent A [%]
0	100
5	80
10	79
12	64
31	60
33	53
34	0
35	0
36	100
40	100

Data were acquired and analysed using the Kroma2000 Software, version 1.83 (Bio-TEK. Neufahrn, G).

2.8. Extraction of phenolic compounds from *Physcomitrella* tissue and culture medium

For the extraction of phenolic compounds, approx. 2 - 4 g protonema tissue from 5 day old standard liquid cultures was harvested (2.2.5) and disrupted in liquid nitrogen with mortar and pestle. Extraction was accomplished by the addition of ice cold 60 % acetone solution (v/v), stirring for 15 min, incubation for 1 - 2 min in an ultrasonic bath (Sonorex Super RK 510H, Bandelin, Berlin, G), and centrifugation for 10 min at 5,000 rpm (Labofuge GL, Kendro, Hanau, G). This extraction procedure was repeated three times, and the supernatants from the three extractions were pooled. The resulting extract was subsequently acidified by the addition of acetic acid in order to stabilise phenols. Acetone was removed with a rotating evaporator (LaboRota SE 320, Resona Technics, Gossau, CH) at 40 °C and 30 mbar and extracted compounds were transferred to the organic phase by a triple extraction of the solution with ethyl acetate in a separating funnel. Sodiumsulphate was added to bind residual H_2O from the pooled extracts, and afterwards removed by filtration through a fluted filter. The samples were dried in the rotating evaporator, subsequently dissolved in 1/60 (of the original acetone extraction) volume of methanol and incubated in an ultrasonic bath to improve resuspension of dried compounds.

For the extraction of phenolic compounds from *Physcomitrella* culture medium, 100 mL culture medium (2.2.1) was freeze-dried by lyophilisation at -20 °C (Alpha I-6 Christ, Osterode, G; pump Duo 5M, Pfeiffer, Asslar, G). Subsequently, lyophilised powder was resuspended in 3 mL 60 % methanol.

2.9. Reverse phase HPLC and LC-MS HPLC for separation of acetone extracts

Extracted compounds (2.8) were separated by RP-HPLC (HPLC Pump 64, degasser and HPLC Programmer 50, Knauer, Berlin, G; auto sampler AS-4000, Merck, Darmstadt, G) and detected by DAD analysis at 280 nm with the PDA detector 996 (Waters, Eschborn, G). Separation was performed on a LiChroCART 250-4 [Lichrospher 100 RP-18 (5 µm)] column (Merck, Darmstadt, G) at a flow rate of 1.2 ml/min and approx. 130 bar at 26 °C in gradients A or B described below. Gradients of solvent A (acetic acid 2 % v/v) and solvent B (acetonitrile/H_2O/acetic acid (40/9/1 v/v/v) were applied as followed:

Gradient 1	time [min]	solvent B [%]	Gradient 2	time [min]	solvent B [%]
	0	10		0	25
	8	10		6	35
	38	23		15	35
	50	40		31	45
	70	90		35	90
	73	90		38	90
	78	10		43	25
	93	10		50	25

Data were acquired using the Millenium Software 3.2 (Waters. Eschborn, G).

For the separation of phenolic compound from *Physcomitrella* tissue, the extract was prepared as described above (2.8), and 20 - 100 µL were injected for HPLC analysis performed with either gradient 1 or gradient 2.

Multiple MS (MS^n) experiments were performed in cooperation with Dr. S. Franke of the Department of Chemistry (University of Hamburg) by electrospray ionisation-mass spectroscopy/mass spectroscopy (ESI-MS/MS) of preparative enriched single peaks on a MAT95XL-Trap instrument (Thermo Electron, Allschwil, CH) in negative ion mode with direct infusion as well as coupled to reverse-phase HPLC with DAD analysis (gradient 2). High-resolution accurate mass was determined five times at 10 000 resolution using the reference mass PEGMME sulphate 550 (375.13304 and 419.15926) as a calibration standard.

2.10. Flow cytometric measurement

For the determination of the ploidy level of generated transformants, protonema was harvested from liquid cultures and resuspended in 2 mL of DAPI stain solution (CyStain UV Ploidy, Partec, Münster, G), chopped with a razor blade in a Petri dish and filtered through a sieve of 30 µm pore size. UV fluorescence intensity was measured using a ploidy analyser PA (Partec, Münster, G) equipped with a mercury arc lamp for detection (settings: gain 450, speed 1.5 µL/sec). From the resulting histogram the ploidy level was derived: with these settings histograms of haploid plants exhibited a prominent peak at about 50, whereas histograms of diploids plants exhibit a signal at about 100.

2.11. Brightfield and fluorescence microscopy

Microscopic analysis was carried out with the BH-2 microscope (Olympus, Hamburg, G). For fluorescence microscopy blue light excitation (filter combination BBY455) from a mercury lamp was applied. Images were acquired with the imaging software analySIS (Software Imaging Systems, Münster, G).

2.12. Sequence analysis

2.12.1. Sequence search and comparison using basic local alignment tool (BLAST)

For *Physcomitrella* sequences, BLAST analysis was performed with the applications on the cosmoss server (http://www.cosmoss.org/) searching in the *Physcomitrella* genome V1.2 (Rensing *et al.*, 2008) and EST databases. Sequence searches in other plant genomes were carried out in the GenBank databases of the NCBI (http://www.ncbi.nlm.nih.gov/blast/Blast.cgi) for *Arabidopsis thaliana*, *Lycopersicon esculentum*, *Triticum aestivum* and *Vitis vinifera*. Sequences in the genome of *Oryza sativa* were identified from the TIGR rice browser (http://www.tigr.org/tigr-scripts/osa1_web/gbrowse/rice/). Sequences in the genome of *Selaginella moellendorffii*, *Populus trichocarpa, Chlamydomonas reinhardtii* and *Ostreococcus tauri* were searched by BLAST analysis on the JGI web server (http://genome.jgi-psf.org/cgi-bin/runAlignment?db=Selmo1&advanced=1, http://genome.jgi-psf.org/cgi-bin/runAlignment?db=Poptr1_1&advanced=1, http://genome.jgi-psf.org/cgi-bin/runAlignment?db=Chlre3&advanced=1, and http://genome.jgi-psf.org/cgi-bin/runAlignment?db=Ostta4&advanced=1).

Comparison of nucleotide sequences was carried out on the NCBI server (http://www.ncbi.nlm.nih.gov/blast/bl2seq/wblast2.cgi). Global pairwise alignments of two amino

acid sequences were performed with EMBOSS::needle pairwise alignment algorithm (http://www.ebi.ac.uk/emboss/align/index.html?).

2.12.2. Gene model prediction

The cosmoss genome browser (http://www.cosmoss.org/cgi/gbrowse/physcome/) was used for gene structure predictions of *Physcomitrella* genes obtained from BLAST analysis against the *Physcomitrella* genome V1.2 (Rensing *et al.*, 2008). Gene models were evaluated manually according to EST evidences, presence of the tyrosinase domain PF00264 and homology to other already published PPO amino acid sequences.

2.12.3. Prediction of protein properties

Molecular weights and isoelectric points of proteins were calculated with an application on the scansite server (http://scansite.mit.edu/calc_mw_pi.html). Conserved domain search was carried on the NCBI web server (http://www.ncbi.nlm.nih.gov/Structure/cdd/wrpsb.cgi). *In silico* predictions for subcellular localisation of proteins were performed with the prediction tools MultiLoc (http://www-bs.informatik.uni-tuebingen.de/Services/MultiLoc/) (Hoeglund *et al.*, 2006) and with the online application TargetP (http://www.cbs.dtu.dk/services/TargetP/) (Emanuelsson *et al.*, 2007).

2.12.4. Sequence alignments and phylogenetic tree construction

Multiple sequence alignments of amino acid sequences were generated using MAFFT L-INS-I v5.860 (Katoh *et al.*, 2005) and manually curated based on column conservation using Jalview 2.4 (Clamp *et al.*, 2004). Phylogenetic analyses were carried out in cooperation with Dr. S. Rensing from the Faculty of Biology (University of Freiburg). Phylogenetic trees were inferred using different methods. Neighbour-joining (NJ) trees were calculated using Quicktree v1.1 (Howe *et al.*, 2002) with 1000 times of bootstrap re-sampling. The most appropriate evolutionary model was selected using ProtTest v1.3 (Abascal *et al.*, 2005) and turned out to be WAG (Whelan and Goldman, 2001) with gamma-distributed rate categories. Bayesian inference (BI) was performed with the predetermined model using MrBayes 3.1.2 (Ronquist and Huelsenbeck, 2003) with eight gamma-distributed rate categories until convergence (548,000 generations, average standard deviation < 0.01). Trees were visualised using FigTree 1.1.2 (http://tree.bio.ed.ac.uk/software/figtree/). For NJ trees, nodes possessing bootstrap values between 100 and 95 were considered to be significant; support values at the nodes of BI trees are BI posterior probabilities and significant between 1 and 0.95.

3. RESULTS

The *PPO* gene family of *Physcomitrella* was identified and characterised *in silico*, and its gene and protein properties as well as the phylogeny of the gene family was analysed. Expression of the gene family members was determined by real-time RT-PCR from tissue cultivated under standard conditions, under strong light irradiation and in the presence of a putative PPO substrate. Additionally, *Physcomitrella PPO1* knockout plants were generated and analysed molecularly and phenotypically under different conditions as well as with respect to developmental processes in differentiation.

3.1. Cloning and characterisation of the *PpPPO1* gene

Within this study the sequence of the polyphenol oxidase encoding gene *PpPPO1* of *Physcomitrella*, of which part of the gene had been previously identified (diploma thesis, Richter, 2003), was extended and completed. Using the publicly accessible EST databases (http://www.cosmoss.org/bm/BLAST?type=0), non overlapping ESTs with homology to known plant PPOs were selected. Based on these BLAST results, the PPO encoding gene *PpPPO1* was reconstructed *in silico*: The longest *PpPPO1* mRNA sequence was found to be 2402 bp long consisting of an ORF of 1611 bp encoding for a 536 aa protein, 289 bp of 5´UTR and 502 bp of 3´UTR (Fig. 3.1). Based on the *in silico* reconstruction, the primers *cPPO1_forw* and *cPPO1_rev* were designed (2.3.3) and the complete coding sequence of *PpPPO1* was amplified from a protonema cDNA library (provided by Reski *et al.*, 1995) with a proof reading polymerase (2.3.4.1). The amplified sequence was cut with *SalI* and *NcoI* and cloned *in frame* with a C-terminal His-tag encoding region into the *SalI/NcoI* cut plasmid pET28a (2.3.8 and 2.3.9). Sequence confirmation was obtained by sequencing both strands (using the primers *T7prom, PPO1_3, PPO1_4, PPO1_5, PPO1_6, PPO1_7* and *cPPO1_rev*), and the mRNA sequence including the 5´ and 3´UTRs was entered into the GenBank database under accession number AY904721 (Richter *et al.*, 2005).

The *PpPPO1* gene is predicted to encode a 536 aa protein with a calculated molecular mass of 60.1 kDa. Comparison of the derived amino acid sequence, PPO1, with known seed plant PPOs (*o*-diphenol oxidases) revealed the presence of two highly conserved copper-binding domains in PPO1, each with a set of three histidines (Pfam domain Tyr PF00264), which is an important characteristic for a catechol-oxidase type PPO.

Through *in silico* analysis of the N-terminus using the MultiLoc and the TargetP algorithm (2.12.3), important differences of the bryophyte sequence to the seed plant PPOs, usually targeted to the chloroplast were found: PPO1 possesses a short signal sequence of 23 aa, which is predicted to lead the protein into the secretory pathway. Consequently, the mature form of PPO1 would consist of 513 amino acids with a calculated molecular mass of 57.6 kDa.

Cloning and sequencing of a DNA fragment amplified from genomic DNA using the primers *PPO1_3* and *PPO1_7* (2.3.3) and comparison to the corresponding cDNA sequence revealed *PpPPO1* having a 94 bp intron located after nucleotide 1344 of the annotated cDNA sequence as indicated in Fig. 3.1.

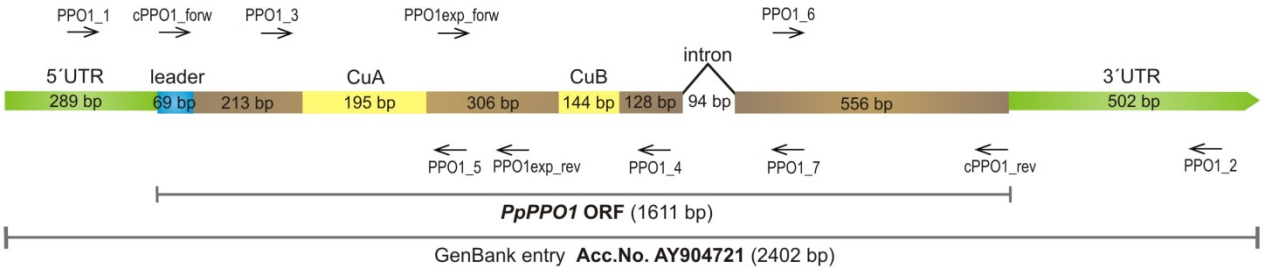

Fig. 3.1 Scheme of *PpPPO1* gene structure. The 5´ and 3´UTRs are marked in green, regions encoding for the copper-binding domains CuA and CuB are coloured yellow and the leader sequence encoding for the predicted N-terminal 23 aa signal sequence is marked in blue. The positions of the primers (2.3.3) used for cloning and sequencing are indicated by arrows.

3.2. *In vitro* PPO activity in culture medium of *Physcomitrella*

Intracellular *in vitro* PPO activity of protein extracts obtained from *Physcomitrella* tissue was previously determined (Richter *et al.*, 2005). As described in 3.1, *in silico* analysis of the deduced amino acid sequence revealed that *PpPPO1* possesses a signal sequence at the N-terminus predicted to target PPO1 to the secretory pathway. Therefore, extracellular PPO activity was determined in protein extracts prepared from culture medium and compared to PPO activity in intracellular protein extracts. *Physcomitrella* tissue was grown for 20 days in liquid culture under standard conditions (2.2.1), and protein extracts were prepared from tissue as well as from culture medium (2.4.1 and 2.4.2). PPO activity was determined polarographically using 4-methyl catechol as a substrate (2.4.5).

Specific PPO activity in protein extracts from culture medium (1574.76 ± 123.6 nmol O_2/h*mg protein) was approximately 15-fold higher than activity in tissue extracts (95.58 ± 30 nmol O_2/h*mg protein), suggesting that a portion of overall PPO was secreted (Fig. 3.2A). However, it should be noted that a major proportion of the total PPO activity was intracellular, if relating activities to culture volume as a reference parameter (Fig. 3.2B).

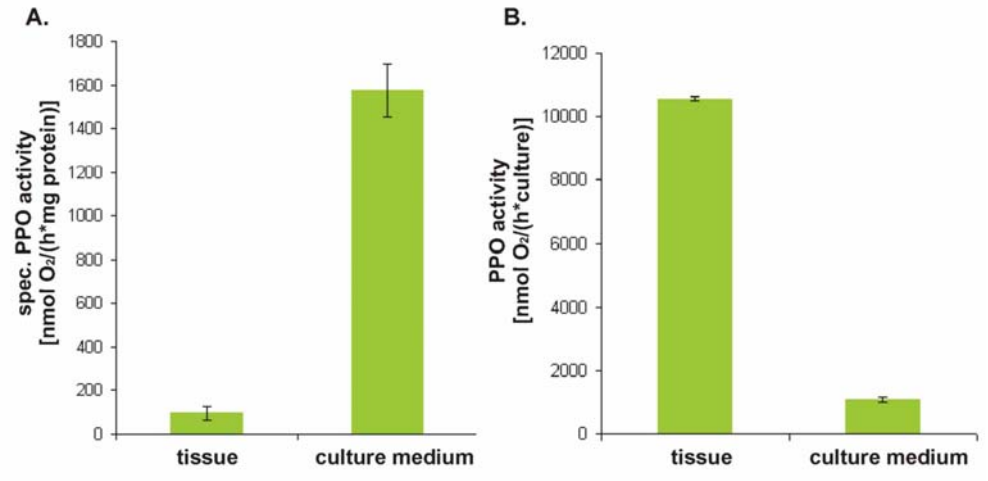

Fig. 3.2 Specific *in vitro* PPO activity in protein extracts of *Physcomitrella* tissue and culture medium. Extracts were prepared from 20 day old liquid cultures grown under standard conditions (2.2.1). (A.) specific PPO activity (B.) PPO activity per 2 L-culture. Activity was determined polarographically using 4-methyl catechol as a substrate (2.4.5). (n=4)

3.3. Identification and characterisation of the *PPO* multigene family from *Physcomitrella*

As genomic data from the *Physcomitrella* genome sequencing project became available (Rensing *et al.*, 2008), it was possible to search for further *PPO* genes in the genome. BLAST analysis using *PpPPO1* as a query revealed that *Physcomitrella* possesses a *PPO* multigene family.

3.3.1. Identification, manual adaptation and sequence comparison of *PPO* genes on DNA level

In order to obtain a more profound understanding of the organisation of PPOs in the bryophyte, further *PPO* gene family members were identified and characterised.

Using the derived amino acid sequence of *PpPPO1* (3.1) as a query for BLASTp in the *P.patens V1.2_protein* database and for tBLASTn in the *P.patens V1.2_genome* database (2.12.1), 15 loci were identified possessing similarities to PPO1 (cut-off 35% identity over a length of 80 aa) (Fig. 3.3).

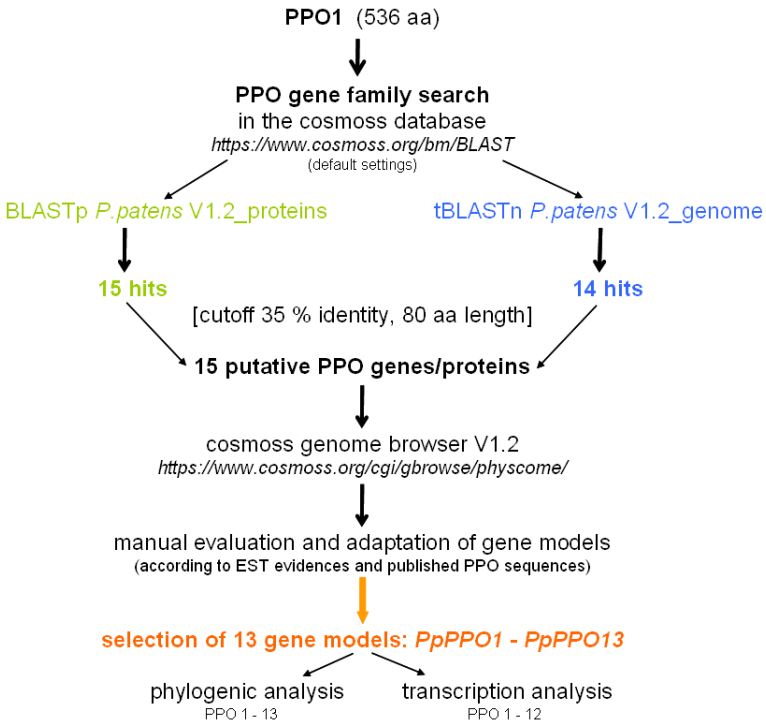

Fig. 3.3 Flow chart of bioinformatic identification of the *PPO* gene family members of *Physcomitrella*. Using the amino acid sequence of *PpPPO1*, BLAST analysis was carried out (2.12.1) and 15 putative PPOs were identified. After manual evaluation and correction of the gene models according to transcript evidence and the presence of the complete tyrosinase domain PF00264 (2.12.2 and 2.12.3), 13 PPOs were selected for further studies.

These 15 loci were selected and named *PpPPO1* to *PpPPO15* in descending order according to their hit appearance in the BLAST results with PPO1 as a query. Their predicted gene models (*Phypa* numbers according to version V1.2) with their intron/exon structure were evaluated in detail according to transcript evidences, the presence of the two copper-binding domains CuA and CuB (tyrosinase domain Pfam Tyr PF00264), and homology to PpPPO1 as well as published plant PPO sequences (2.12.2). If necessary, other gene models, available on cosmoss.org, were selected and proposed (Tab. 3.1).

For the putative polyphenol oxidase encoding genes *PPO6, PPO13, PPO14,* and *PPO15* no ESTs were available to support the predicted gene models (Tab. 3.1). All other *PPO* gene models were sustained by EST evidences, although only the gene models of *PPO1, PPO9,* and *PPO11* were covered completely by ESTs. For the gene models of *PPO2, PPO3, PPO4, PPO5, PPO7, PPO8, PPO10,* and *PPO12*, ESTs were present covering parts of the predicted gene structure.

According to BLAST homology analysis, for *PPO12* and *PPO13*, no appropriate gene model was proposed by the cosmoss.org genome browser. For this reason, the *Phypa* models predicted by

version V1.2 were prolonged manually at the 5′ end in the case of *PPO12*, and at the 3′ end in the case of *PPO13*.

After manual evaluation and verification, the *Phypa* gene models proposed by version V1.2 were confirmed for *PPO1, -2, -3, -7, -8, -14,* and *-15*, whereas for *PPO4, -5, -6, -9, -10, -11, -12*, and *-13* other than the server-proposed gene models (*all_Phypa* numbers, available on cosmoss.org) were selected, based on EST evidences supporting the intron/exon structure and homology analysis with other plant PPOs. In Tab. 3.1 the gene models with their introns before and after manual correction are summarised, along with the total number of corresponding ESTs and properties of the derived amino acid sequences. Further detailed information on evaluation of *PPO* gene models according to the analysis described in 2.12.2 can be found in the appendix (6.2.1).

Analysis of the organisation of the gene family within the genome revealed, that *PPO6* and *PPO12* are located *tail to tail* in relative proximity on the same scaffold No. 83 separated by approximately 15 kbp.

PPO7 and *PPO10* are also located on the same scaffold No. 3 *head to head*, but approx. 1.89 Mbp apart from each other. Due to the preparative procedure of the genomic DNA prior to sequencing and assembly of the sequenced DNA in scaffolds, genes located on the same scaffold are localised on the same chromosome. Hence, *PPO6* and *PPO12* as well as *PPO7* and *PPO10* are located on the same corresponding chromosomes.

Tab. 3.1 Adaptation and properties of *PPO* gene family members selected by BLAST analysis on cosmoss.org using *PpPPO1* as a query. For *PPO1, -2, -3, -7, -8, -14* and *-15* gene models of the *Physcomitrella* genome version V1.2 (available on the cosmoss genome browser, 2.12.2) were considered to be correct (*Phypa* model). For *PPO4, -5, -6, -9, -10, -11, -12* and *-13* a better fitting model according to homology analysis was selected (*all_Phypa* model). ([a]): gene models available on http://www.cosmoss.org/cgi/gbrowse/physcome/; ([b]): determined on http://scansite.mit.edu/calc_mw_pi.html; ([c]) conserved domain search (http://www.ncbi.nlm.nih.gov/Structure/cdd/wrpsb.cgi); ([d]): simple prediction determined with MultiLoc, (http://www-bs.informatik.uni-tuebingen.de/Services/MultiLoc/); ([e]): prediction performed with TargetP (http://www.cbs.dtu.dk/services/TargetP/) as described in 2.12.3.

	BLAST V1.2 results[a]			Selected gene models[a]				Properties of the deduced amino acid sequences					
	gene model (V1.2)	intron [bp]	EST [no]	gene model after evaluation	scaff_no: from..to	intron [bp]	Pos. of intron(s)	ORF [aa]	MW[b] [kDa]	pI[b]	Pfam Tyr[c] PF00264	MultiLoc prediction[d] [likelihood]	TargetP prediction[e] [cleavage site]
PPO1	**Phypa_215905**	94	15	**Phypa_215905**	121: 167271..169785	94	after CuB	536	60.15	9.38	yes	Golgi [0.51]	secretory pathway [23]
PPO2	**Phypa_173565**	128	1	**Phypa_173565**	491: 123370..124362	128	after CuB	537	60.71	9.18	yes	Golgi [0.97]	secretory pathway [23]
PPO3	**Phypa_140409**	138	6	**Phypa_140409**	167: 513054..514871	138	after CuB	559	62.71	7.26	yes	extracellular [0.54]	secretory pathway [22]
PPO4	Phypa_2725	0	2	**all_Phypa_116543**	16: 1780468..1782075	0	no intron	535	60.78	5.50	yes	plasma membr. [0.68]	secretory pathway [29]
PPO5	Phypa_102269	88	2	**all_Phypa_156596**	559: 43493..45206	88	after CuB	541	61.28	5.31	yes	plasma membr. [0.97]	mitochondrial [11]
PPO6	Phypa_2707	93	0	**all_Phypa_130554**	83: 1328380..1330047	93	after CuB	524	59.61	5.31	yes	plasma membr. [0.93]	- [-]
PPO7	**Phypa_158623**	143 54	5	**Phypa_158623**	3: 1801505..1803375	143 54	after CuB	557	62.89	5.94	yes	plasma membr. [0.94]	secretory pathway [24]
PPO8	**Phypa_130903**	0	12	**Phypa_130903**	85: 1247599..1249239	0	no intron	546	61.94	5.74	yes	plasma membr. [0.92]	secretory pathway [28]
PPO9	Phypa_155214	45	25	**all_Phypa_173397**	455: 71482..73437	0	no intron	549	62.12	6.23	yes	vacuolar [0.27]	secretory pathway [26]
PPO10	Phypa_111922	0	2	**all_Phypa_174105**	3: 3692578..3694295	0	no intron	541	61.23	6.79	yes	ER [0.34]	secretory pathway [20]
PPO11	Phypa_186186	139	59	**all_Phypa_131684**	90: 966474..968220	139	after CuB	535	60.81	8.62	yes	plasma membr. [0.92]	secretory pathway [19]
PPO12	Phypa_212826	233	5	**138 nt (5´-end) + Phypa_212826**	83: 1344874..1347619	233	after CuB	535	60.50	8.21	yes	plasma membr. [0.9]	secretory pathway [19]
PPO13	Phypa_122830	845	0	**Phypa_122830 + 576 nt (3´-end)**	41: 343237..345686	845	within CuA	535	60.61	7.28	yes	cytoplasmic [0.33]	- [-]
PPO14	**Phypa_169836**	329	0	**Phypa_169836**	222: 7055..8088	329	in front of CuB	234	26.34	6.75	no	n.a.	n.a
PPO15	**Phypa_86565**	61	0	**Phypa_86565**	147: 625749..626220	61	in front of CuB	136	15.87	4.76	no	n.a	n.a

In Fig. 3.4 the intron/exon structure of the evaluated gene models defined in Tab. 3.1 is schematically shown. On genomic level, the four *PPO* genes, *PPO4, -8, -9,* and *-10*, were found to have no introns. By contrast, *PPO1, -2, -3, -5, -6, -7, -11,* and *-12* possess a small intron that varies in size from 88 to 233 bp. These introns are located at the same corresponding position downstream of the CuB encoding region. For the gene model of *PPO7*, a second intron (54 bp) was predicted to be located 84 bp downstream of the first intron. The predicted intron in the selected gene model of *PPO13* was found to be very large (845 bp) and located within the CuA encoding region, unlike those of the gene models of *PPO1* to *PPO12*.

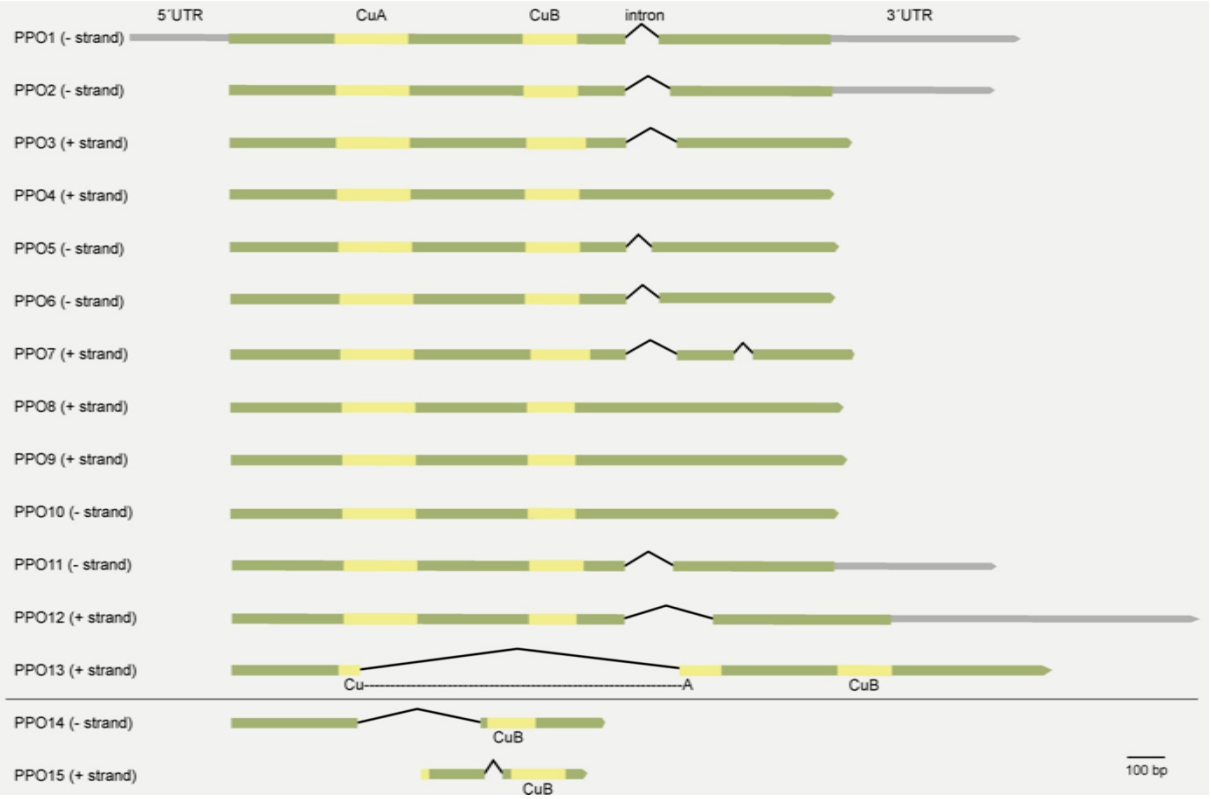

Fig. 3.4 Scheme of *PPO* gene models after manual adaptation according to Tab. 3.1. Coding sequences are displayed in green and yellow, UTRs in grey, position and length of introns are marked by black spikes. The sequence regions encoding for the copper-binding domains CuA and CuB are indicated in yellow. *PPO14* and *PPO15*, were considered to be incomplete genes, because the Pfam domain Tyr PF00264 was not present in the gene models.

As shown in Tab. 3.1 and Fig. 3.4, the Pfam domain Tyr PF00264, consisting of the two copper-binding domains CuA and CuB, was found in the ORFs of the selected gene models of *PPO1* to *PPO13*, but could not be detected for *PPO14* and *PPO15*. Both latter sequences encode only a short ORF (234 and 136 aa, respectively) and contain only one copper-binding domain encoding region (CuB). *PPO15* also possesses a small fragment homologous to a part of the copper-binding domain CuA. Other gene models for *PPO14* and *PPO15* with prolonged ORFs were not

available due to start and stop codons upstream and downstream of the existing models. Moreover, LTR retrotransposons were found ca. 340 bp downstream of the *PPO14* gene model and ca. 2100 bp upstream and ca. 1800 bp downstream of the predicted gene model for *PPO15*. These results suggested that *PPO14* and *PPO15* are incomplete, probably due to an insertion of transposable elements. Therefore, they were excluded from the putative *PPO* gene family.

Based on these observations, it was concluded that *Physcomitrella* possesses thirteen putative polyphenol oxidase encoding genes, *PpPPO1* to *PpPPO13*. Further studies including detailed amino acid sequence comparison as well as phylogenetic analyses were conducted on these genes (3.3.2 and 3.3.3). Transcription levels of *PPO1* to *PPO12* were analysed under standard cultivation conditions as well as under influence of certain stress conditions (3.5).

3.3.2. Sequence comparison of PpPPO1 to PpPPO13 on amino acid level

Properties of the derived amino acid sequences of *PPO1* to *PPO13* were analysed according to the *in silico* methods described in 2.12.3 and are summarised in Tab. 3.1.

The ORFs of the thirteen *PPO* genes encode for proteins with a length ranging from 524 (PPO6) to 559 (PPO3) amino acids with a calculated molecular weight of 59.61 to 62.89 kDa. The predicted isoelectric points (pI) of the derived amino acid sequences range from 9.38 to 5.31, and can be grouped as follows:
PPO1/PPO2 > PPO11/PPO12 > PPO13 > PPO3 > PPO7/PPO8/PPO9/PPO10 > PPO4/PPO5/PPO6.

Sequence comparison of PPO1 to PPO13 on amino acid level was performed using the MAFFT algorithm (2.12.4). Percentage identity of pairwise alignment of the overall amino acid sequences was determined using the EMBOSS::needle algorithm (2.12.1) and ranged from 28.9 % (PPO8 with PPO13) to 74.7 % (PPO1 with PPO2). Based on the MAFFT alignment, an average distance tree using the calculated BLOSUM62 scores was generated in Jalview 2.4 (2.12.4) as shown in Fig. 3.5.

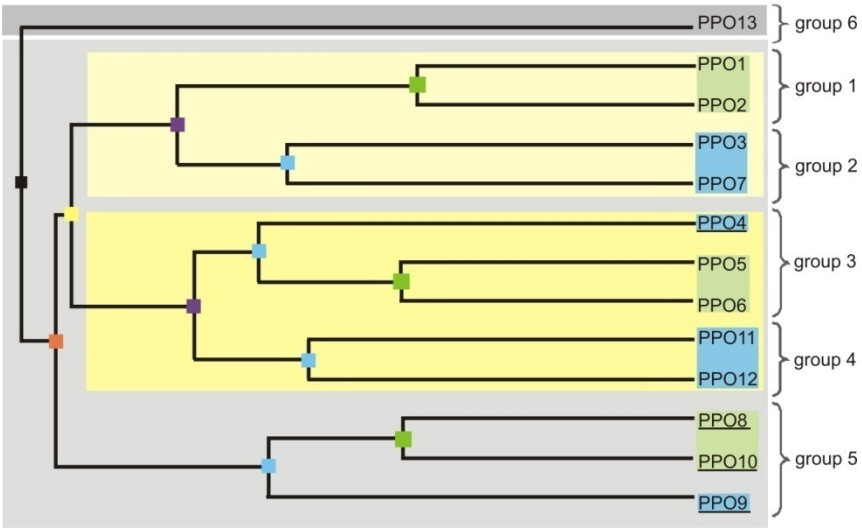

Fig. 3.5 Average distance tree (based on BLOSUM62 score calculated with the MAFFT algorithm) of PPO1 to PPO13. Parts of the alignment are given in Fig. 3.6. PPOs without introns are underlined. Groups formed by the fifth separation at the blue nodes are coloured in blue, groups formed by the sixth separation at the green nodes are marked in green.

The identified PPO family members were found to cluster in six groups. PPO13 is separated and stands apart from the other twelve PPOs. The other five groups consist of group 1 [PPO1/PPO2] and group 2 [PPO3/PPO7], together assembling to an upper-level grouping, group 3 [PPO4/PPO5/PPO6] and group 4 [PPO11/PPO12], both being part of a second upper-level grouping, and group 5 [PPO8/PPO9/PPO10]. PPOs within one group share similar protein properties such as similar isoelectric points and target predictions (Tab. 3.1).

In Fig. 3.6 parts of the MAFFT alignment that was used to establish the tree depicted in Fig. 3.5 are shown.

The alignment revealed that the copper-binding domain CuA consists of exactly 65 aa in all *Physcomitrella* PPOs and is highly conserved within the PPO family (Fig. 3.6B). Percentage identity of the copper-binding domain CuA within one group was high and ranged from 81 % to 90 % (PPO1 with PPO2). Compared across groups, lower identities were found (e.g., 49 % identity of CuA of PPO10 with CuA of PPO13).

The length of the copper-binding domain CuB was found to be less conserved than CuA and ranged from 41 aa to 59 aa (Fig. 3.6C). Although conservation of CuB within one group was very high and ranged from 72.9 % identity (PPO3 with PPO7) to 95.8 % identity (PPO1 with PPO2), lower identities were determined, when comparing across groups (32.2 % identity of PPO7 CuB with PPO9 CuB).

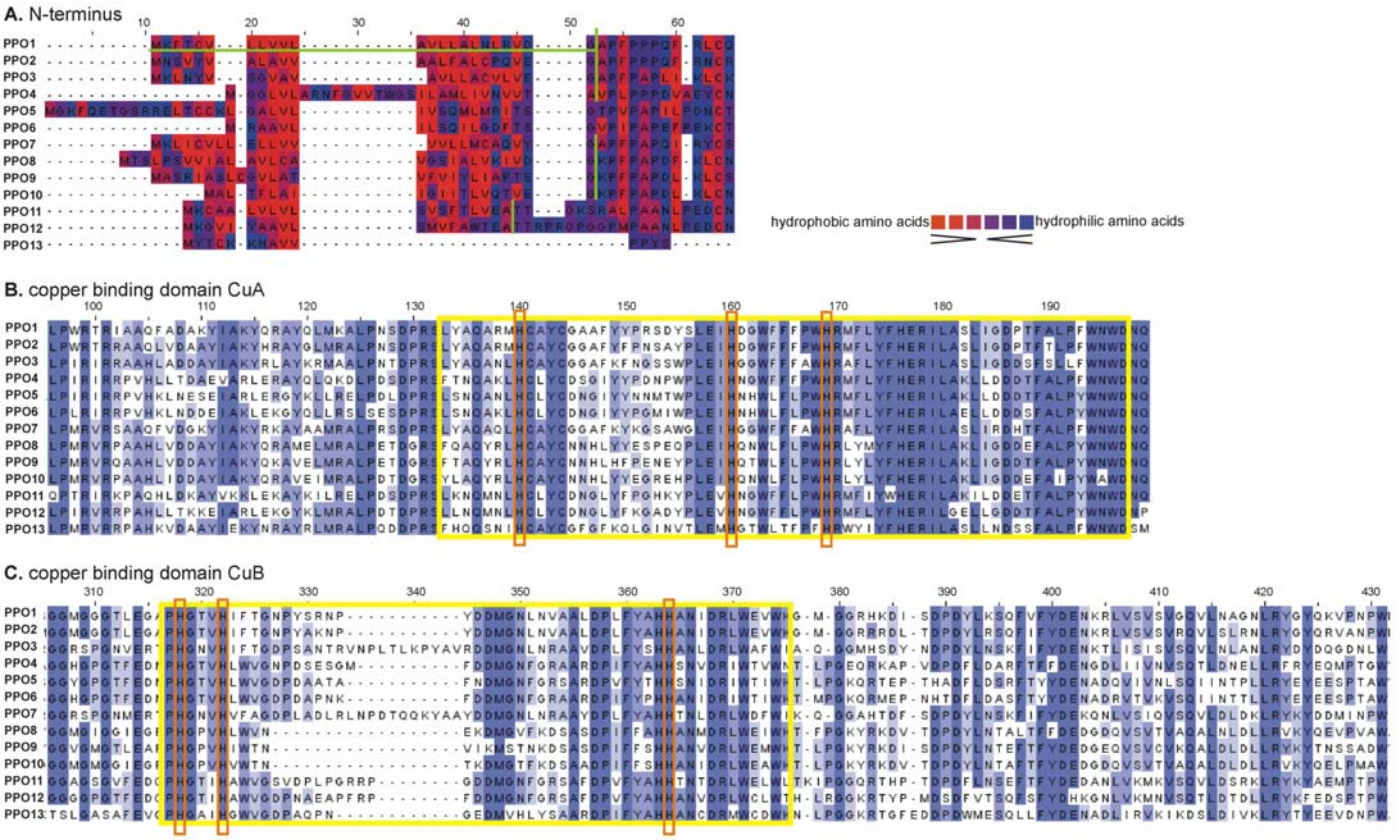

Fig. 3.6 Multiple sequence alignment of PPO1 to PPO13 of the N-terminus (A.) and the region of the copper-binding domain CuA (B.) and CuB (C.). The alignment was calculated using the MAFFT algorithm and graphically displayed in Jalview 2.4 (2.12.4); sequences were not edited. The predicted signal sequence of PPO1 is underlined. The start of the putative mature form of PPOs, possessing a signal sequence as predicted by TargetP, is indicated by a vertical green line (for PPO5, PPO6 and PPO13 no signal peptides were predicted). In A. the alignment is coloured according to hydrophobicity: hydrophobic amino acids are coloured in red, intermediates in purple and hydrophilic amino acids are coloured in blue (Kyle and Doolittle, 1982). In B. and C. the colours indicate the BLOSOM62 score: high scores are designated by dark blue, lower scores in light blue. The regions of the copper-binding domains are framed in yellow; the three histidines within each copper-binding domain are framed in orange.

The subcellular localisations of the thirteen selected *PPO* gene products from *Physcomitrella* were predicted using the online applications TargetP and MultiLoc (2.12.3). As indicated in Tab. 3.1, in most cases both applications predicted similar targets. TargetP predicted that all PPOs except PPO5, -6 and -13 enter the secretory pathway. MultiLoc predicted nearly the same targets but specified the organelle that the protein was targeted to, such as Golgi, endoplasmatic reticulum (ER), extracellular, vacuolar or plasma membrane. PPO5 was predicted to be localised in the mitochondria by TargetP, although analysis using MultiLoc predicted the sequence to be targeted to the plasma membrane. No targets were predicted for PPO6 and PPO13 with TargetP, whereas MultiLoc analysis suggested that PPO6 is targeted to the plasma membrane, and that PPO13 is a cytoplasmic protein (likelihood 0.33).

TargetP was further used to determine the length of the putative N-terminal signal sequences, which were found to vary in length from 19 aa (PPO11) to 29 aa (PPO4) (Tab. 3.1).

In Fig. 3.6A the alignment of the N-terminal signal sequences of PPO1 to PPO13 is presented, and amino acids are coloured according to their hydrophobicity. All PPOs with a predicted signal peptide possess a hydrophobic region in their N-terminal sequence consisting of five amino acids with the consensus sequence G[A/L/V]LVL and eleven amino acids with the consensus sequence IV[S/V][F/I/L]ALV[A/E][A/I/Q]VE.

Pairwise alignments revealed that the N-terminal sequences were less conserved across groups (e.g., 13 % identity of PPO10 with PPO13), while percentage identities were higher within the same group (e.g., 57 % for PPO1 with PPO2).

3.3.3. Phylogeny and classification of *PpPPO1* to *PpPPO13*

To analyse the evolution of the *Physcomitrella PPO* family, and to compare the *PPO* multigene family with *PPO* families from other plant species, phylogenetic analyses were performed.

Initially, a metagenome analysis was carried out including the sequenced genomes of the green algae, *Chlamydomonas reinhardtii* and *Ostreococcus tauri*, the genome of the club moss, *Selaginella moellendorffii*, as well as the sequenced seed plant genomes of *Arabidopsis thaliana*, *Oryza sativa*, *Populus trichocarpa* and *Vitis vinifera* (2.12.1). Using PpPPO1 to PpPPO13 from *Physcomitrella* as a query to search for putative *o*-diphenol oxidases, twelve putative PPOs were identified in the genome of *S. moellendorffii* (SmPPO1 to SmPPO12), nine PPOs in the genome of *P. trichocarpa* (PtPPO1 to PtPPO9), two PPOs in the *O. sativa* genome (OsPPO1 and OsPPO2) and nine PPOs in the genome of *V. vinifera* (VvPPO1 to VvPPO9). No *o*-diphenol oxidases were found in the *Arabidopsis* genome; here 17 *p*-diphenol oxidases (laccases, AtLAC1 to AtLAC17, firstly described by McCaig *et al.*, 2005) are present.

In addition, the seven members of the PPO family of *Lycopersicon esculentum* characterised by Newman *et al.* (1993) and four PPOs from *Triticum aestivum* described by He *et al.* (2007) were included for sequence comparison along with four fungal tyrosinases (monophenol monooxygenases) from *Aspergillus fumigatus* (Q8J130), *Hypocrea jecorina* (CAL90884), *Aspergillus oryzae* (BAA07149.1) and *Agaricus bisporus* (O42713.1).

Finally, also tyrosinases (TYR) and laccases (LAC) were searched in the *Physcomitrella* genome *P. patens*_version V1.2 as described in Fig. 3.3. Searches with the mentioned fungal tyrosinases did not yield any positive results. By contrast, three putative laccases were identified in the *Physcomitrella* genome using an *Arabidopsis* laccase (Acc.No. NP_199621) as a query for the

BLAST search. These putative *Physcomitrella* laccases, designated here as PpLAC1, PpLAC2, and PpLAC3, were also included in the phylogenetic analyses.

Genome analysis of the sequenced genomes of *C. reinhardtii* and *O. tauri* revealed that green algae entirely lack the extended group of polyphenol oxidases, as no *o*-diphenol oxidases, laccases or tyrosinase could be found in these genomes using amino acid sequences of the above identified plant PPOs, a tyrosinase of *Aspergillus fumigatus* (Acc.No. Q8J130) or a laccase from *Arabidopsis* (Acc.No. NP_199621) as a BLAST query.

At first, phylogenetic analysis was performed with the extended group of polyphenol oxidases. For this purpose, all collected amino acid sequences including PPOs, laccases and tyrosinases were aligned using the MAFFT algorithm, and based on column conservation, the alignment was manually edited. The following computational analyses were carried out in cooperation with Dr. S. Rensing (University of Freiburg). A Bayesian tree was constructed using the program MrBayes 3.1.2, and the evolutionary model of WAG (Whelan and Goldman, 2001) (2.12.4) was used to build the Bayesian tree, which was displayed and re-rooted using the program FigTree 1.1.2 (Fig. 3.7).

Phylogenetic tree analysis for the extended group of the polyphenol oxidases revealed that the identified *Physcomitrella* PPOs were clustered together with the group of *o*-diphenol oxidases of vascular plants, and not with the tyrosinases (TYR) or the *p*-diphenol oxidases (LAC). Comparison of *Physcomitrella* PPOs with laccases from *Arabidopsis* as well as with the three identified putative laccases from *Physcomitrella* (2.12.1) yielded in 2- to 3-fold lower percentage identities compared to *o*-diphenol oxidases (e.g., 12 - 15 % identity with *Arabidopsis* laccases; 6 - 17 % identity with the putative laccases from *Physcomitrella*). Also further comparison of *Physcomitrella* PPOs with selected tyrosinases from fungi resulted in 2- to 3-fold lower identities (15 - 19 % identity with tyrosinases from *A. fumigatus* and *H. jecorina*). Moreover, conserved domain search (2.12.3) revealed that both the *Physcomitrella* PPOs and the collected kormophyte PPOs possess the tyrosinase Pfam domain Tyr PF00264, whereas putative *Physcomitrella* laccases and *Arabidopsis* laccases possess three domains of the Cu-oxidase superfamily (Cu-Ox3 PF07732; Cu-Ox PF00394 and Cu-Ox2 PF07731, respectively).

Hence, the phylogeny analysis of the extended group of polyphenol oxidases confirmed the classification of the identified *Physcomitrella* sequences PPO1 to PPO13 as *o*-diphenol oxidases, as previously suggested by their sequence properties and domain structures.

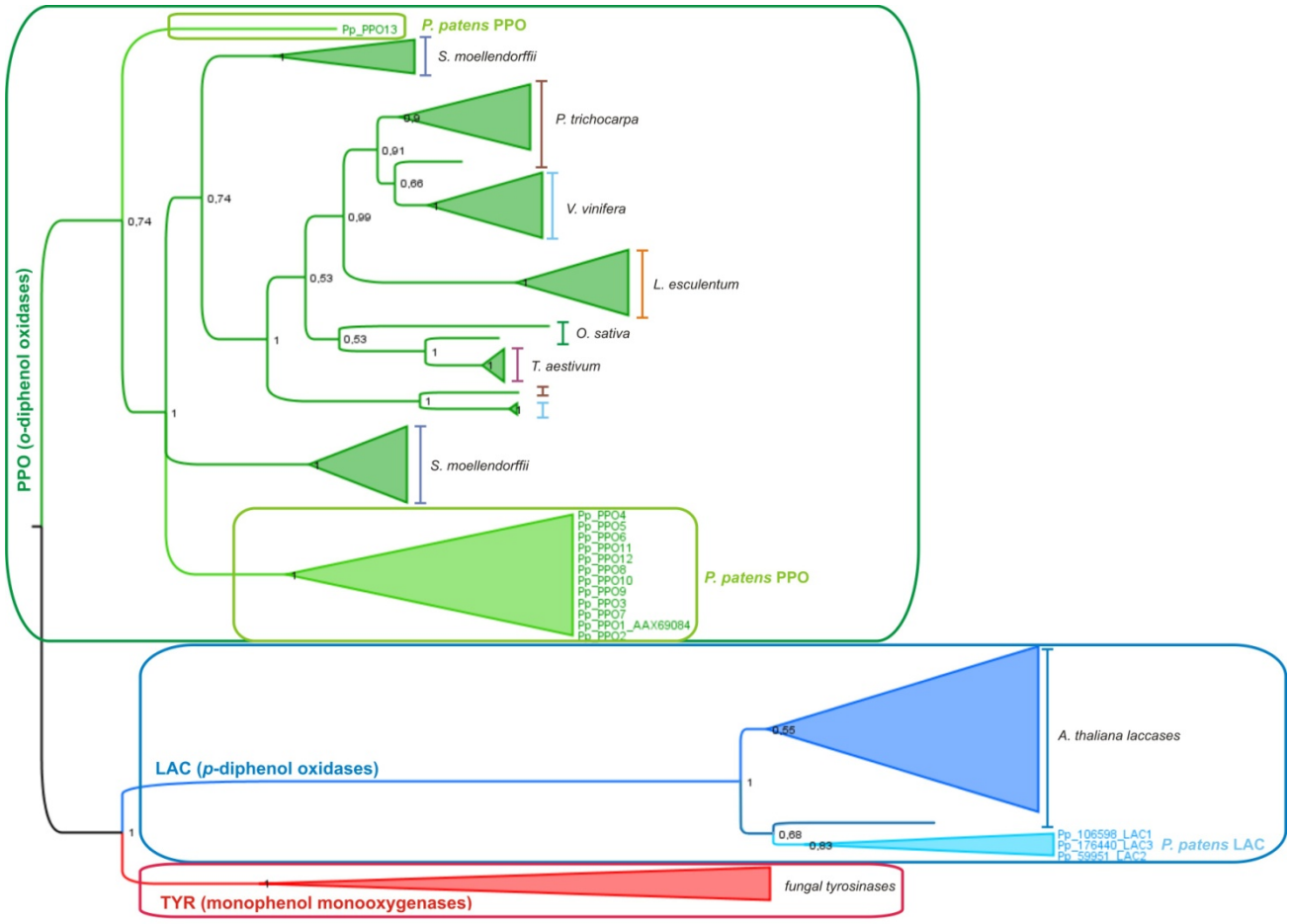

Fig. 3.7 Phylogenetic (Bayesian) tree of the extended group of polyphenol oxidases including *o*-diphenol oxidases (PPOs), laccases (LAC) and tyrosinases (TYR) Sequences were collected by metagenome analysis. The Bayesian tree was calculated according to the evolutionary model of WAG (Whelan and Goldman, 2001) using the program MrBayes 3.1.2 (in cooperation with Dr. S. Rensing), and the tree was displayed, re-rooted and processed in FigTree 1.1.2 (2.12.4). Only the main branches are displayed, the division of the sequences within each clade is schematically displayed by a triangle. The subgroup of *o*-diphenol oxidases is coloured in green, the laccases are coloured in blue and the tyrosinases are coloured in red. Nodes possessing posterior probabilities between 0.95 and 1 calculated by MrBayes are considered as significant.

Subsequently, a more detailed phylogenetic analysis of the subgroup of the *o*-diphenol oxidases (PPO) was carried out. For the construction of a phylogenetic tree, only the collected *o*-diphenol oxidases were aligned using the MAFFT algorithm and edited based on column conservation. According to the evolutionary model of WAG (Whelan and Goldman, 2001) a neighbour joining tree was calculated using QuickTree with 1000 bootstrap re-samplings, as well as a Bayesian tree using the program MrBayes (2.12.4). The phylogenetic trees were then displayed and re-rooted using the program FigTree 1.1.2. In Fig. 3.8 the neighbour joining tree is presented with bootstrap values displaying the significance of the nodes; the bayesian tree is not displayed. A comparison of the neighbour joining tree and the Bayesian tree revealed that the nodes supported by bootstrap values between 95 and 100 within the *Physcomitrella* clade of PPO1 to PPO12 were

fully supported by posterior probabilities between 0.95 and 1 derived from the Bayesian inference (marked by red asterisks in Fig. 3.8).

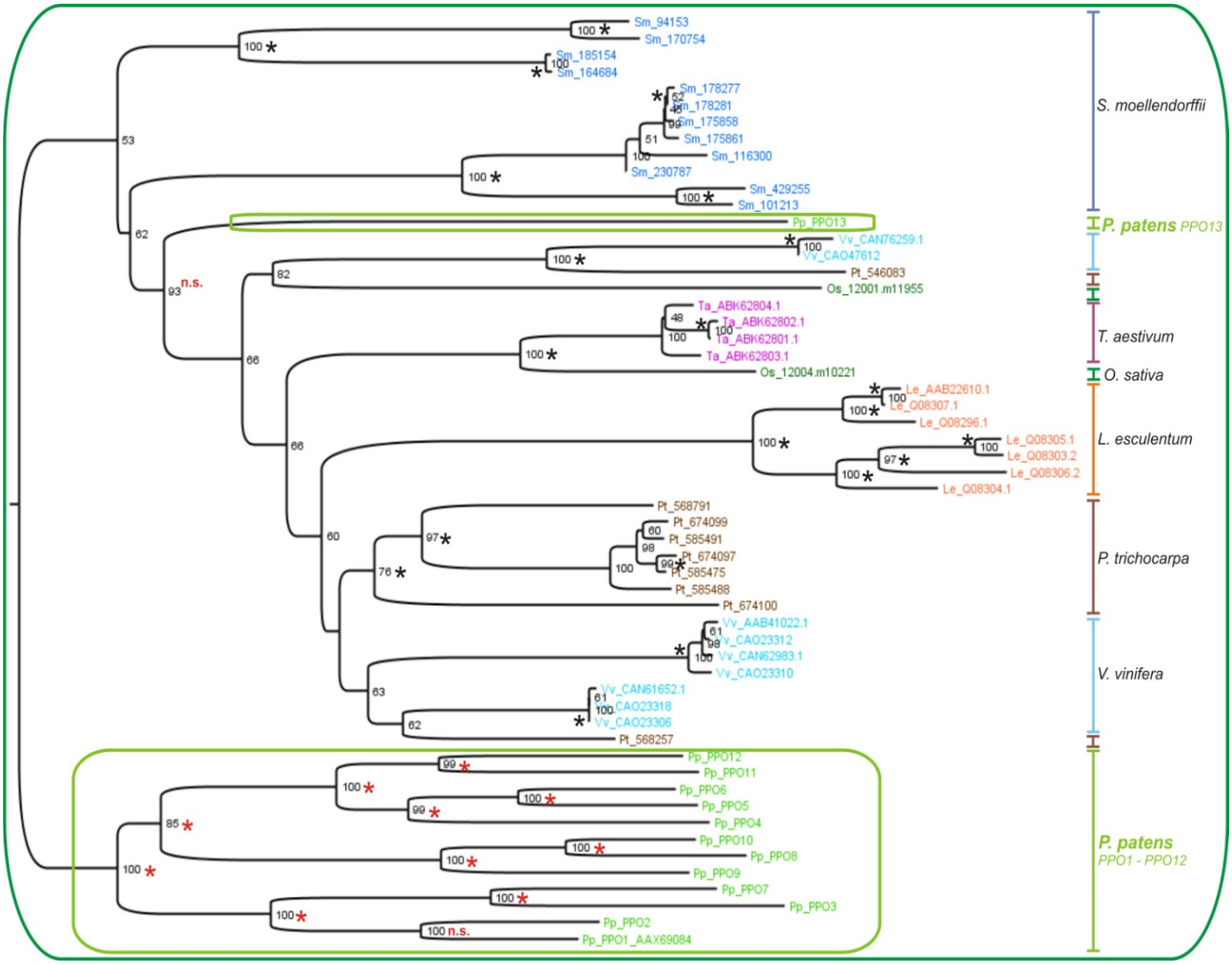

Fig. 3.8 Phylogenetic (neighbour joining) tree of PpPPO1 to PpPPO13 of *Physcomitrella* and PPOs of *Vitis vinifera* [Vv], *Triticum aestivum* [Ta], *Lycopersicon esculentum* [Le] (Acc.No.: http://www.ncbi.nlm.nih.gov/), *Oryza sativa* [Os] (TIGR proteins IDs: http://www.tigr.org/tigr-scripts/osa1_web/gbrowse/rice/), *Populus trichocarpa* [Pt] (JGI protein IDs: http://genome.jgi-psf.org/cgi-bin/browserLoad/484e9ff422e743aa3caedbb9), and *Selaginella moellendorffii* [Sm] (JGI protein IDs: http://genome.jgi-psf.org/cgi-bin/browserLoad/484e9fa80bfc94516e3f5666). The gene models of the characterised *Physcomitrella* PPOs are summarised in Tab. 3.1. Phylogeny was calculated as described in 2.12.4 with 1000 bootstrap re-samplings. Nodes with bootstrap values between 95 and 100 are considered as significant. Bootstrap values supported by posterior probabilities derived from Bayesian tree calculations (not shown) are marked by asterisks (red asterisks within the *Physcomitrella* clade). Bootstrap values within the *Physcomitrella* clade not supported by Bayesian posterior probabilities are marked by "n.s.".

Therefore, as graphically displayed in Fig. 3.8, phylogenetic examination of the *Physcomitrella* PPO family with bootstrap analysis (1000 re-samplings) confirmed results observed for the sequence comparison of PpPPO1 to PpPPO13 (Fig. 3.5). PpPPO1 to PpPPO12 are clustered in five groups with 2 - 3 PPOs per group as described above (3.3.2). This clustering was strongly supported by bootstrap values between 95 and 100. PpPPO13 was found to be isolated from the other twelve PPOs (bootstrap value 93). However, the bootstrap value displayed for the

separation of PPO13 within the neighbour joining tree was not supported by the second calculation method using Bayesian inference. Within the Bayesian tree PPO13 clustered with the putative PPOs from *S. moellendorffii* (posterior probability 0.98).

Moreover, pairwise alignments revealed overall identities within the *Physcomitrella* PPO family ranging from 30 % (PPO7 with PPO8) to 74.7 % (PPO1 with PPO2). The club moss *S. moellendorffii* possesses high identities up to 98 % within the group of its putative PPOs and up to 42 % identity to the analysed seed plant PPOs. Seed plant PPO family members possess higher identities to each other ranging from 34 % to 99 %. PpPPO1 was found to have the highest identity of all *Physcomitrella* PPOs to the analysed vascular plant PPOs ranging from 30 % - 36 % to putative PPOs of *S. moellendorffii* and 32 - 35 % to PPOs of *P. trichocarpa*.

As shown in Fig. 3.8, *Physcomitrella* PPO1 to PPO12 formed a monophyletic clade. In addition, the phylogenetic tree displayed the separation of the large *Physcomitrella PPO* gene family (with the exception of PPO13) from the vascular plant PPOs. This revealed that *PPO* gene duplications in *Physcomitrella* occurred after separation from the vascular plant lineage, which here contains the kormophytes *S. moellendorffii* and several seed plant species.

3.4. Heterologous expression of *PpPPO11* in *E. coli* and *in vitro* PPO activity of recombinant PPO

To prove the functionality of the *Physcomitrella PPO* gene family, *PPO1* and *PPO11* were chosen exemplary for heterologous expression in *E. coli* under the control of the IPTG-inducible *trc*-promoter (a hybrid promoter consisting of the *trpB*- and the *lacUV5*-promoter) using the pTrcHis2-TOPO-TA expression kit from Invitrogen (2.3.11).

The expression vector pTrc_PpPPO11his was created by amplification of the *PPO11* sequences encoding for the predicted mature protein (3.3) from a cDNA library (provided by Reski *et al.*, 1995) with the primers *cPPO11_forw* and *cPPO11_rev* (2.3.3 and 2.3.4.1), and ligation of *PPO11* into the plasmid pTrcHis2_TOPO *in frame* to a sequence encoding for a C-terminal His-tag (2.3.11). *E. coli* TOP10 clones with the ligation product were selected and plasmid DNA was analysed by restriction digests.

To construct the vector pTrc_PpPPO1his, the same cloning procedure was carried out with the cDNA encoding for the predicted mature form of *PPO1* (3.1) amplified with the primers *cPPO1_forw1* and *cPPO1_rev1* (2.3.3 and 2.3.4.1).

Expression was carried out with selected TOP10 *E. coli* clones expressing PPO1:his and PPO11:his, and protein extracts were prepared, enriched and purified using His-tag-binding columns as described in 2.4.3. Additionally, control expressions were performed with TOP10 clones (pTrcHis2_TOPO/*lacZ*) expressing a His-tagged lacZ protein as well as with BL21(DE3) clones expressing His-tagged PPO1 of *Trifolium pratense* (TpPPO1) obtained from Dr. Sullivan (Sullivan *et al.*, 2004). Protein extracts obtained from these expression systems served as positive controls for proper expression (lacZ:his and TpPPO1:his) and as negative (lacZ:his) as well as positive controls (TpPPO1:his) for PPO activity determinations from *E. coli* protein extracts.

Western blot analysis using an anti-His-tag antibody (2.4.8) revealed, that a major portion of the expressed PPO1:his and PPO11:his protein was accumulated in inclusion bodies (lane 3 and 4 in Fig. 3.9) and apparently insoluble. Besides, PPO11 expressing *E. coli* cultures yielded higher levels of recombinant PPO11 protein than PPO1 expressing cultures. No His-tagged protein was detected in the soluble non-enriched extracts of PPO1:his and PPO11:his expressing *E. coli* clones (lane 7 and 8). However, PPO11:his could be enriched from soluble extracts of clones expressing the protein, using a Ni-column (lane 9), indicating that a small portion of the recombinant PPO11:his protein was soluble. By contrast, no PPO1:his protein could be enriched from soluble extracts of PPO1:his expressing cultures (lane 10). Therefore, no activity measurements were carried out with PPO1.

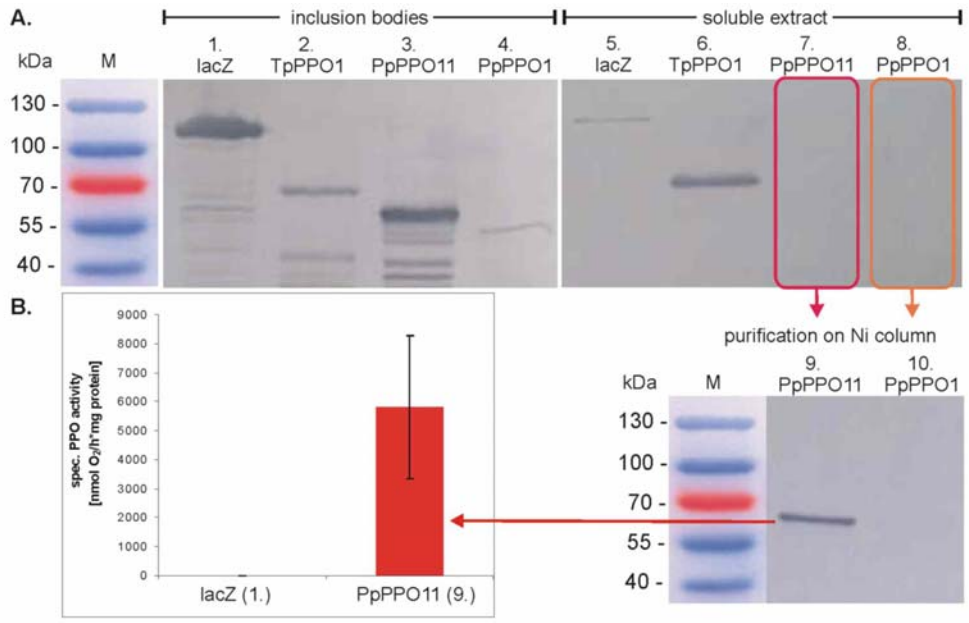

Fig. 3.9 Western blots of recombinant protein expressed in *E. coli* (A.) and PPO activity of purified His-tagged PPO11 (B.). Protein extracts of 6 h IPTG-induced *E. coli* cultures expressing His-tagged proteins were separated on a 12.5 % SDS-gel (2.4.6). (A.) The His-tagged proteins were detected by Western blot analysis (2.4.8) of insoluble (left panel), and soluble protein extracts (right panel), as well as enriched and purified extracts (lower, right panel) using an anti-His-tag antibody: lacZ:his (120 kDa, lane 1 and 5), TpPPO1:his (59 kDa, migrates at 65 kDa according to Sullivan *et al.* (2004), lane 2 and 6), PPO11:his (62 kDa, lane 3 and 9) and PPO1:his (60 kDa, lane 4). (B.) PPO activity was determined polarographically using 4-methyl catechol as a substrate (2.4.5). (n=3).

The recombinant His-tagged PPO11 protein was used for polarographic PPO activity determinations using 4-methyl catechol as a substrate (2.4.5). These extracts were found to have a significant PPO activity, while control protein extracts prepared from *E. coli* clones expressing lacZ:his in the same expression vector had no measurable *in vitro* PPO activity (Fig. 3.9B). PPO activities in the enriched and purified PPO11:his protein extracts were inhibitable by the addition of KCN to the reaction mixture, which was defined as a necessary prerequisite for a specific PPO activity assay.

Thereby the functionality of a *PPO* gene from *Physcomitrella* was unequivocally proven for the example of PPO11.

3.5. Expression profiles of *PPO* gene family members in *Physcomitrella*

In order to analyse the expression pattern of the *PPO* gene family members, gene-specific primers were designed for *PpPPO1* to *PpPPO12* (2.3.3) using the online application "Primique" (http://cgi-www.daimi.au.dk/cgi-chili/primique/front.py) and (real-time) RT-PCR was performed.

The expression patterns under different conditions (standard growth conditions, strong light irradiation and application of caffeic acid to the culture medium) of the *PPO* gene family members were analysed as described in the following three sections.

3.5.1. *PPO* expression under standard growth conditions

To determine the expression of *PPO* genes under standard growth conditions (2.2.1), RNA was isolated (2.3.13 and 2.3.14) from 8 day old protonema cultivated in liquid cultures, and (real-time) RT-PCR was carried out (2.3.4.1 and 2.3.4.3).

Prior to the examination and interpretation of the (real-time) RT-PCR experiments, the specificity of amplifications for each *PPO* gene was verified by sequencing the PCR products with the appropriate primers already used for the amplification of the respective fragments (2.3.15). Sequence analysis revealed highest specificity of each *PPO* primer pair for its expected template, as each amplified PCR product was found to be identical with the expected DNA fragment (data not shown).

Furthermore, as a prerequisite for the comparability of real-time RT-PCRs performed with different primer pairs, the different PCR efficiencies needed to be highly similar, ranging from 100 to 95 %. Thus, prior to examination of real-time RT-PCR results, PCR efficiency for each *PPO* primer pair (as well as for the control amplifications of *PpACT3*) was tested with different dilution series of genomic DNA as a template in real-time PCR analysis (2.3.4.3). PCR efficiencies for *PPO1* to *PPO12* and *ACT3* were found to range between 95 and 99 % depending on the primer pair. As examples, the efficiencies of PCRs performed with the primer pair for *PPO1* and *PPO4* are graphically shown in Fig. 3.10.

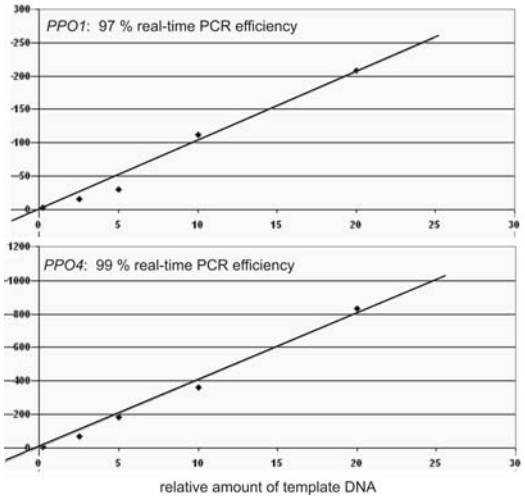

Fig. 3.10 Efficiency of real-time PCRs with *PPO* gene specific primers shown for the example of *PPO1* (upper panel) and *PPO4* amplification (lower panel). PCR efficiencies were 97 and 99 %, respectively. Efficiencies for all other amplifications were: 99 % (*ACT3, PPO4, -7, -10*), 97 % (*PPO1,- 2, -6, -8, -11*, *-12*), 96 % (*PPO3*) and 95 % (*PPO5, -9*).

Subsequent RT-PCR analysis revealed that nine of the twelve analysed *PPO* genes were expressed in 8 day old protonema liquid cultures (Fig. 3.11A). Only transcripts for *PPO7, -8* and *-10* were not detectable at this stage. However, in the case of *PPO10*, control PCRs on a protonema cDNA library (provided by Reski *et al.*, 1995) revealed that *PPO10* transcript can be present in protonema tissue.

Afterwards, real-time RT-PCRs were carried out using the same primers and cDNAs, in order to analyse the relative transcript amounts of each *PPO* gene (2.3.4.3), To compare expression levels of different gene family members, cycle threshold (CT) values for each *PPO* gene obtained from real-time RT-PCRs were adjusted according to equation 1, and relative transcript levels were determined using equation 4 as described in 2.3.4.3.

These analyses revealed different expression levels for the nine expressed *PPO* genes. *PPO1* had the highest expression level, followed by *PPO2, -3, -4, -11,* and *-12*, whereas *PPO5, -6,* and *-9* had only marginal expression levels in 8 day old protonema cultivated under standard conditions (Fig. 3.11B).

In comparison to the results in Fig. 3.11B, the number of expressed sequence tags (ESTs) from gametophytic and sporophytic EST databases (http://www.cosmoss.org/) found for each *PPO* gene is given as a diagram in Fig. 3.11C. According to these EST frequencies, *PPO11* had by far the highest expression level in gametophytic tissue within the *PPO* gene family (59 ESTs), followed by *PPO9* and *PPO1* (25 and 15 ESTs, respectively). ESTs in sporophytic databases were found for *PPO7, -8, -9,* and *-12*, of which *PPO8* had the highest number of ESTs.

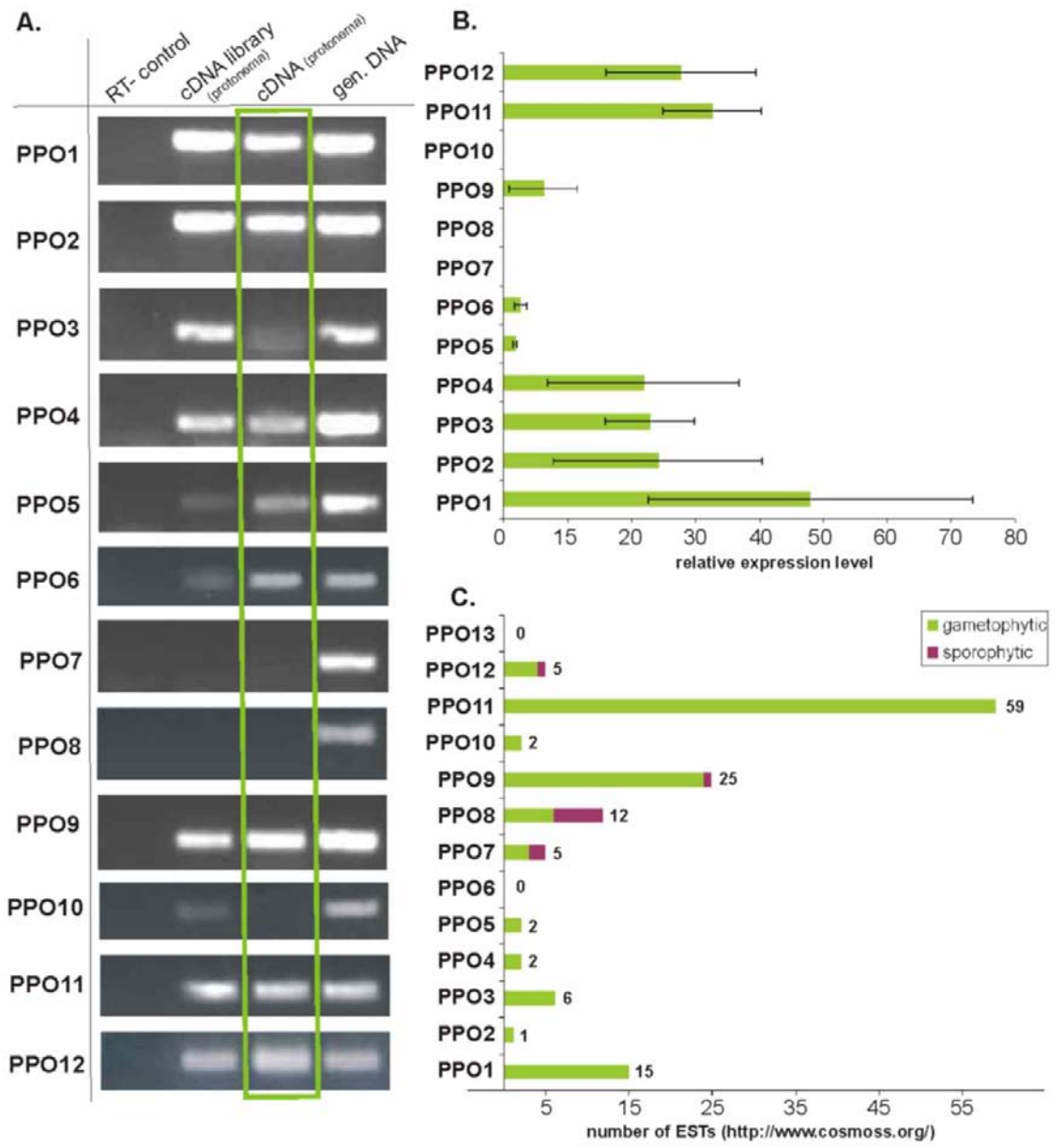

Fig. 3.11 Expression of *PPO1* to *PPO12*. (A.) Results of the RT-PCR with *PPO* gene specific primers on cDNA and cDNA library, as well as genomic DNA as a control for PCR. (B.) real-time RT-PCR analysis (n=3) (C.) EST frequencies for each *PPO* gene (http://www.cosmoss.org/). In A. and B. RNA from 8 day old wild type liquid culture was used as a template for cDNA synthesis (2.3.13 and 2.3.14). For comparison between the expression levels of the different *PPO*s, CT values of genomic DNA amplifications were used to adjust cDNA CT values, and relative transcript amounts were determined using equations 1 and 4 (2.3.4.3). Specificity of the amplification with the *PPO* gene specific primers was confirmed by sequencing the PCR products.

3.5.2. *PPO* expression under strong light irradiation with a sunlight like spectrum

In order to analyse the expression level of the *PPO* gene family members under strong light irradiation, part of a protonema liquid culture cultivated under standard condition for 5 days (~50 µmol $m^{-2}s^{-1}$) was transferred to ½ sunlight like light of ~1000 µmol $m^{-2}s^{-1}$ intensity and irradiated for four hours (2.2.3).

To monitor stress of irradiated tissue, samples were taken every hour, and the optimal quantum yield of photosystem II (PSII) electron transport [F_v/F_m] was determined as an indirect parameter for photosynthetic activity using a PAM fluorometer (2.5.2). After one hour of irradiation, activity of PSII decreased to 66 % of the initial photosynthetic activity (following the equation given in 2.5.2 that F_v/F_m of 0.8 corresponds to 100 % photosynthesis activity), and decreased further to 56 % (F_v/F_m 0.45) after four hours of irradiation (Fig. 3.12). Photosynthetic activity was restored to 76 % after four hours of cultivation under standard light conditions (~50 µmol $m^{-2}s^{-1}$) in the growth chamber subsequent to the strong light irradiation.

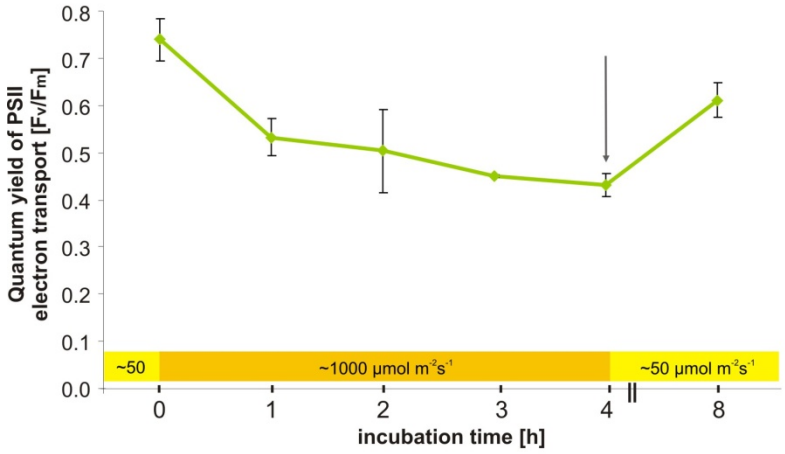

Fig. 3.12 Quantum yield of PSII electron transport (F_v/F_m) of WT liquid cultures in the time course of a culture irradiated with ½ sunlight like light (~1000 µmol $m^{-2}s^{-1}$) for 4 h and subsequent regeneration for 4 h at ~50 µmol $m^{-2}s^{-1}$ (2.2.3). A value of 0.8 was defined as 100 % photosynthetic activity of PSII according to Krause and Weis (1991). (n=3). Tissue for RNA extraction was harvested after 4 h of irradiation indicated here by the arrow.

After four hours of irradiation, RNA was isolated from strong light treated protonema samples as well as from control cultures cultivated under standard light conditions (2.3.13). cDNA was synthesised (2.3.14) and real-time RT-PCR was performed using the gene specific primers for *PPO1* to *PPO12* (2.3.3 and 2.3.4.3). The obtained CT values for *PPO* gene amplifications were corrected with the appropriate *PPO* CT values of genomic PCRs as well as with the CT values for the reference gene *PpACT3* of the appropriate cDNA PCRs according to the equation 3; the relative transcript amounts were determined using equation 4 described in 2.3.4.3.

Additionally, PPO activity of the differently treated tissue samples was determined polarographically (2.4.1 and 2.4.5), but slight changes in specific PPO activity of irradiated tissue in comparison to activity of untreated tissue were considered as insignificant (data not shown).

In Fig. 3.13 the expression levels of *PPO1* to *PPO12* from two independent real-time RT-PCR experiments (A. and B.) are displayed.

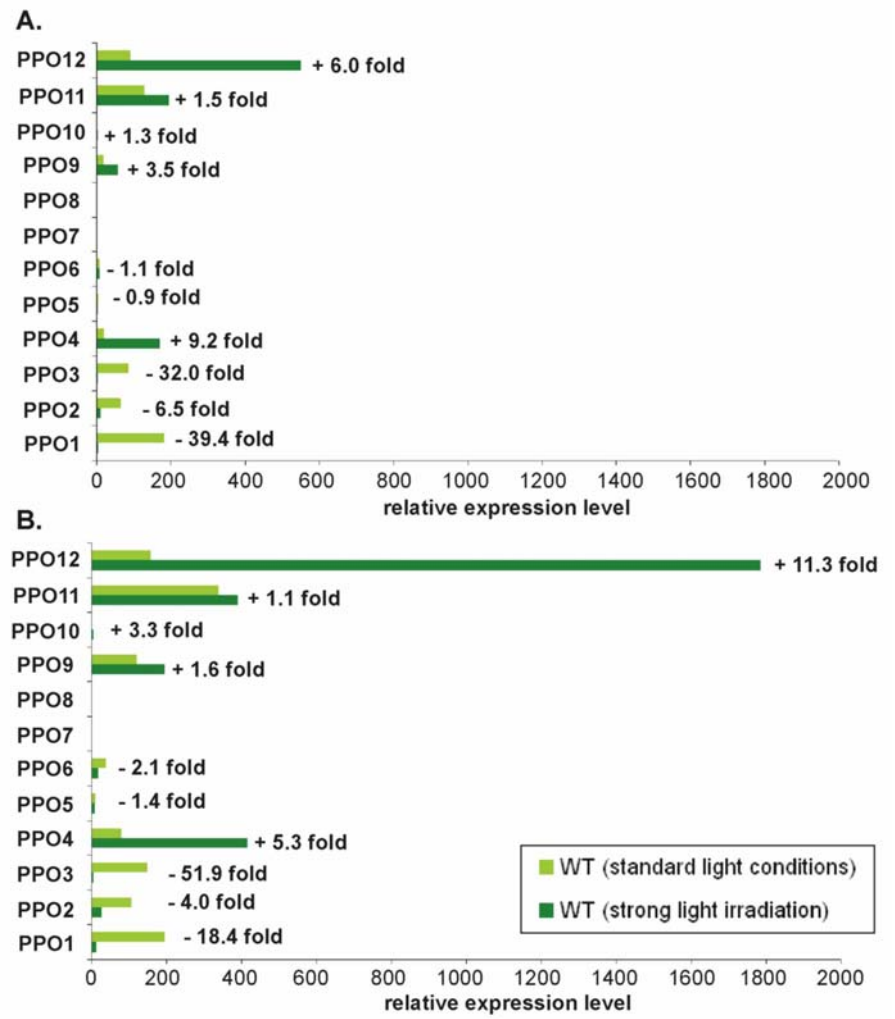

Fig. 3.13 Expression profile of *PPO1* to *PPO12* of wild type protonema irradiated with strong sun like light and of protonema cultivated under standard growth conditions. CT values determined by real-time RT-PCR were corrected for PCR efficiencies and the reference gene *PpACT3*, and relative transcript levels were calculated as described in 2.3.4.3 (equation 3 and 4). *PPO10* was expressed only under strong light conditions. *PPO7* and *PPO8* were neither expressed under standard nor under strong light irradiation. A. and B. are two independent real-time RT-PCR experiments. For each *PPO* gene the increase (+ x-fold) or decrease (- x-fold) of the relative expression level in strong light irradiated tissue in comparison to expression in standard cultivated tissue is indicated next to the columns.

Both graphs show the same pattern of increase and decrease of the different *PPO* genes in strong light irradiated tissue compared to expression levels under standard conditions. *PPO1, -3, -11,* and *-12* had the highest expression levels in 5 day old tissue cultivated under standard conditions. In strong light irradiated protonema the expression pattern of the *PPO* gene family changed, and due to the upregulation of *PPO4, -9, -11,* and *-12*, these genes were the major expressed *PPO* genes, with *PPO12* having the highest expression levels.

Gene expression of *PPO1* decreased ca. 18- to ca. 39-fold, *PPO3* gene expression decreased 30- to 50-fold, and *PPO2* expression decreased on average 5.3-fold in strong light irradiated tissue. The expression level of *PPO5* and *PPO6* was decreased 1.2-fold and respectively 1.6-fold on average after irradiation with sunlight like light. A slight increase in the expression level of *PPO9*

and *PPO11* was detected (2.5-fold and 1.3-fold in average in strong light irradiated tissue, respectively), whereas expression of *PPO4* and *PPO12* increased 7.3- to ca. 8.7-fold in average.

For the *PPO* genes *PPO7* and *PPO8,* which were not expressed under standard conditions (Fig. 3.11), also no expression was detectable under strong light irradiation. However, *PPO10* transcript was detected in strong light treated tissue, in contrast to tissue cultivated under standard conditions, where no expression was measured.

In summary, from these results it can be concluded, that the expression pattern of the *PPO* gene family changed drastically, and that the *PPO* gene family members reacted differently to the strong light irradiation.

3.5.3. *PPO* expression after caffeic acid (CA) application to the culture medium

With the aim to analyse the expression levels of the *PPO* gene family members in the presence of a putative PPO substrate, caffeic acid (CA) was applied to the culture medium and *PPO* transcript levels were determined by real-time RT-PCR using *PPO* gene specific primers (2.3.4.3 and 2.3.3).

Prior to the determination of *PPO* expression levels, preliminary tests were carried out to examine the effect of CA on *Physcomitrella* wild type growth. Protonema from standard liquid cultures was transferred to solid ABCNTV culture medium supplemented with various concentrations of CA ranging from 50 to 1000 µM, as well as to control agar plates without CA (2.2.2). Increase in "colony" diameter was examined after four weeks of cultivation under standard conditions (2.2.1). As indicated in Fig. 3.14A, diameters of the colonies were lower with increasing CA concentrations in the culture medium. In Fig. 3.14B examples of *Physcomitrella* colonies cultivated with 1000 µM CA are shown, displaying growth reduction in comparison to the controls.

A.

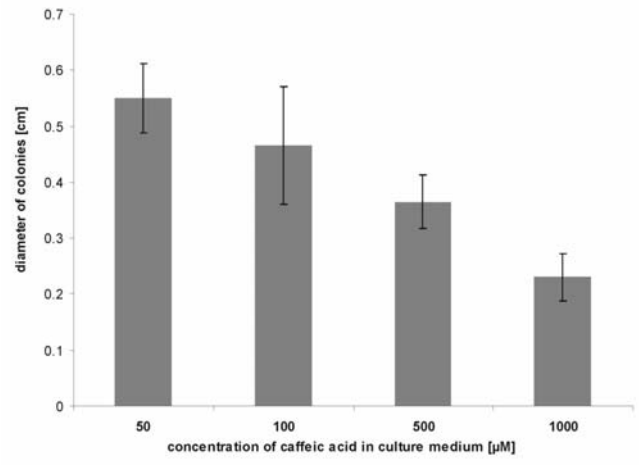

B.

Fig. 3.14 Growth inhibition of *Physcomitrella* wild type by caffeic acid measured after four weeks of cultivation (2.2.2). (A.) diameter of colonies on solid ABCNTV medium supplemented with different concentrations of CA (n=10). (B.) *Physcomitrella* growth on ABCNTV medium supplemented with 1000 µM CA (lower plate) and on medium without CA as a control (upper plate).

After determination of the influence of CA on *Physcomitrella* growth, subsequent experiments were conducted to determine the *PPO* expression levels in the presence of a putative PPO substrate. CA was added to the culture medium of freshly disintegrated protonema liquid cultures to a final concentration of 100 µM (2.2.2), and *Physcomitrella* tissue was cultivated for three days in the growth chamber using standard light and temperature parameters (2.2.1). Tissue from three different cultures for both treatments (grown either with or without CA) was harvested, RNA was extracted and cDNA was synthesised (2.3.13 and 2.3.14). Real-time RT-PCRs were performed with the gene specific primers for *PPO1* to *PPO12* as well as with the primers for the constitutively expressed control gene *PpACT3* (2.3.4.3 and 2.3.3). The relative transcript amounts for each *PPO* gene were determined using the equations 3 and 4 given in 2.3.4.3, and are displayed in Fig. 3.15.

Real-time RT-PCR analysis revealed that *PPO9* and *PPO12* had the highest expression level in 3 day old protonema cultivated under standard conditions. This was not altered in the case of protonema cultivated for three days in the presence of CA, although *PPO9* expression decreased 3.6-fold on average. Furthermore, in the presence of CA, *PPO11* transcription decreased 5.5-fold on average, and gene expression of *PPO2, -3, -4, -5,* and *-6* decreased about 2-fold to 4-fold.

From genes expressed under standard conditions, only *PPO1* gene expression increased (approx. 3-fold) in the presence of 100 µM CA.

As in tissue cultivated without CA, *PPO7* and *PPO10* were also not expressed in tissue incubated with CA. In contrast, *PPO8*, which was not expressed under standard conditions, showed low levels of expression in tissue cultivated with CA.

However, taking in account the relatively high standard deviations, only the changes in expression levels determined for *PPO8, PPO9* and *PPO11* were considered as significant in comparison to the transcript levels in untreated tissue (marked by asterisks in Fig. 3.15).

Additionally, PPO activity, determined polarographically, was found to be decreased in tissue cultivated with CA (227.95 ± 28.91 nmol O_2/h*mg protein) compared to tissue cultivated without CA (287.60 ± 13.93 nmol O_2/h*mg protein) (insert in Fig. 3.15).

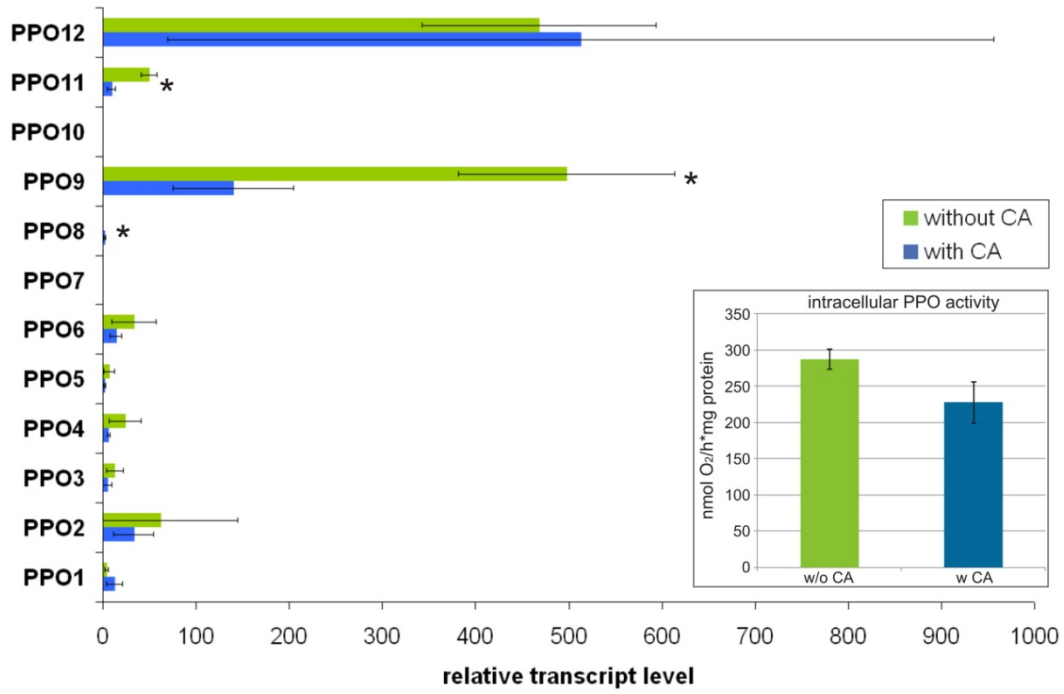

Fig. 3.15 Expression profile of *PPO1* to *PPO12* and PPO activity in wild type protonema incubated with 100 µM caffeic acid (CA). Tissue was cultivated for three days and under standard growth conditions with and without CA (2.2.1 and 2.2.2). Relative transcript levels were determined by real-time RT-PCR and corrected to *PpACT3* mRNA and to the different PCR efficiencies (according to equation 3 and 4 in 2.3.4.3). *PPO8* was found to be expressed only in the presence of caffeic acid. *PPO7* and *PPO10* were neither expressed under standard conditions nor in the presence of caffeic acid (n=3). Non-overlapping standard deviations are designated by asterisks. PPO activity (insert) was determined polarographically (2.4.5) in protein extracts of the same tissue samples as used for transcriptional analysis (n=6).

Thus, most of the *PPO* gene family members, except *PPO1, PPO8* (and *PPO12*) reacted with a transcriptional decrease after incubation with CA, which was also reflected in a reduction of overall intracellular PPO activity.

3.6. Analysis of putative PPO substrates from *Physcomitrella* tissue and culture medium

In order to investigate polyphenol-like compounds as potential substrates of bryophyte PPOs, extracts of *Physcomitrella* protonema tissue as well as of concentrated culture medium were analysed (2.8).

3.6.1. Analysis of *Physcomitrella* tissue for phenolic substances

To identify potential PPO substrates from tissue, acetone/water extracts of 5 day old *Physcomitrella* protonema were prepared and processed for HPLC analysis as described in 2.8. No peaks were detected within the first 45 min of chromatography, which was the elution frame of the reference substances tested, by separation of the extracts by RP-HPLC on gradient 1 (Fig. 3.16A). However, six major peaks (A to F) were observed after 45 min of separation (Fig. 3.16B).

In order to disperse these six peaks, the extracts were separated on a different gradient (gradient 2) as shown in Fig. 3.16C.

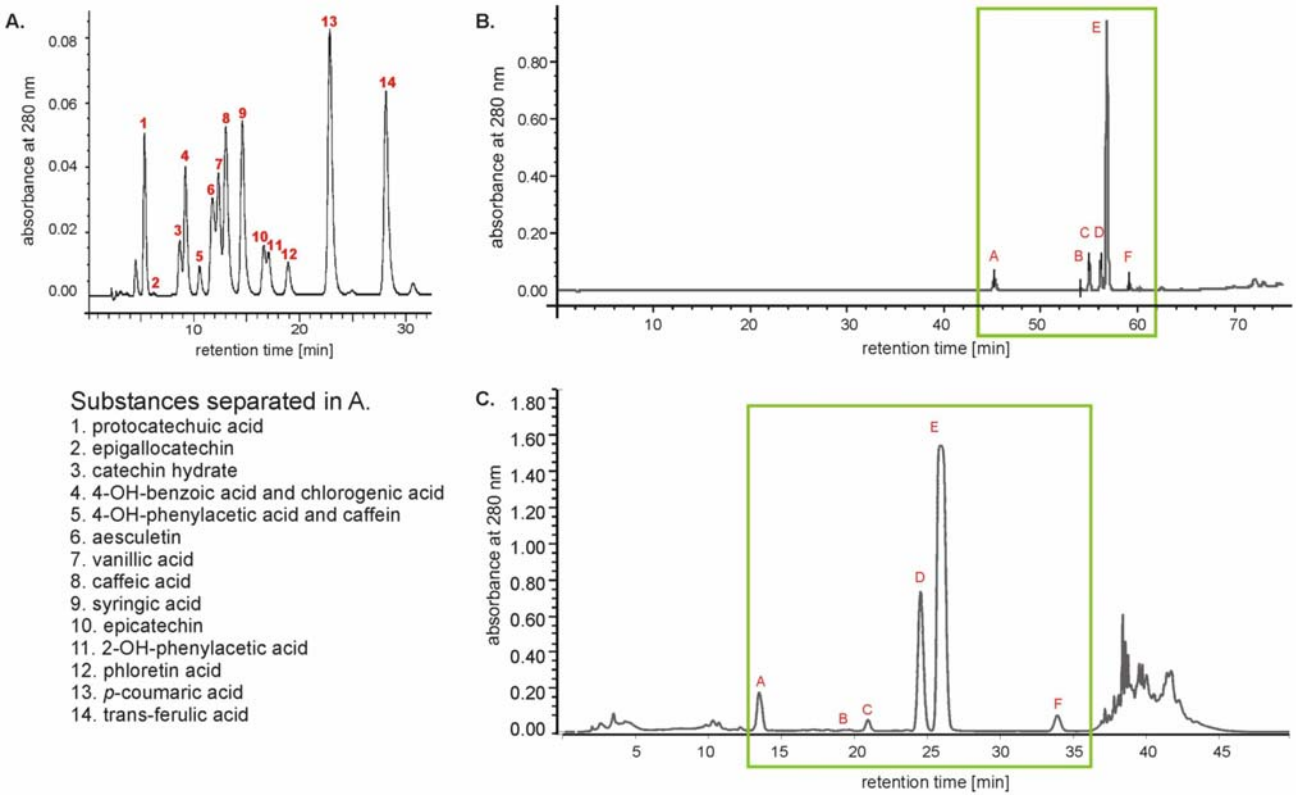

Fig. 3.16 HPLC analysis of acetone extracts isolated from *Physcomitrella* wild type tissue. (A.) phenolic reference compounds separated on gradient 1 (2.9). (B.) separation of compounds extracted from *Physcomitrella* tissue on gradient 1, but with prolonged data registration. (C.) improved conditions (gradient 2, described in 2.9) for separation of apolar substances from *Physcomitrella* extracts. Chromatograms were recorded at 280 nm.

Hence, none of the six major compounds had the same properties than the phenolic reference substances tested. In addition, later elution times of the six compounds than those of the polar reference compounds (Fig. 3.16A) indicated apolar properties of substances A to F.

With the aim to identify the structure of these six substances detected in *Physcomitrella* tissue, gradient 2 (2.9) was employed for a preparative HPLC separation. Larger volumes of fractions corresponding to the peaks of compounds A to F were collected and subsequently analysed by LC-MS in cooperation with Dr. S. Franke (Department of Chemistry, University of Hamburg) (2.9). MS-MS analysis (Tab. 3.2) revealed that the isolated substances A to F were not phenolic compounds but carboxylic acid aldehydes, of which two (substance B and E) were already described by Wichard *et al.* (2005). The four other compounds were not described in the mentioned publication, but due to the resulting MS/MS fragmentations, it was concluded that these substances were also members of this group of carboxylic acid aldehydes.

Tab. 3.2 Properties of compounds A to F extracted from *Physcomitrella* protonema tissue. (*): retention time observed in gradient 2 described in (2.9); ([a]): exact mass was determined by high resolution MS; ([b]): substances described by Wichard *et al.* (2005)

peak	λ_{max} [nm]	Retention time [min]*		mass [m/z] +H	empirical formula	MS/MS fragments [m/z]	Reference
		RT_{UV}	RT_{MS}				
A	281	13.61	14.40	182	$C_{10}H_{14}O_3$	163 (-18), 137 (-44), 119 (-18 -44)	
B	279	18.41	19.08	196	$C_{11}H_{16}O_3$	n.a.	subst.10[b]
C	268	19.32	20.11	224	$C_{12}H_{16}O_4$	205 (-18), 179 (-44), 163 (-60), 141 (-82)	
D	279.5	22.42	23.21	208	$C_{12}H_{16}O_3$	189 (-18), 179 (-28), 163 (-44), 145 (-44 -18), 121 (-44 - 42)	
E	283	23.52	24.43	208[a]	$C_{12}H_{16}O_3$	189 (-18), 179 (-28), 163 (-44), 145 (-44 -18), 135 (-44 -28)	subst. 7[b]
F	280	30.63	31.54	210	$C_{12}H_{19}O_3$	191 (-18), 181 (-28), 173 (-18 -18), 165 (-44), 153 (-56, -2 x 28), 111 (-98, - 2 x 28 – 42)	

According to these results, it can be stated that *Physcomitrella* did not produce or enrich significant amounts of phenolic compounds under standard *in vitro* cultivation conditions (recovery of > 95 % of epicatechin during the extraction procedure tested in control experiments, not shown here).

3.6.2. Analysis of *Physcomitrella* culture medium for phenolic substances

As described above, no measurable amounts of phenolic compounds were detectable in *Physcomitrella* tissue grown under standard growth conditions (3.6.1). However, under certain cultivation conditions, browning of the culture medium occurred indicating extracellular accumulation of phenolic compounds. To identify such putative phenolic substances, *Physcomitrella* wild type protonema was cultivated under standard conditions in liquid medium (2.2.1), supplemented with 0.45 % (w/v) D-glucose. Browning of the culture medium and the tissue was already visible by eye after 7 days of cultivation.

After 14 days of cultivation, media with (+Glu) and without D-glucose (-Glu) were freeze-dried, and the lyophilised powders were resuspended in 60% methanol (2.8). These extracts were separated by RP-HPLC on gradient 1 (2.9).

In the HPLC chromatograms for concentrated culture medium of wild type tissue cultivated without glucose (designated as "medium-Glu" in the following), 13 peaks with very low amplitude

were detected (Fig. 3.17A). In contrast, chromatograms for concentrated medium supplemented with glucose (designated as "medium+Glu" in the following) revealed 24 major peaks with higher amplitudes (Fig. 3.17B). According to the elution time of the compounds from medium+Glu, the peaks were named "a" to "x". The absorption spectra recorded from 225 to 540 nm of these compounds are given in Fig. 3.18B.

Analyses of the absorption spectra revealed that some of the substances occurring in medium+Glu were also present in medium-Glu. Hence, the corresponding peaks were named identical in chromatogram A (Fig. 3.17), and spectra for these compounds are coloured purple in Fig. 3.18B. Most of the detectable peaks occurred only in medium+Glu, and the appropriate spectra are coloured dark blue in Fig. 3.18B.

Substances detected only in medium-Glu were named by their retention time in Fig. 3.17A, and the appropriate absorption spectra of these compounds are shown in light blue in Fig. 3.18A.

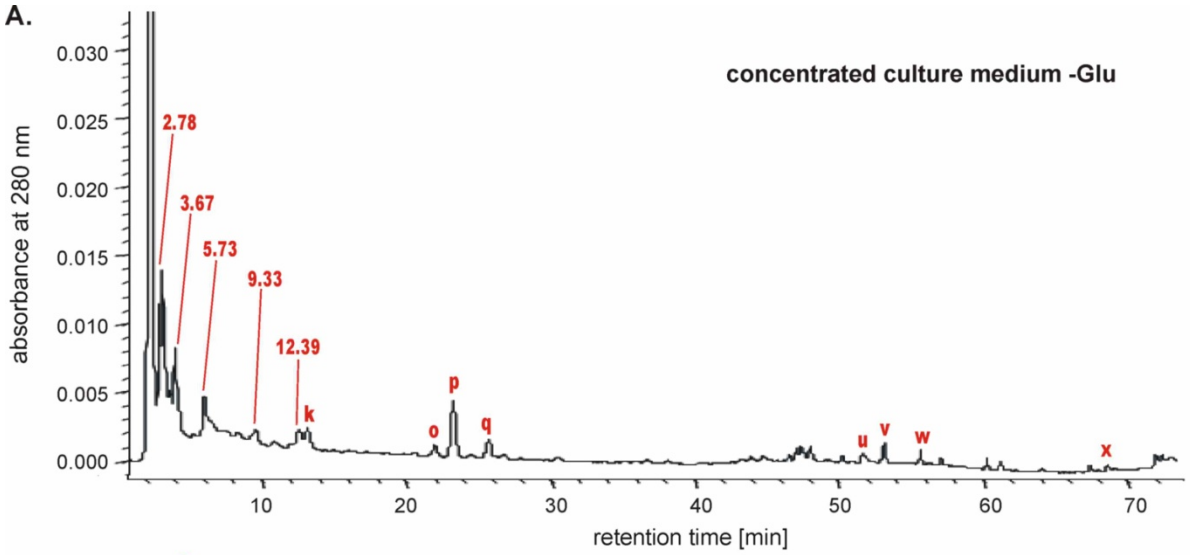

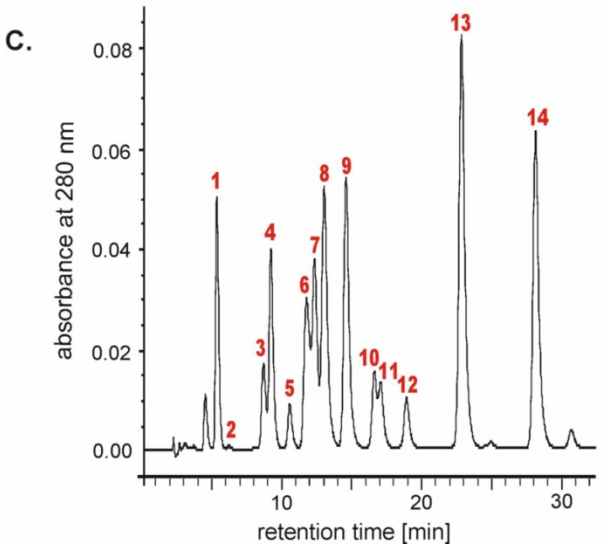

Reference substances separated in C.	RT [min]	lambda max [nm]
1. protocatechuic acid	5.271	259.7 / 294.1
2. epigallocatechin	6.249	265.6
3. catechin hydrate	8.431	278.7
4. 4-OH-benzoic acid	9.289	255.0
5. 4-OH-phenylacetic acid	11.003	275.1
6. aesculetin	12.104	297.7 / 345.5
7. vanillic acid	12.688	260.9 / 292.9
8. caffeic acid	13.397	234.9 / 323.9
9. syringic acid	15.047	275.1
10. epicatechin	16.551	278.7
11. 2-OH-phenylacetic acid	17.683	272.7
12. phloretin acid	19.478	276.3
13. *p*-coumaric acid	22.979	309.6
14. trans-ferulic acid	28.134	322.7

Fig. 3.17 HPLC analysis of phenolic-like compounds in concentrated culture medium of wild type. (A.) separation of compounds from concentrated medium of tissue cultivated without glucose ("medium-Glu"). (B.) separation of compounds from concentrated medium of tissue cultivated with 0.45 % D-glucose ("medium+Glu"). Separation was performed on gradient 1 with data registration at 280 nm (2.9). Equal integration parameters were applied for chromatogram A and B. (C.) reference compounds separated on gradient 1 with shortened data registration. Retention times and lambda max of the reference compounds are given in the table aside.

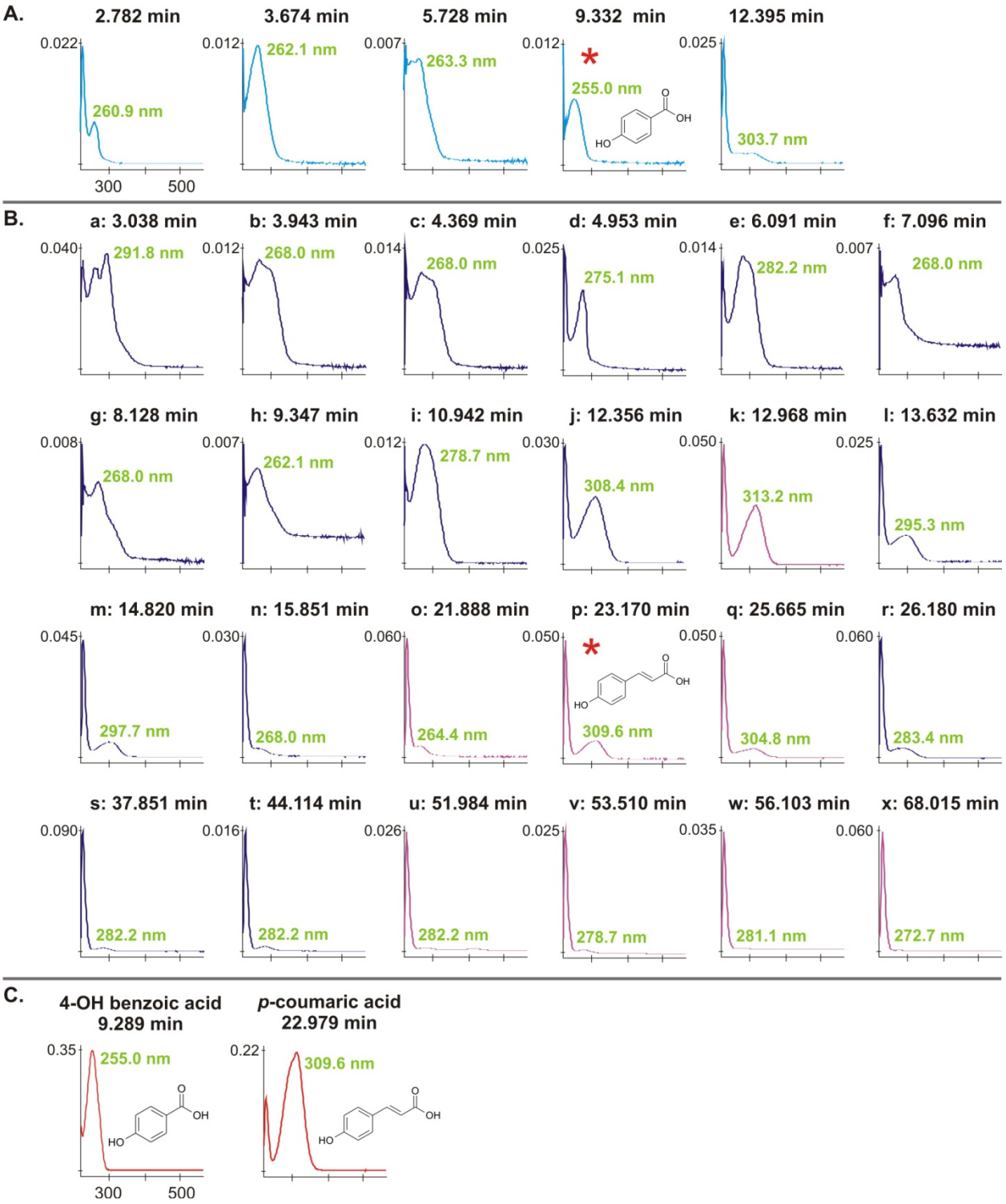

Fig. 3.18 Absorption spectra of compounds extracted from *Physcomitrella* culture medium analysed by HPLC. Corresponding HPLC profiles are given in Fig. 3.17. Absorbance of each compound was recorded from 225 to 540 nm. (A.) spectra of substances named by their retention times as in Fig. 3.17A extracted from standard culture medium ("medium-Glu"). (B.) spectra of substances "a" to "x" (Fig. 3.17B) from medium supplemented with 0.45 % D-glucose ("medium+Glu"). For each spectrum lambda max is displayed in green. Spectra coloured in light blue belong to substances occurring only in medium-Glu, spectra in dark blue belong to compounds that were only detected in medium+Glu; spectra coloured in purple were derived from substances detected under both conditions (medium-Glu and medium+Glu). Two substances (spectra marked by a red asterisk) were tentatively identified by the reference compounds given in C. according to the retention time and lambda max. (C.) spectra of the reference compounds 4-hydroxybenzoic acid and *p*-coumaric acid.

As shown in Fig. 3.17 and Fig. 3.18, the substances "k, o, p, q, u, v, w and x" were present in both culture media, with and without glucose. However, the amplitude of the peaks in the chromatogram B from medium+Glu were, with the exception of compound "p", much higher compared to the amplitude of the same peaks in A (Fig. 3.17). Thus, higher amounts of these substances were present in medium+Glu in comparison to medium-Glu.

Therefore, it can be suggested that the supplementation of culture medium with 0.45 % D-glucose led to a release of phenolic-like compounds, which were not secreted under standard conditions. Furthermore, an increased production of compounds already present under standard growth conditions was observed after supplementation of the culture medium with glucose.

A comparison of the elution times and the absorption spectra of the compounds detected in the concentrated culture media of *Physcomitrella* with the reference substances (table in Fig. 3.17C and Fig. 3.18C) revealed that two compounds in the culture media had properties matching two of these reference substances.

The peak "9.332" detected from medium-Glu with a retention time of 9.33 min and a lambda max of 255.0 nm could tentatively be identify as 4-hydroxybenzoic acid (9.289 min, 255.0 nm). Moreover, the peak "p" detected from medium-Glu and medium+Glu with a retention time of 23.170 min and a lambda max of 309.6 nm was identified as *p*-coumaric acid (22.979 min, 309.6 nm). All other detected substances possessed typical phenolic properties, although none of the substances could be assigned to one of the reference compounds used in the experiment (Fig. 3.17C).

3.7. Targeted knockout of *PpPPO1* in *Physcomitrella*

To obtain information on PPO function, knockout plants for one of the *PPO* gene family members, from which *PPO1* was chosen exemplary, were generated. Knockout lines were analysed, to determine the contribution of PPO1 activity to the overall PPO activity. Transcripts of the *PPO* gene family were measured to elucidate, whether the expression pattern changed in *PPO1* knockout lines. Moreover, phenotypic changes were analysed to obtain information on possible functions of PPO in *Physcomitrella*.

3.7.1. Generation and molecular analysis of targeted knockout lines of *PpPPO1*

A *PPO1* knockout vector pET_PPO1_nptII was constructed by blunt end insertion of an *nptII* resistance cassette into the coding sequence of *PpPPO1*. For this purpose, the plasmid pET28a_PpPPO1 containing the coding sequence of *PpPPO1* (3.1) was digested with *Ecl136II* and

Bsp1407 releasing a 106 bp fragment that was removed by gel purification (2.3.8 and 2.3.6). Sticky ends were filled in using the Klenow fragment, and self circulation of the vector was prevented by CIAP treatment prior to ligation (2.3.9). The *nptII* resistance cassette (*neomycin phosphotransferase* II gene under control of the 35S promoter, terminated by the *nos* terminator) was released from the vector pHP23 by digestion with *EcoRI*, gel purified, and blunted by a Klenow reaction. After ligation and transformation (2.3.9 and 2.3.10), *E. coli* clones carrying the ligation product were selected by colony PCR screening using the primers *nptII*_3 and *nptII*_4 (2.3.3 and 2.3.4.2) and confirmed by restriction enzyme analysis (2.3.8).

Afterwards, the "*PPO1* knockout cassette" (*nptII* cassette flanked by 730 and 853 bp of *PPO1* coding sequence) was amplified from the knockout construct using the primers *cPPO1_forw* and *cPPO1_rev* (2.3.3 and 2.3.4.1). *PPO1* knockout plants were generated by protoplast transformation with 25 µg of the PCR product (2.2.6 and 2.2.7).

For molecular analysis of putative *PPO1* knockout plants, genomic DNA was isolated from 13 stable transformants resistant to G418 (2.3.12), and PCRs were carried out to analyse the integration of the *nptII* cassette into the genomic locus of *PpPPO1* (2.3.4.1). Four of the screened lines (#1, #3, #5, and #8) showed correct 5′ and 3′ integration of *nptII* (Fig. 3.19). In line #5 probably a multiple insertion of *nptII* occurred, because no PCR product could be obtained by amplification with primers *PPO1_3* and *PPO1_4* (PCR product 3). For line #6 only the PCR product 1 was obtained, while PCR product 2 could not be amplified. Amplification of PCR product 3 resulted in a short fragment, as that obtained for wild type. These results suggested an insertion of the *PPO1* knockout cassette at the 5′ end in *PPO1*_ko line #6 instead of a gene replacement. Nevertheless, all five transgenic lines (#1, #3, #5, #6, and #8) would theoretically possess no *PPO1* transcript, and were therefore regarded as *PPO1* knockout lines (*PPO1*_ko) and used for further studies.

Additionally, the disruption of the genomic *PpPPO1* locus in the knockout lines #1 and #5 was proven by sequencing the PCR products 1 and 2 using the primers *PPO1_1* and *nptII_1* as well as *PPO1_2* and *nptII_2,* respectively. Analysis revealed that the PCR products consisted of the expected sequences from genomic *PpPPO1* and *nptII*.

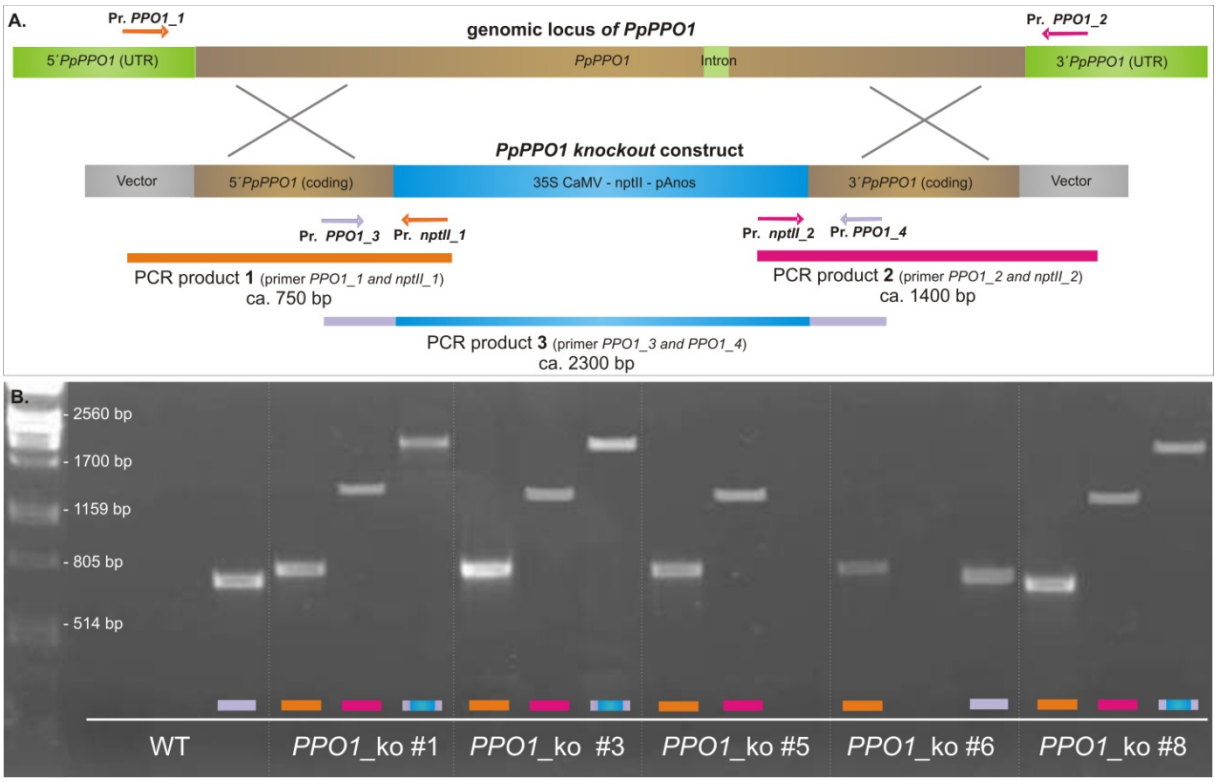

Fig. 3.19 Schematic integration of the *nptII* cassette into the genomic locus of *PPO1* and molecular analysis of the *PPO1* knockout lines. (A.) Disruption of the genomic locus of *PpPPO1* by insertion of the *nptII* cassette mediated by homologous recombination (blue) conferring to G418 resistance. The 5' and 3' *nptII* flanking regions originated from the *PPO1* coding sequence are coloured brown; regions of the *PPO1* gene not present in the knockout construct are displayed in green. Primers used in B. are indicated as arrows. (B.) PCR analysis of genomic DNA testing for disruption of the WT locus (purpel/blue amplificate) and 5' and 3' integration (orange and pink amplificate) of the *PPO1* knockout construct for five transgenic lines. Primers and expected PCR products are displayed in A. with the same corresponding colours.

As described by Schween *et al.* (2005a), during the transformation procedure the ploidy of the protoplasts changes with a certain frequency, resulting in regenerating di- or tetraploid *Physcomitrella* plants. This necessitated that the ploidy of the generated knockout plants was tested.

Haploidy of all analysed stable transformants was demonstrated by flow cytometry (2.10). Plants identified and confirmed above as *PPO1* knockout lines (#1, #3, #5, #6, and #8) exhibited a major peak at 50 (shown for the example of *PPO1*_ko #1 in Fig. 3.20), typical for haploid status. One of the analysed plants, for which correct 5´ and 3´ integration was demonstrated by PCR (data not shown), was found to be diploid (*PPO1*_ko #12 in Fig. 3.20) and therefore excluded from further studies.

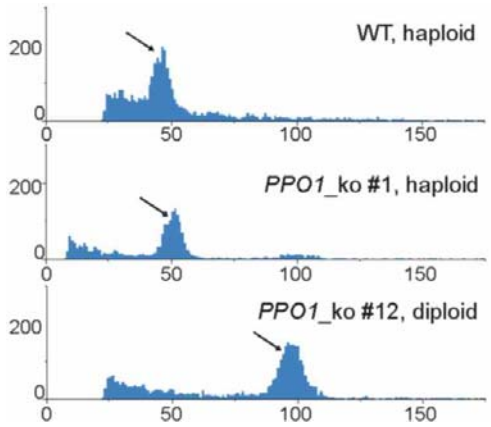

Fig. 3.20 Ploidy analysis of *PPO1* knockout plants. Flow cytometric histograms (2.10) for the example of haploid *PPO1*_ko #1 and diploid *PPO1*_ko #12 (not used in further studies) in comparison to wild type (grown on ABCNTV medium). The x-axis indicates the relative fluorescence intensities of analysed nuclei; the ordinate represents the number of counted events.

To prove the absence of *PPO1* transcript, RNA was isolated from 10 day old cultures of *PPO1*_ko lines #1, #3, #5, #6 and #8 grown under standard conditions (2.3.13) and cDNA was synthesised (2.3.14). RT-PCR was carried out using the *PPO1* specific primer pair *PPO1expr* (2.3.3) as described in 2.3.4.1. As a positive control for proper RNA extraction and RT-PCR, the primers *act3_forw* and *act3_rev* were used to amplify the constitutively expressed *PpACT3* gene.

As shown in Fig. 3.21, the absence of *PPO1* transcript was confirmed for all five knockout lines by RT-PCR with *PPO1* specific primers.

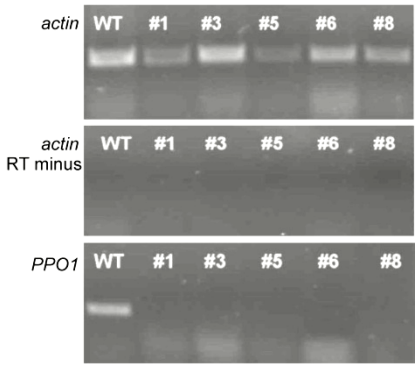

Fig. 3.21 Expression analysis of *PPO1* knockout lines. RT-PCR of *PPO1* knockout plants was performed with *PPO1* specific primers (2.3.3). *PPO1* was found to be expressed only in WT, but not in the transgenic *PPO1*_ko lines (lower panel). As a positive control, RT-PCR was carried out with the primers *act3_forw* and *act3_rev*, corresponding to the constitutively expressed *actin3* gene (upper panel). RT minus controls showed RT reactions being free from DNA contamination (central panel).

3.7.2. Analysis of *PPO1* knockout lines: PPO activity, *PPO* expression pattern and phenotypic changes

Subsequent to the molecular identification of *PPO1* knockout lines and demonstration of the absence of *PPO1* transcript (3.7.1), the *in vitro* PPO activity was determined, expression levels of *PPO2* to *PPO12* were analysed and phenotypic changes of *PPO1* knockout lines were studied as described in the following sections.

3.7.2.1. *in vitro* PPO activity in tissue and culture medium of *PPO1* knockout lines

To investigate whether *PPO1* knockout plants exhibit a decreased PPO activity, the total *in vitro* PPO activity was determined, using *PPO1*_ko #1 and *PPO1*_ko #5 as examples. Protein extracts from *Physcomitrella* tissue as well as from culture medium of 7 day old liquid cultures were prepared as described in 2.4.1 and 2.4.2, and PPO activity was determined polarographically (2.4.5). As already described (3.2), the specific PPO activity was found to be higher in extracellular protein extracts than in intracellular extracts (Fig. 3.22).

For the total intracellular PPO activity from tissue extracts, no considerable differences between wild type and *PPO1* knockout lines were observed (Fig. 3.22B). However, PPO activities from extracellular medium extracts were found to be significantly reduced in *PPO1*_ko lines #1 and #5 compared to wild type. In Fig. 3.22, the specific *in vitro* PPO activities are shown for *PPO1*_ko #1 and #5 possessing a remaining extracellular PPO activity of only 32 and 31 %, respectively compared to wild type. All measured PPO activities were inhibitable by the addition of KCN to the reaction mixture, which was defined as a necessary requirement for enzymatic PPO activity.

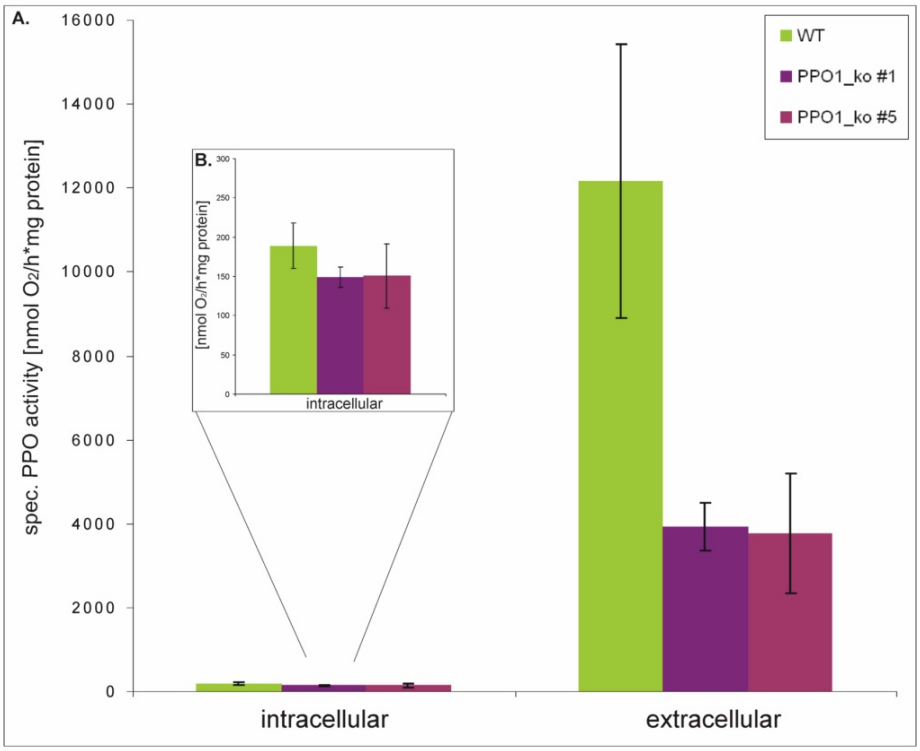

Fig. 3.22 *in vitro* PPO activity of *PPO1* knockout plants and wild type. Protein extracts were prepared from tissue and culture medium from cultures grown under standard conditions for 7 days (2.4.1 and 2.4.2) and PPO activity displayed as [nmol O_2/h*mg protein] was determined polarographically using 4-methyl catechol as a substrate (2.4.5). (B.) is a magnification of the intracellular PPO activity shown in A. (n=3)

Besides the indirect functional evidence for PPO1 being an *o*-diphenol oxidase, these findings suggested, that PPO1 with its *in silico* predicted secretion signal (3.1), provides a major portion of the extracellular PPO activity detectable with 4-methyl catechol.

3.7.2.2. Expression pattern of *PPO2* to *PPO12* in *PPO1* knockout plants under standard conditions and strong light irradiation

With the aim to analyse the effect of the *PPO1* knockout on the expression pattern of the remaining *PPO* gene family members, the relative transcript amounts of *PPO2* to *PPO12* were analysed in the *PPO1* knockout plants. Expression profiles of the *PPO* genes under standard conditions were compared with the expression profiles recorded under strong light irradiation.

Aliquots of 5 day old protonema cultures of *PPO1*_ko lines#1 and #5 as well as of wild type were transferred from standard cultivation conditions (~50 µmol $m^{-2}s^{-1}$) to the sunlight simulator and irradiated with strong sunlight like light (~1000 µmol $m^{-2}s^{-1}$) for four hours as described in 2.2.3.

In order to monitor stress caused by strong light irradiation, prior to analysing the *PPO* transcript amounts, the quantum yield of photosystem II (PSII) electron transport of *PPO1* knockout lines in comparison to wild type was determined during the irradiation procedure. Tissue samples were taken every hour, and F_v/F_m was measured using a PAM fluorometer (2.5.2). Results displayed in Fig. 3.23, demonstrated that after the first hour of strong light irradiation F_v/F_m decreased to 0.53 (equals 66 % initial photosynthetic activity) for wild type and to 0.53 and 0.49 (equals 66 % and 61 %) for the *PPO1*_ko lines (F_v/F_m of 0.8 corresponds to 100 % photosynthesis activity, 2.5.2). After four hours of strong light irradiation, F_v/F_m decreased further to 0.45 (equals 56 %) for wild type and 0.52 and 0.35 (equals 65 % to 43.8 %) for *PPO1*_ko lines #1 and #5, respectively. Tissue was re-transferred to the growth chamber with standard light conditions subsequent to the strong light irradiation and cultivated for another four hours, at which the photosynthetic activity was restored to 76 % for wild type (F_v/F_m 0.61) and 83.8 % and 82.5 % (F_v/F_m 0.67 and 0.66) for the *PPO1*_ko lines #1 and #5.

Thus, no significant differences in light stress reactions, monitored by F_v/F_m measurements, were observed between *PPO1* knockout plants and wild type.

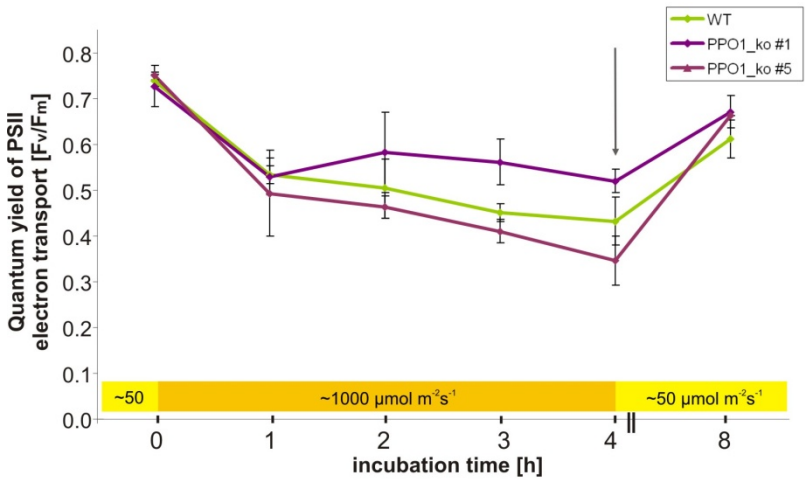

Fig. 3.23 Quantum yield of PSII electron transport (F_v/F_m) of *PPO1*_ko plants #1 and #5 and wild type in the time course of cultures irradiated with ½ sunlight like light (~1000 µmol $m^{-2}s^{-1}$) for 4 h and subsequent regeneration for 4 h at ~50 µmol $m^{-2}s^{-1}$ (2.2.3). A value of 0.8 was defined as 100 % photosynthetic activity of PSII (Krause and Weis, 1991, 2.5.2). (n=3). Tissue for RNA isolation was harvested after 4 h of irradiation indicated by the arrow.

To analyse whether the gene expression pattern of *PPO2* to *PPO12* changed in *PPO1* knockout plants, after four hours of irradiation, tissue was harvested from strong light irradiated cultures as well as from cultures grown under standard conditions. RNA was isolated and cDNA was synthesised (2.3.13 and 2.3.14). Real-time RT-PCR experiments using the *PPO* gene-specific primers as well as the primers for the constitutively expressed control gene *ACT3* (2.3.3) were performed, and the relative transcript amounts for each *PPO* gene in each cDNA preparation were calculated according to equation 3 and 4 as described in 2.3.4.3.

In Fig. 3.24 the relative expression levels of the *PPO* gene family members in *PPO1*_ko lines #1 (B.) and #5 (C.) compared to wild type (A.) are given as two graphs resulting from two independent real-time RT-PCR experiments.

The expression pattern of the *PPO* gene family members in the *PPO1*_ko plants was found to resemble that of wild type under standard light conditions, except that the *PPO1* transcript was absent in *PPO1*_ko lines, as already demonstrated in 3.7.1. Thus, the lack of *PPO1,* being one of the strongly expressed *PPO* genes in wild type under standard conditions, did not lead to significant changes in the expression pattern of the remaining *PPO* genes in *PPO1*_ko lines #1 and #5. In 5 day old *PPO1*_ko lines cultivated under standard conditions, the highest expression levels were found for *PPO3, -11,* and *-12*. *PPO4, -5, -6,* and *-9* were moderately expressed, and transcripts for *PPO7*, *-8,* and *-10* were not detectable.

Furthermore, in both *PPO1*_ko and wild type plants a similar pattern of changes in the *PPO2* to *PPO12* expression was observed under strong light irradiation compared to standard conditions. However, in *PPO1*_ko #5 as in wild type the expression of *PPO11* was increased ca. 1-fold to 3-fold, whereas in *PPO1*_ko #1 the expression was decreased ca. 3.5-fold in strong light irradiated tissue.

In strong light irradiated protonema of *PPO1*_ko plants and wild type, the *PPO* genes *PPO4, -9, (-11),* and *-12* were upregulated, resulting in the high expression levels for these gene family members, with *PPO12* having the highest expression levels in all analysed genotypes. Stronger increase of *PPO4* expression in strong light irradiated *PPO1*_ko plants #1 and #5 (24.2-fold to 29.8-fold and 13.9-fold to 16-fold, respectively) was observed compared to wild type (5.3-fold to 9.2-fold).

Decrease of *PPO2, -5,* and *-6* gene expression in strong light irradiated *PPO1*_ko plants was in the same range as observed for wild type, whereas *PPO3* gene expression decreased only 9.8-fold to 12.1-fold in *PPO1*_ko #5 compared to a 30- to 50-fold decrease in wild type. However, in strong light irradiated *PPO1*_ko #1 the *PPO3* gene expression decreased 24.3- to 36.8-fold.

As in strong light irradiated wild type, *PPO7* and *PPO8* were also not expressed in strong light irradiated *PPO1*_ko lines. Yet, expression of *PPO10* transcript, not expressed under standard conditions, was detectable in both *PPO1*_ko lines and wild type irradiated with strong light.

Moreover, specific PPO activities in protein extracts of the differently treated *PPO1*_ko plants and wild type were determined polarographically (2.4.1 and 2.4.5), but no significant changes were observed (data not shown).

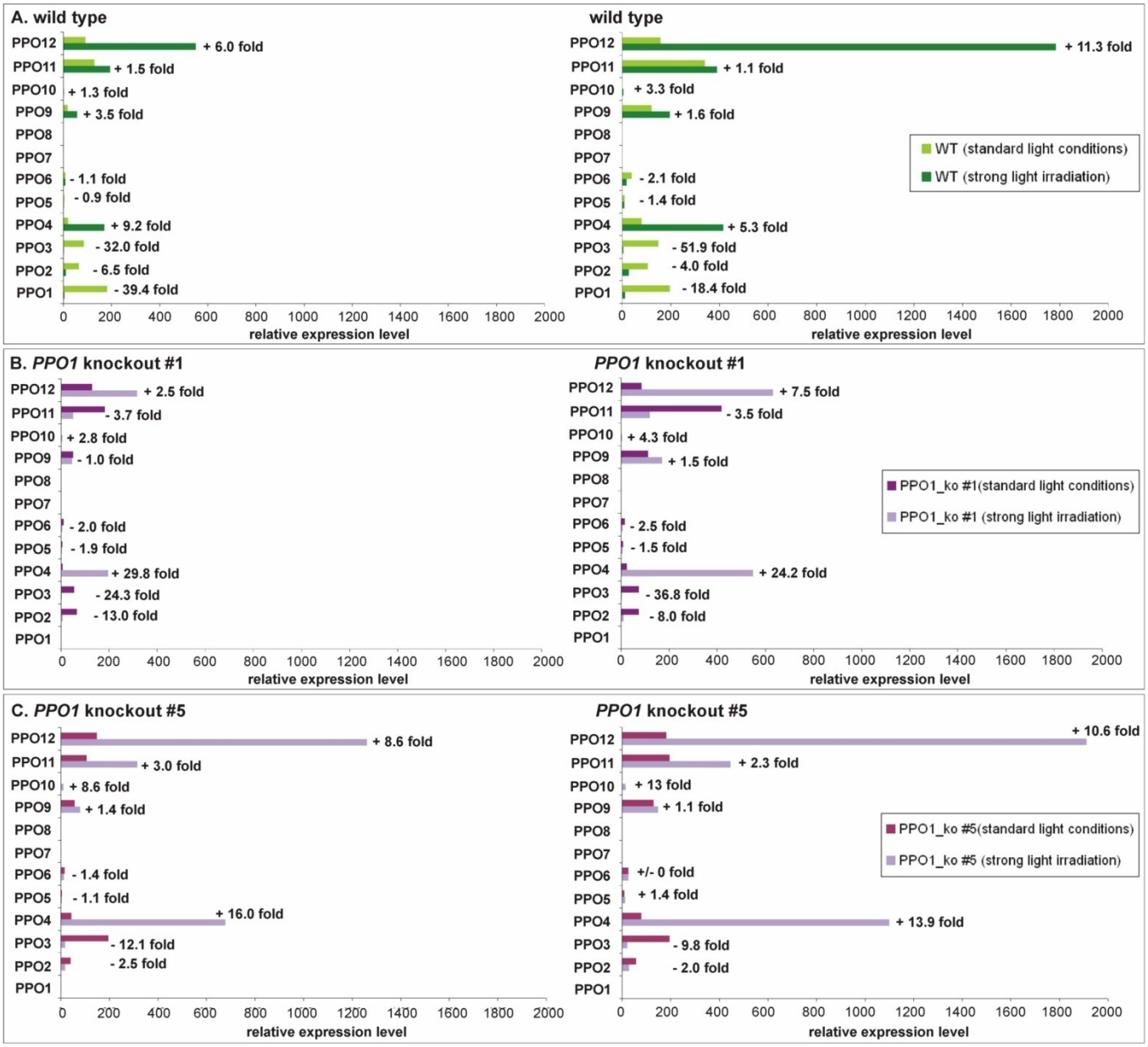

Fig. 3.24 Relative expression levels of *PPO1* to *PPO12* in wild type (A.) and *PPO1*_ko lines #1 (B.) and #5 (C.) under standard growth conditions and after strong light irradiation. RNA was extracted from of 5 day old tissue irradiated for 4 h with ~1000 µmol $m^{-2}s^{-1}$ light (2.2.3) as well as from tissue cultivated under standard growth conditions. CT values were corrected for different PCR efficiencies and for *ACT3,* and relative transcript amounts were determined according to the equations 3 and 4 given in 2.3.4.3. For each *PPO* gene the increase (+ x-fold) or decrease (- x-fold) of the relative expression level under strong light irradiation in comparison to expression under standard growth conditions is given next to the columns. Two independent real-time RT-PCR experiments are displayed for each genotype (Numeric values of the relative expression levels are listed in the appendix, Tab. 6.1).

In summary, the expression pattern of *PPO2* to *PPO12* did not change significantly under standard conditions in *PPO1* knockout lines in comparison to wild type, thus revealing that the regulation of each *PPO* gene was almost independent from *PPO1* gene expression. Under strong light irradiation, regulation of *PPO* genes (with the exception of *PPO4,* and possibly *PPO3* and *PPO11*), was to a great extent independent from *PPO1* expression.

3.7.2.3. Reaction of *PPO1* knockout plants to 4-methyl catechol in the culture media

In order to test whether the addition of phenolic compounds had a different effect on *PPO1* knockout plants in comparison to wild type, the different genotypes were grown in the presence of a polyphenol.

As shown in 3.2, 3.4 and 3.7.2.1 the phenolic compound 4-methyl catechol (4-MC) was found to be a substrate for *Physcomitrella* PPOs from tissue and culture medium. Thus, 4-MC was added to 5 day old standard liquid cultures of wild type and *PPO1*_ko lines #1, #3, #5, #6, and #8 to a final concentration of 50 and 100 µM (2.2.2), and vitality of the tissue was monitored over a period of 48 h by F_v/F_m measurements (2.5.2) as well as by cell vitality staining (2.5.1).

Because very similar results were obtained for all five *PPO1* knockout lines, data are exemplary shown for the *PPO1*_ko #1 in Fig. 3.25. Die back in *PPO1*_ko lines visible by browning of protonema tissue was already visible by eye after 24 h, whereas wild type tissue remained green and healthy looking (Fig. 3.25A).

However, F_v/F_m values determined by PAM fluorometry (2.5.2) and reflecting the cell vitality were already reduced after 6 h in *PPO1* knockout lines and wild type as given in Fig. 3.25B. After 6 h of incubation, photosynthetic activity of PSII was reduced to 65 % in wild type and to 44 % and 43 % for the *PPO1*_ko lines #1 and #5, respectively (related to F_v/F_m at t0). After 24 h of 4-MC incubation a residual photosynthetic capacity of 12 % and 10 % for *PPO1*_ko plants #1 and #5, respectively was measured, whereas for wild type only a 40 % reduction was monitored.

Additionally, cell vitality was determined by fluorescein diacetate (FDA) staining visualised under UV light as described in 2.5.1 (Fig. 3.25C.). FDA staining showed that protonema of 4-MC treated wild type fluoresced green under UV light indicating cell vitality. By contrast, *PPO1*_ko protonema cells appeared red without green fluorescence under UV light and were therefore considered to be dead.

In summary, the methods of macroscopic observation, F_v/F_m monitoring and FDA staining consistently demonstrated, that the *PPO1* knockout protonema was more heavily damaged by the 4-MC application than wild type protonema. Besides, the degree of tissue damage was shown to be dependent on the concentration of 4-MC in the culture medium (Fig. 3.25A. and C.). A concentration of 100 µM 4-MC in the medium caused a more intense damaging of the tissue compared to 50 µM 4-MC.

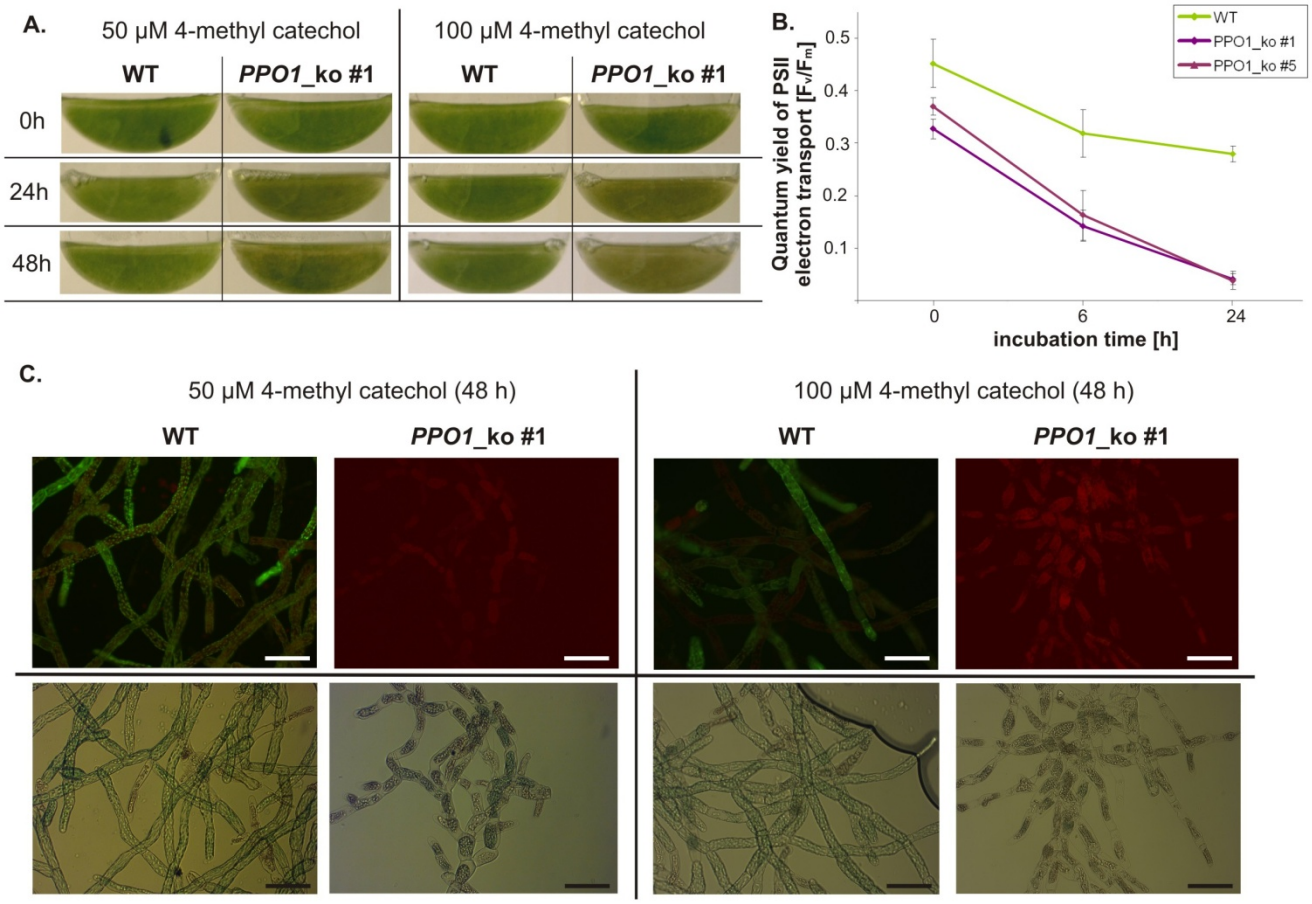

Fig. 3.25 Effect of 4-methyl catechol application on liquid cultures of *PPO1* knockouts and wild type. Protonema was cultivated in a volume of 10 mL in 100 mL flasks under standard conditions with 50 µM 4-MC (left panel in A. and C.) or 100 µM 4-MC (right panel in A. and C.; and B.) as described in 2.2.2 (A.) Macroscopic observation of die back of *PPO1*_ko #1 protonema cultures 24 and 48 h after 4-MC application in comparison to WT. (B.) F_v/F_m values of tissue after 0, 6 and 24 h of incubation with 100 µM 4-MC determined by PAM fluorometry (n=4). (C.) Microscopic analysis of protonema cultivated for 48 h with 4-MC. Upper row: cell vitality of protonema cultivated for of 48 h with 4-MC displayed by FDA staining under UV light. Lower row: Bright light microscopy of the same section as above. The scale bars correspond to 100 µm.

3.7.2.4. General phenotypic analysis of *PPO1* knockout lines

With the aim to analyse possible morphological changes of plants lacking *PPO1*, growth of *PPO1*_ko lines #1, #3, #5, #6 and #8 under standard growth conditions in liquid culture medium (2.2.1) was monitored in comparison to wild type.

Microscopic analysis of liquid cultures revealed protonema of *PPO1*_ko lines consisting of shorter and roundly shaped chloronema cells than wild type protonema (Fig. 3.26). Cell length of *PPO1*_ko plants was approx. 32 % decreased (e.g., *PPO1*_ko #5: 46.5 ±8.3 µM; WT: 69.5 ± 7.4 µM; n=10), whereas the cell width of *PPO1*_ko plants was increased approx. 43 % compared to wild type protonema (e.g., *PPO1*_ko #5: 22.9 ± 3.3 µM; WT: 15.9 ± 1.5 µM; n=10).

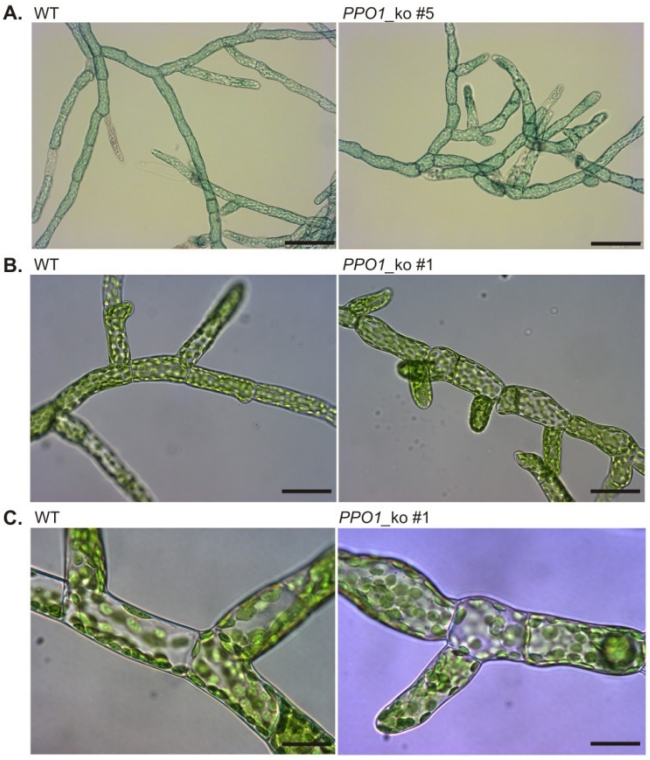

Fig. 3.26 Protonema growth of *PPO1* knockout plants and wild type. Bright field microscopic images of protonema from 3 to 7 day old liquid cultures grown under standard conditions (2.2.1). The scale bars correspond to 100 µm in A.; 50 µm in B. and 20 µm in C.

Furthermore, also developmental changes of the *PPO1* knockout plants grown on solid culture medium under standard conditions were observed. The *PPO1*_ko lines produced notably more gametophores than wild type. The increased gametophore formation was observed for all five analysed *PPO1* knockout lines, shown for the example of 17 day old *PPO1*_ko lines #1 and #5 compared to wild type of the same age in Fig. 3.27.

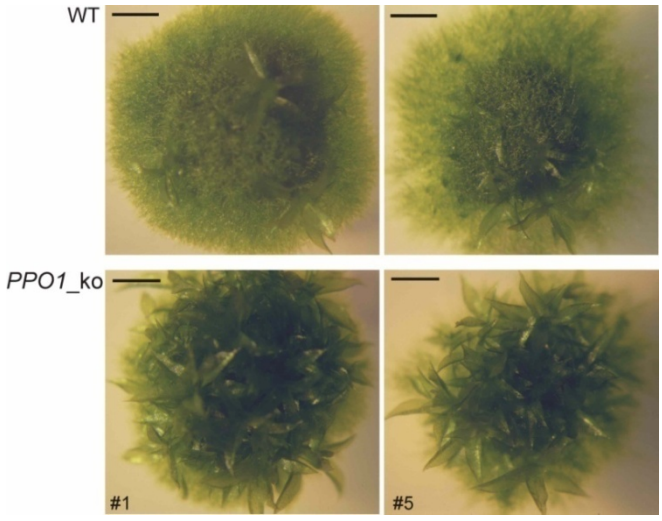

Fig. 3.27 Phenotype of *PPO1* knockout plants and wild type. WT (upper row) and *PPO1* knockout lines #1 and #5 (lower row) of the same age cultivated under standard growth conditions for 17 days on the same ABCNTV culture plate (2.2.1). The scale bars correspond to 1 mm.

To quantify the enhanced gametophore production of *PPO1*_ko plants and wild type, protonema tissue from freshly disintegrated liquid cultures (t0) of both genotypes was used to inoculated solid growth medium (ABCNTV, 2.2.1). The increase of gametophores was monitored over a period of one week by counting the number of gametophores every three days under the stereomicroscope in four observation fields (4 x 3 cm^2) per plate.

That way, it was observed that the number of gametophores significantly increased more rapidly in all five transgenic *PPO1*_ko lines compared to wild type cultures within seven days of cultivation. The number of gametophores per cm^2 counted at day 0, 3 and 7 is displayed in Fig. 3.28 for the example of *PPO1*_ko plants #1 and #5 in comparison to wild type. The relative increase of gametophores from day 0 to day 7 for all *PPO1*_ko lines and wild type is given in the table aside.

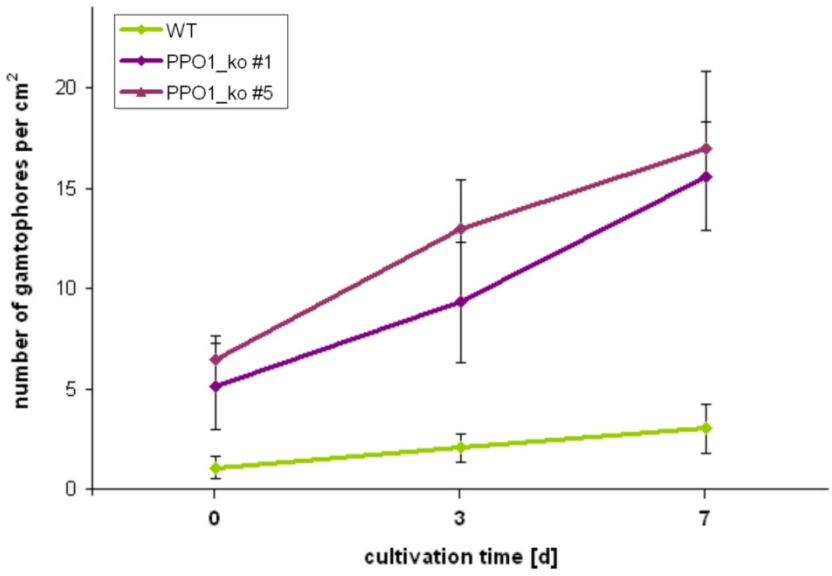

	increase of gametophores/cm^2 within 7 days
WT	1.96 ± 0.81
*PPO1*_ko #1	10.48 ± 1.22
*PPO1*_ko #3	8.75 ± 1.30
*PPO1*_ko #5	10.50 ± 1.36
*PPO1*_ko #6	7.33 ± 1.93
*PPO1*_ko #8	9.42 ± 2.83

Fig. 3.28 Gametophore production of *PPO1* knockout plants and wild type. Freshly disintegrated protonema tissue was transferred to agar plates (d0) and cultivated for 7 days under standard conditions (2.2.1). *PPO1*_ko lines showed an enhanced production of gametophores compared to wild type of the same age. The relative increase of gametophores (per cm^2) formed in *PPO1*_ko lines and wild type within 7 days of cultivation is given in the table aside. (n=16).

3.7.2.5. *In vivo* CKX activity of *PPO1* knockout plants

The increased production of gametophores in *PPO1* knockout plants described in 3.7.2.4 might be caused by an increased cytokinin level related to a decreased cytokinin oxidase/dehydrogenase (CKX) activity. To test whether, *PPO1*_ko lines possessed a reduced CKX activity, *in vivo* feeding experiments using tritiated isopentenyladenine (^{3}H-iP) were performed, and this way *in vivo* CKX activity was determined indirectly (Schwartzenberg *et al.*, 2003).

5 pmol ^{3}H-iP was applied to 7 day old protonema liquid culture of *PPO1*_ko lines #1 and #5 as well as of wild type, and cultures were incubated for 8 h (2.2.4). For each genotype three replicates were incubated and analysed.

Overall radioactivity was determined by liquid scintillation counting of medium samples taken after 0, 2, 4 and 8 h as described in 2.6. The disintegrations per minute (dpm) determined for t0 were defined as 100 % ^{3}H-iP in the culture medium. In Fig. 3.29 the relative radioactivity corresponding to ^{3}H-iP in the culture medium during the incubation time is graphically displayed. As already described in 2.6, ^{3}H-iP is metabolised by CKX to 3-methyl-2-butenal and ^{3}H-adenine, which is rapidly taken up by the plant cell. Thus, in the initial phase of feeding overall radioactivity in the culture medium reflects the amount of radiolabelled iP.

Analysis revealed, that the amount of ^{3}H-iP after 8 h of incubation was significantly higher in culture media of *PPO1*_ko lines #1 and #5 (60 ± 1.8 % and 57.4 ± 3.3 %, respectively) compared to wild type (49.4 % ± 2.3 %). Thus, these results are consistent with the assumption, that *PPO1* knockout plants have a reduced CKX activity compared to wild type.

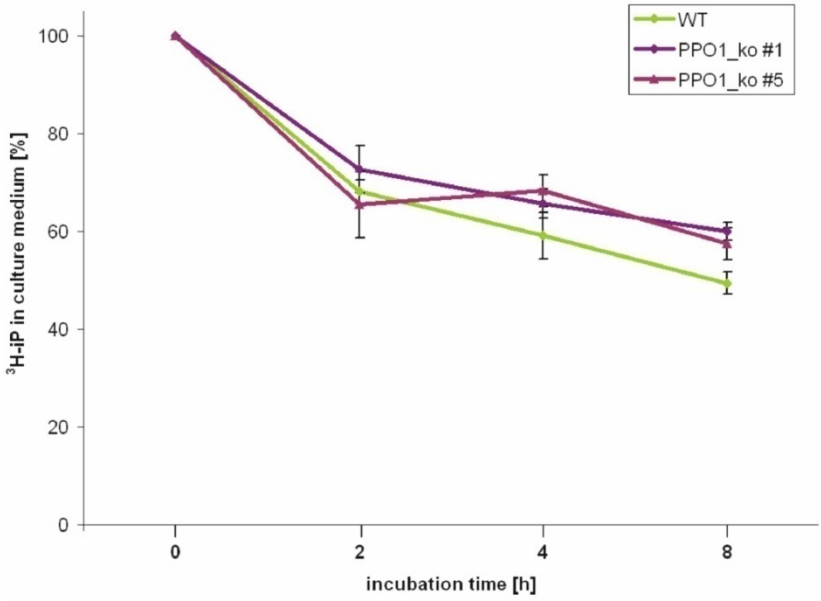

Fig. 3.29 Amount of applied tritiated isopentenyladenine in the culture medium of *Physcomitrella PPO1*_ko plants and wild type in the time course of a culture. Total radioactivity in culture medium was determined by liquid scintillation counting (2.6) and is given here as percentage radiolabelled iP (t0 = 100 %). (n=6)

To verify that the measured overall radioactivity determined from culture medium by liquid scintillation counting corresponded indeed to the tritiated iP, part of the samples was analysed by HPLC-LSC (2.7). The resulting chromatograms, given in Fig. 3.30 for the example of *PPO1*_ko #1 and wild type, demonstrated that the samples contained only one radioactive substance, which co-eluted with the reference substance, tritiated isopentenyladenine (chromatogram not shown). Furthermore, the integration of the ^{3}H-iP peak from each chromatogram confirmed the results obtained by liquid scintillation counting of the overall extracellular radioactivity. In medium of one single wild type culture, the consumption of ^{3}H-iP was higher within 8 h (9562 dpm - 4626 dpm = 4936 dpm, equals 51.6 % iP depletion) than in medium of one single *PPO1*_ko #1 culture (8159 dpm - 6183 dpm = 1976 dpm, equals 24.2 % iP depletion).

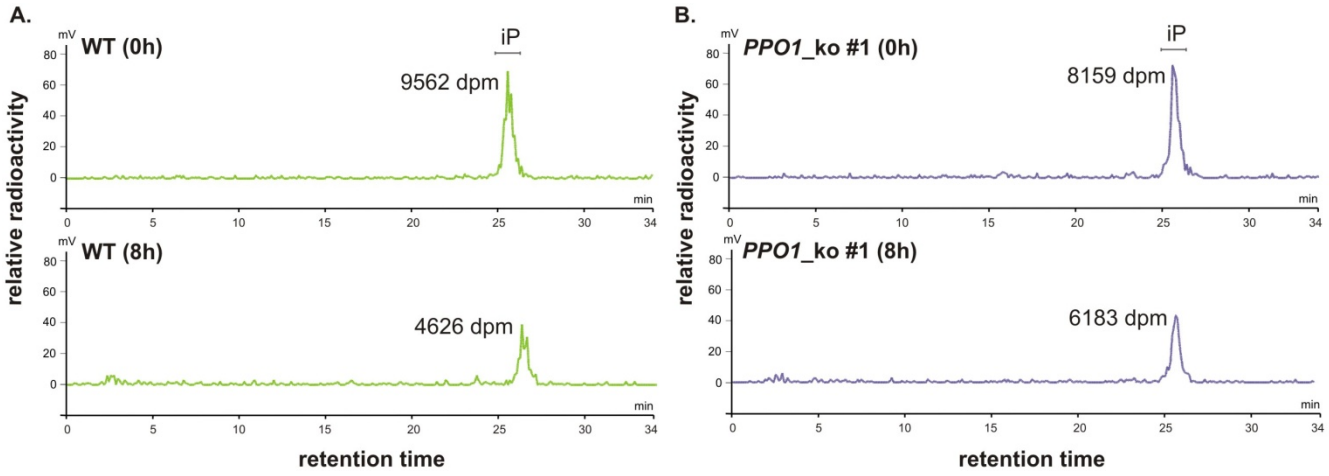

Fig. 3.30 HPLC-LSC based quantification of ^{3}H-iP in culture medium of wild type (A.) and *PPO1*_ko line #1 (B.) Measurements (2.7) were performed directly after application of radiolabelled iP (0 h) and after 8 h of incubation (8 h) (2.2.4). Dpm correspond to the iP peak after integration of the radioactivity profile.

These data strengthen the conclusions derived from measurements of overall radioactivity (Fig. 3.29) and demonstrate a lower cytokinin breakdown in *PPO1* knockout lines compared to wild type under the given experimental conditions.

4. DISCUSSION

In the field of PPO research a main focus was put on seed plant PPOs, and numerous publications exist on gene and protein characterisation of these PPOs. Although several different functions were attributed for PPOs in different organisms, a general function could not be related to PPO. In order to obtain more information on land plant PPOs, this research aimed to identify and characterise PPOs of the bryophyte *Physcomitrella* having evolved 450 million years ago.

In this work it was demonstrated, that *Physcomitrella* possesses intra- and extracellular PPO activity and a large *PPO* gene family. Analysis of the architecture and the transcriptional regulation of the *PPO* genes revealed the *Physcomitrella PPO* gene family to share several characteristics with seed plant PPOs, but at the same time differing from these in gene and protein properties. These results are discussed with respect to the evolutionary position of *Physcomitrella* within the green land plant lineage, and with a focus on the development of PPO regarding regulation and possible functions in the bryophyte.

4.1. PPO activity from *Physcomitrella* tissue and culture medium

Initially, it was aimed to elucidate, whether the bryophyte *Physcomitrella* possesses *o*-diphenol oxidase (PPO) activity as described for numerous seed plants. Very little information has so far been published on PPOs in mosses. The genera *Dicranum, Sphagnum and Thuidium* exhibit no PPO activity as demonstrated within a study performed by Sherman *et al.* (1991). In contrast, the moss *Funaria hygrometrica* possesses PPO activity as determined photometrically (Kapoor and Bhatla, 1999).

Physcomitrella *exhibits PPO activity*

PPO activity in gametophytic tissue of *Physcomitrella* was determined polarographically using 4-methyl catechol as a substrate and was further shown to change during the time course of a culture (Richter *et al.*, 2005).

Yet, only little specific PPO activities from tissue extracts were measurable. Defining the specific PPO activity as 1 unit equalling 1 µmol O_2 consumption per min, activities of 0.0016 units/mg protein for tissue cultured for 20 days were obtained. Compared to PPO activities in *Vicia faba* leaf extracts (0.7 units/mg protein) (Robinson and Dry, 1992) and in *Vitis vinifera* leaf extracts (0.4 units/mg protein) (Dry and Robinson, 1994), *Physcomitrella* possesses only little intracellular PPO activity.

Portion of total PPO activity is secreted to the culture medium

Moreover, PPO activity was also determined from protein extracts derived from extracellular culture medium (3.2). Interestingly, higher specific PPO activities (0.026 units/mg protein) were detected from extracellular protein extracts and already suggest an extracellular targeting of PPO.

PPO activity from *Physcomitrella* tissue or medium extracts was measured in the presence of SDS (final concentration 0.3 % in the reaction assay). It was assumed, that the addition of SDS to the reaction assay leads to a membrane detachment releasing membrane-bound PPO and thereby causing higher enzyme activities (Richter *et al.*, 2005). In contrast, Kanade *et al.* (2006) proposed a general activation of the PPO protein due to unfolding of the protein to a certain stage, making the protein more active for substrate turnover. This unfolding is certainly only possible up to a critical concentration of SDS in the reaction assay, high concentrations of SDS would lead to a total denaturation of the protein. The fact that the addition of SDS increased the PPO activity also in extracellular protein extracts, where no membrane fragments are present, suggests an SDS mediated activation of the PPO protein by mild denaturation.

4.2. Comparison of the moss *PPO* gene family with PPOs from vascular plants

To further analyse PPO in *Physcomitrella*, the *PPO* gene family was identified from the sequenced *Physcomitrella* genome, and detailed analysis of the gene structure and architecture as well as organisation and phylogeny of the gene family was conducted (3.3).

Defining the Physcomitrella PPO *gene family – Evidence for* PPO13 *being a pseudogene*

From the sequenced *Physcomitrella* genome, initially 15 gene models with similarities to PpPPO1 and plant PPOs were identified.

As already mentioned, the gene models of *PPO14* and *PPO15* were found to be incomplete and were therefore excluded from further studies. As a result, it was concluded that *Physcomitrella* possesses 13 putative *PPO* genes. However, due to the different gene structure of *PPO13*, missing EST support and a disputable position within three differently calculated phylogenetic trees, it is assumed that *PPO13* is a pseudogene. Phylogenetic analysis was carried out with the gene model of *PPO13* described above, however, it has to be mentioned that this gene model of *PPO13* can be fused to another gene model upstream on the scaffold (*all_Phypa_7364*), resulting in a longer amino acid sequence at the N-terminus. Using this fused gene model for phylogenetic tree construction, *PPO13* was still in an isolated and questionable

position within the phylogenetic tree not being in line with the other *Physcomitrella PPO* gene family members.

Based on these observations, it is finally concluded that *Physcomitrella* possesses a *PPO* gene family with 12 expressed members. For the above mentioned reasons, the 13th member is considered to be a pseudogene and thus, designated as *psPPO13* in the following.

Physcomitrella *possesses a large, monophyletic* PPO *gene family*

Detailed analysis of the gene family organisation and phylogenetic analysis revealed that *Physcomitrella* possesses 12 paralogous *PPO* genes that are arranged as a monophyletic clade (Fig. 4.1). Hence, *PPO* gene duplication in *Physcomitrella* occurred after separation from the seed plant lineage.

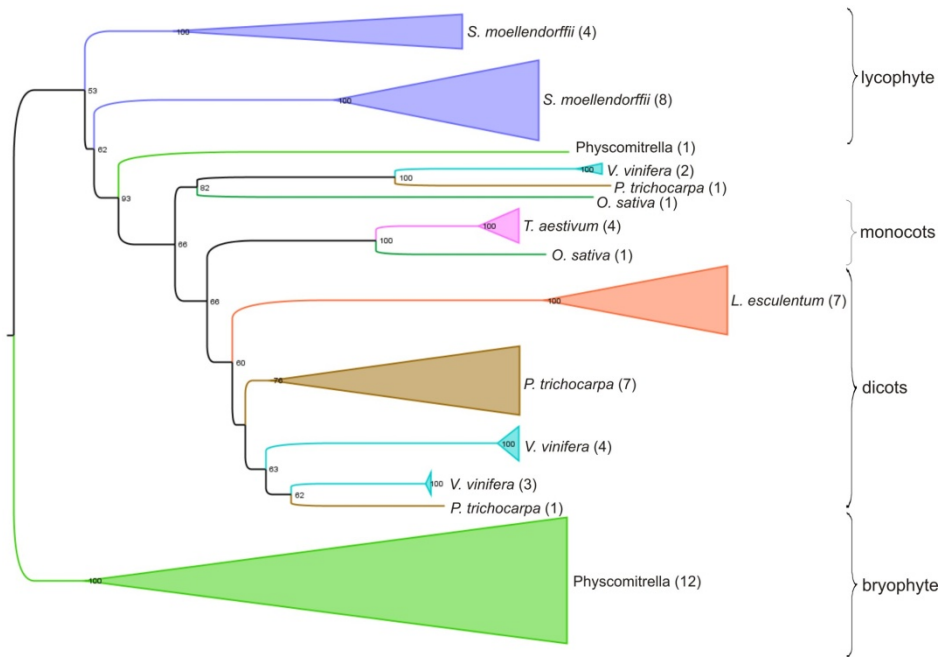

Fig. 4.1 Schematic tree of the *PPO* gene families of the bryophyte *Physcomitrella* and vascular plants (*S. moellendorffii*, monocotyledonous and dicotyledonous plants). *PPO* gene families are displayed schematically as triangles. Numbers in brackets behind the species name indicate the number of *PPO* genes within one clade.

The *PPO* gene families of the *Physcomitrella* genome and of the club moss *S. moellendorffii* were found to be the largest compared to all other analysed *PPO* gene families in this study. *PPO* gene families of seed plants were found to be more condensed with two to nine gene family members. With respect to the evolutionary position it can be assumed, that *PPO* genes expanded to a greater extent in organisms with a more basal position in evolution than in organisms developed later in evolution.

As the *Physcomitrella PPO* gene family is represented as a monophyletic group with paralogous genes, it is most likely that *Physcomitrella* inherited one primal *PPO* gene, which expanded by gene and genome duplication to a large gene family. Regarding the polyphyletic *PPO* gene families of seed plants and *S. moellendorffii*, it can be assumed that these plants originally obtained more *PPO* ancestors, which evolved independently in different plant lines.

PPO gene duplication within the *Physcomitrella* genome occurred most likely six times. As one whole-genome duplication occurred approximately 45 million years ago (Rensing *et al.*, 2007), the sixth node in the *PPO* gene family formation (green node in Fig. 3.5) forming PPO1/PPO2, PPO3/PPO7, PPO5/PPO6, PPO8/PPO10, PPO11/PPO12 might correspond to this genome duplication. The groups comprising three *PPO* genes, PPO4/[5/6] and PPO9/[8/10], might have lost one *PPO* gene formed in the whole-genome duplication.

As indicated by the branch length within the phylogenetic tree, the formation of *PPO* gene families by gene and genome duplications occurred later in *S. moellendorffii* and seed plants, reflecting the earlier occurrence of *Physcomitrella* in evolution. However, it should be noted that mosses are evolving on average 2 -3 fold slower compared to seed plant (Stenøien, 2008).

PPOs evolved with the conquest of land

Interestingly, neither *o*-diphenol oxidases and laccases nor tyrosinases were found in the sequenced genomes of the green algae *C. reinhardtii* and *O. tauri*. Hence, it is most likely that *o*-diphenol oxidases (PPO) encoding genes newly occurred during the evolution of land plants (Fig. 4.2). A potential bacterial origin will be discussed later in this section.

As reviewed by Lang and co-authors (2008), the adaptation of the first land plants to harsh conditions such as (UV) radiation, floating and desiccation caused substantial changes in morphology and regulatory processes leading to the development of newly generated pathways in *Physcomitrella* (Lang *et al.*, 2008). Sherman *et al.* (1991) analysed the distribution of PPO activity in a broad variety of aquatic and terrestrial plant species (summarised in Fig. 4.2) and proposed that PPOs may have developed simultaneously with the adaptation to oxygenated atmosphere.

As mentioned, the water to land transition was also accompanied by an enhanced exposure to light radiation (including UV), a newly occurring stress factor for plants. Influence of strong light irradiation on *PPO* gene expression in *Physcomitrella* was therefore analysed in this research and will be discussed later (4.4).

The occurrence of *o*-diphenol oxidases with the water to land transition might point towards an early function of PPOs in land plants, developing further in higher organisation forms and evolved to perform diverse functions in different plant species. Thus, characterisation of the *PPO* gene family of *Physcomitrella*, exhibiting an important position in land plant evolution, opens new possibilities to obtain information on potential and probably more original function(s) of PPOs. Involvements of *Physcomitrella* PPOs in potential functions are further discussed in the summarising section 4.8.

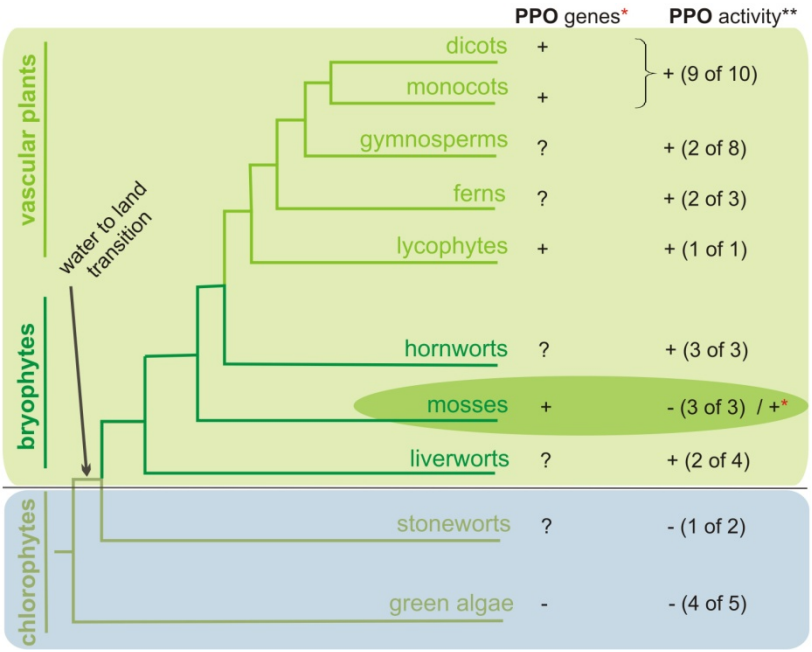

Fig. 4.2 Schematic phylogenetic relationship among plants and the occurrence of *PPO* genes and *o*-diphenol oxidase activity. Data obtained from this work are marked by a red asterisk. Data on PPO activity from a study of Sherman *et al.* (1991) are marked by two black asterisks, displaying how many of the analysed species exhibited activity (+) or exhibited no activity (-).

Although *o*-diphenol oxidases might not have evolved until the conquest of land, laccases and tyrosinases occurred earlier in evolution. Numerous tyrosinase and laccase genes have been characterised from several fungi, e.g., from *Trichoderma reesei* (Selinheimo *et al.*, 2006) and *Pycnoporus sanguineus* (Halaouli *et al.*, 2006). Also several bacteria possess laccases and tyrosinases, e.g., the plant pathogen *Ralstonia solanacearum* (Hernandez-Romero *et al.*, 2005) and the marine bacterium *Marinomonas mediterranea*, the latter with a multipotent laccase (Sanchez-Amat *et al.*, 2001). Hence, it can be speculated that the *o*-diphenol oxidases, which apparently have newly occurred in land plants, derived from bacterial tyrosinases.

Surprisingly, *Arabidopsis* does not possess *o*-diphenol oxidases, but is known to have a large laccase gene family (first described by McCaig *et al.*, 2005). Nevertheless, 4-methyl catechol conversion was observed in polarographic enzyme assays with tissue extracts (data not shown).

Possibly, this conversion was mediated by laccase gene products. Hence, in *Arabidopsis* the subclass of laccases might account for PPO activity.

Moreover, genome analysis revealed that *Physcomitrella* also possesses three putative laccase encoding genes. No tyrosinase encoding genes were found in the *Physcomitrella* genome. Consequently, *Physcomitrella* possesses two types of enzymes from the extended group of polyphenol oxidases, three *p*-diphenol oxidases (laccases) and 12 *o*-diphenol oxidases. In the current study, analysis was focussed on the characterisation of *o*-diphenol oxidases; therefore no assumptions are made regarding regulatory mechanisms or possible functions of *Physcomitrella* laccases at this point.

Intron/exon structure of PpPPOs *with respect to phylogeny*

On genomic level, eight *Physcomitrella PPO* genes do contain one small intron at corresponding positions downstream of the CuB encoding region; *PPO7* possesses an additional intron downstream of its first intron. In contrast, the pseudogene *psPPO13* contains a large intron located within the region encoding for CuA. Four *PPO* genes were found to be intronless, three of these being in the same group (group 5 with PPO8/PPO9/PPO10). Thus, within the *Physcomitrella PPO* gene family the intron/exon structure partially corresponds to the clustering of PPOs established by amino acid sequence alignment.

In comparison, *PPO* genes characterised from dicotyledonous seed plants e.g. tomato, potato, and apple are reported to contain no introns (Newman *et al.*, 1993; Thygesen *et al.*, 1995 and Haruta *et al.*, 1998), whereas *PPO* genes from monocotyledonous plants like banana (Gooding *et al.*, 2001) and pineapple (Zhou *et al.*, 2003) possess one short intron. Wheat *PPO* genes possess two small introns (Sun *et al.*, 2005). A comparison of the intron position of the *Physcomitrella PPO* genes with the intron positions of *PPO* genes from monocots, revealed that they are located at corresponding positions downstream of the CuB encoding region.

Analysis of the 12 putative *PPO* gene models from *S. moellendorffii* available on the JGI genome browser revealed that six *PPO* genes possess one intron (48 bp to 144 bp) located downstream of the CuB encoding region. The other six gene models contain two small introns: one at the same corresponding position, the second intron in between the regions encoding for CuA and CuB.

Massa *et al.* (2007) suggested that the insertion of introns in *PPO* genes occurred after divergence of monocots and dicots; however, this assumption may have to be revised, due to the

observation that *Physcomitrella* and *S. moellendorffii* already possess *PPO* genes with introns. Correlating the results of this study with the phylogenetic position of the analysed plants, it can be stated that certain primordial *PPO* genes already possessed intron(s). In case of transmission of these *PPO*s to the dicotyledonous line, introns obviously have been removed from *PPO* genes.

Distribution of PPO *sequences in the genome*

Analysing the organisation of the *PPO* genes within the *Physcomitrella* genome revealed that *PPO6* and *PPO12* are located *tail to tail* on the same scaffold (No. 83) separated by 15 kbp, accordingly those loci are located relatively close to each other on the same chromosome. Assuming that the adjacent location of *PPO6* and *PPO12* resulted from gene duplication, their phylogenetic position suggests that this event occurred early in gene family formation. Clustering of the *Physcomitrella* PPOs demonstrated that *PPO6* and *PPO12* are members of two different groups (group 3 and 4), but belong to the same upper-level grouping.

Moreover, *PPO7* and *PPO10* are localised on one scaffold (No. 3) *head to head*, hence, on the same chromosome but approximately 1.89 Mbp apart from each other. Besides very early gene duplication, other events like translocation of chromosomal parts must be taken into account in order to explain the vicinity of *PPO7* and *PPO10*.

Although the pairs *PPO7/PPO10* and *PPO6/PPO12* are located presumably on the same chromosome, they cannot be defined as tandemly arrayed genes (TAGs), as according to Rensing *et al.* (2008), TAGs are indeed highly conserved (sharing up to 99% identity on nucleotide level).

Protein properties of PPOs from Physcomitrella *compared to PPOs from other plant species*

Amino acid sequences of PPO1 to PPO12 were analysed in order to compare PPOs within the *Physcomitrella* gene family as well as across different plant species (3.3.2). Overall identities within the *Physcomitrella* PPO family were lower, compared to identities of PPO family members within one seed plants species and *S. moellendorffii*. Also across different species, *Physcomitrella* PPOs share fewer similarities on amino acid level with other plants. Hence, more diversity within the PPO family from *Physcomitrella* and more distant relationship of PpPPO to *S. moellendorffii* and seed plant PPOs was observed, the latter being highly conserved even across species. Thus, with the identification and characterisation of the *Physcomitrella PPO* gene family, a more basal *PPO* gene family with probably different functions was identified.

Physcomitrella PPOs differ from seed plant PPOs in the predicted targeting and localisation of the proteins. Using bioinformatic applications to predict N-terminal target peptides within the protein sequence, 10 of 12 PPOs were predicted to possess a short N-terminal signal sequences targeting the proteins to the secretory pathway. Localisation of *Physcomitrella* PPOs was further specified predicting the PPOs to be targeted to the plasma membrane, the Golgi apparatus, the ER or the extracellular space. However, all predictions were based on computational analysis of the amino acid sequence and might therefore differ *in vivo*. As discussed in 4.1, the occurrence of detectable PPO activity in the culture medium already pointed towards an extracellular targeting of *Physcomitrella* PPOs. The localisation of *Physcomitrella* PPOs will be discussed in section 4.7, and detailed experimental analysis of the PPO targets is aimed to be further carried out (perspectives 4.9).

Furthermore, phylogenetic analysis of the extended group of polyphenol oxidases revealed that the identified *Physcomitrella* PPOs clustered together with the selected *o*-diphenol oxidases from seed plants and *S. moellendorffii*, but not with the *Arabidopsis* laccases or fungal tyrosinases. Comparison of *Physcomitrella* PPOs with *Arabidopsis* laccases and putative laccases of *Physcomitrella* as well as with fungal tyrosinases yielded in 2- to 3-fold lower percentage identities compared to *o*-diphenol oxidases. Besides, conserved domain search within the amino acid sequence of the PPOs from *Physcomitrella* revealed that all members of the gene family possess the two copper-binding domains CuA and CuB each with three conserved histidines at the same corresponding positions.

Thus, already by sequence comparison and phylogenetic analysis it was strongly presumed, that the identified putative *PPO* genes from *Physcomitrella* encode for *o*-diphenol oxidases. PPO function was proven for the example of *PPO11* and will be discussed in the following section.

4.3. Functional evidence for *PPO11* encoding for an *o*-diphenol oxidase

Even so PPO activity could be detected from *Physcomitrella* tissue and culture medium, functional evidence for the putative *PPO* genes as *o*-diphenol oxidase needed to be proven as a necessary prerequisite for further analyses. Thus, two of the characterised *PPO* genes, *PPO1* and *PPO11*, were chosen exemplary and expressed in *E. coli*, in order to obtain recombinant protein usable for *in vitro* PPO activity assays (3.4).

In vitro *PPO activity from* PPO11 *expressing* E. coli *clones*

The functional evidence could be adduced for the example of *PPO11*. The purified recombinant protein expressed in *E. coli* possessed the ability to oxidise 4-methyl catechol, hence having *o*-diphenol oxidase activity. Thereby the functionality of a *PPO* gene family member of *Physcomitrella* was unequivocally proven, which is the first report on functionality of a bryophyte *PPO* gene.

Unfortunately, only a little amount of soluble PPO11 protein could be obtained from heterologous expression in *E. coli*. Moreover, the extracts exhibited only low PPO activities compared to the PPO11 protein amount used in the polarographic assay. Thus, no further studies on substrate specificity could be carried out in this work.

Similar observations were made earlier by other researchers having expressed plant PPOs in *E. coli*. Haruta *et al.* (1998) expressed an apple PPO in *E. coli* and obtained recombinant protein, which showed no *in vitro* PPO activity at all. The authors proposed that a proper folding of the protein to bind Cu^{2+}, which is essential to obtain active PPO, did obviously not occur under their experimental conditions. However, Sullivan *et al.* (2004) could obtain a small amount of soluble *Trifolium pratense* PPO (TpPPO1) expressed in *E. coli* with measurable *in vitro* PPO activity. *E. coli* clones expressing this *TpPPO1* were also used as a positive control monitoring proper expression conditions in this study, and protein extracts exhibited *in vitro* PPO activity under identical experimental conditions used for *PpPPO11* expression. Nevertheless, as already observed by Sullivan *et al.* (2004), TpPPO1, like PpPPO11, exhibited only little PPO activities relative to the amount of protein used for the assay. Therefore, it can be assumed, that PPOs from *Physcomitrella*, as from higher plants, need to be modified properly after translation to generate a highly active PPO enzyme, although PPO with limited levels of enzyme activity can be produced in a prokaryotic expression system.

To obtain a sufficient amount of active, properly folded recombinant *Physcomitrella* PPO protein, a eukaryotic expression system, such as *Pichia pastoris* or *Physcomitrella* itself should be used instead (perspectives 4.9).

Difficulties expressing recombinant PPO1 *in heterologous systems*

During experiments to generate recombinant protein, no soluble PPO1 protein could be obtained using the same expression system as for PPO11 production. The inability to express PPO1 was already observed earlier using prokaryotic as well as eukaryotic expression systems (data not

shown). No recombinant PPO1 could be obtained by heterologous expression in *E. coli*, *Saccharomyces cerevisiae* and *Pichia pastoris,* although *PPO1* mRNAs were detectable. Summarising, it is suggested that PPO1 might possesses certain sequence properties on either RNA level, which could be responsible for the fast degradation of overexpressed transcript, or on protein level resulting in instabilities and thereby failing protein expression.

Nevertheless, functional evidence for one of the *Physcomitrella PPO* gene family members encoding for an *o*-diphenol oxidase was clearly given by the heterologous expression of *PPO11*, as described above in this section.

4.4. Differential expression of *PPO1-12* under different cultivation conditions

PPO gene family members from seed plants are known to be differentially expressed regarding spatial and temporally distribution. For example, potato *PPO* gene expression was found to be highest in young, developing tissue and declined during further development (Thygesen *et al.*, 1995). Often no transcription was detectable in late stages of plant development as demonstrated for PPO from *Prunus armeniaca* (e.g. Chevalier *et al.*, 1999). Moreover, *PPO* transcription is differentially regulated also concerning spatial distribution: Sullivan *et al.* (2004) showed that the *PPO* genes of *Trifolium pratense* are differently expressed, each being predominant in a certain stage, e.g. *TpPPO1* in young leaves, *TpPPO2* in flowers and petioles.

Because *Physcomitrella* possesses a large *PPO* gene family with 12 members, the question arose, whether these genes are also differentially expressed under standard conditions. As known from recent literature, plant PPOs and PPO-mediated reactions are supposed to be involved in several stress responses, such as drought stress (Thipyapong *et al.*, 2004b) or UV irradiation (Mahdavian *et al.*, 2008; Kondo and Kawashima, 2000), transcription profiles of the 12 *Physcomitrella PPO* gene family members were further analysed under certain stress conditions. *PPO* transcription levels were determined by real-time RT-PCRs using gene specific primers for each *PPO* gene.

In contrast to published data with *PPO* expression profiles mainly derived from sporophytic tissue of seed plants, *PPO* transcription levels in *Physcomitrella* were experimentally analysed in gametophytic tissue, the predominant phase of mosses. However, a comparison between the *PPO* expression patterns of gametophytic tissue from *Physcomitrella* with that of sporophytic tissue

from seed plant, seems reasonable, as in both cases the analysed material represents the vegetative tissue of the predominant phase.

Methodical discussion of real-time PCR experiments

Before discussing the results obtained from real-time RT-PCR experiments, the method for determination of transcript levels itself should be evaluated.

Prior to the determination of transcript amounts by real-time RT-PCR, some essential requirements needed to be tested: At first, design and selection of each different primer pair ensured that the length of amplicons had similar sizes (ranging from 200 to 300 bp) for *PPO1* to *PPO12* as well as for *ACT3*. Secondly, the gene specificity for each primer pair was confirmed by sequencing each PCR product amplified under real-time PCR conditions. Sequencing results revealed highly specific amplifications, as expected for each primer pair. A third and highly important prerequisite for the comparability of results from different real-time PCRs, is the similar PCR efficiency of each primer pair. PCR efficiencies were determined for each primer pair revealing values between 95 % and 99 %, thus, ensuring the comparability between PCR reactions with different primer pairs. Furthermore, high quality RNA and equal amounts of RNA used for cDNA synthesis were ensured by agarose gel electrophoresis and spectrophotometrical determinations.

After having checked all methodical prerequisites for the real-time PCR-based transcript analysis, a correction of raw data was performed. To ensure that different CT values obtained from different samples did not result from different cDNA qualities or PCR efficiencies, correction based on both, CT values for *ACT3* mRNA as well as on CT values obtained with genomic DNA as template, was performed.

PPO *gene family members are differentially expressed under standard growth conditions*

The analysed *PPO* gene family members were found to be differentially expressed in gametophytic tissue under standard growth conditions (3.5.1). *PPO1* was found to have the highest expression level; three *PPO* genes (*PPO7, -8,* and *-10*) were not expressed in 8 day old protonema.

In Fig. 4.3 the data obtained for *PPO* transcript amounts from tissue of different age from three different experiments performed in this work were combined. Mean values obtained for

PPO transcript levels under standard growth conditions were taken from experiments, in which 3, 5 and 8 day old tissue was analysed (3.5.1 - 3.5.3), and assembled to one figure presenting the expression pattern of each *PPO* gene family member in the time course of a *Physcomitrella* protonema culture.

From this graph it becomes apparent, that the expression pattern for each *PPO* gene changes drastically within the time course of a culture, thus, depending on the age of the tissue.

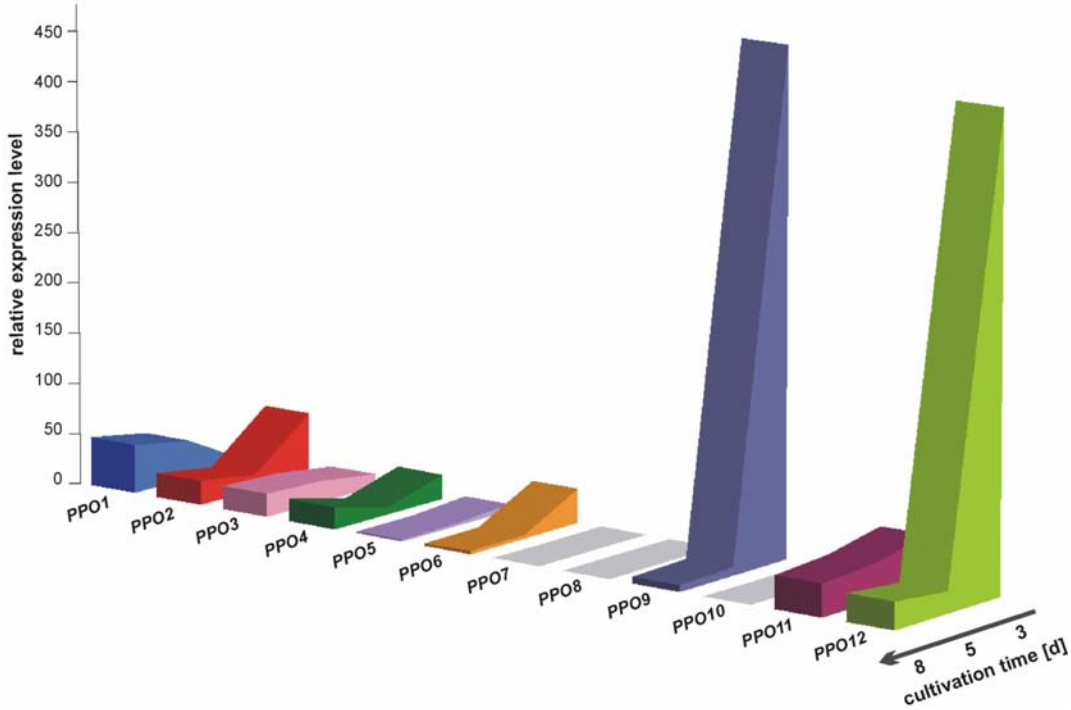

Fig. 4.3 *PPO1* to *PPO12* expression level in protonema grown for 3, 5, and 8 days under standard cultivation conditions. Average values taken from real-time RT-PCR experiments described in 3.5.3 (3 d; n=3), 3.5.2 (5 d, n=2) and 3.5.1 (8 d, n=3). *PPO7, -8* and *-10* were not expressed under standard condition.

Moreover, regarding the overall *PPO* expression level, the amount of *PPO* transcripts was found to be highest in youngest tissue (3 day old), mainly due to high *PPO9* and *-12* expression, decreasing strongly to a moderate expression level with more equally distributed transcript amounts. This pattern was similar to that observed for expression levels of seed plant *PPO* genes. Not only general changes in *PPO* expression levels are comparable to seed plants, also the fact that the highest *PPO* expression levels were detected in youngest tissue (e.g., as described for potato *PPO* genes by Thygesen *et al.* (1995) or for apricot *PPO* genes by Chevalier *et al.* (1999), details see above).

Hence, *PPO2, -4, -5, -6, -9, -11,* and *-12*, were found to have similar expression patterns as many seed plant PPOs, whereas *PPO1* and *PPO3* exhibited a reverse expression pattern with higher transcript levels in older protonema tissue.

Further analyses counting the number of ESTs for each *PPO* gene revealed highest EST frequencies for *PPO11*, followed by *PPO9* and *PPO1*. ESTs from databases derived from sporophytic tissue were found for the four *PPO* genes, *PPO7, -8, -9* and *-12*. Thus, besides changes in *PPO* gene expression during the time course (Fig. 4.3), the *PPO* gene family expression pattern also changes depending on the vegetative or regenerative phase, suggesting potentially different functions or substrate specificities of the different *PPO* genes.

Determined EST frequencies strongly differed from transcription levels measured by real-time RT-PCR for each *PPO* gene. However, as the ESTs derived from a huge cDNA collection of different ages and types of tissue, unlike the experimental data analysed for a specific protonemal stage, the real-time RT-PCR-based expression levels cannot be compared directly with the EST frequencies obtained for each *PPO* gene.

Expression pattern changes drastically under strong light irradiation and PPO *gene family members react differently to strong light exposure*

As mentioned above in this section, PPO-mediated reactions are supposed to be involved in strong light stress response. Thus, *PPO* gene expression patterns were further determined in strong light irradiated *Physcomitrella* tissue (~1000 µmol $m^{-2}s^{-1}$) (3.5.2). Control experiments monitoring the photosynthetic activity by F_v/F_m measurements of irradiated tissue demonstrated, that the strong light intensities caused a certain stress for *Physcomitrella* protonema; however, tissue was not irreversible damaged, as PSII activity could be restored after a regeneration period under standard conditions.

Determination of *PPO* transcription levels in strong light irradiated tissue revealed different reaction patterns of *PPO* gene expression. Three major groups were identified: *PPO4* and *PPO12* were highly upregulated, *PPO10* was only transcribed under strong light conditions, and *PPO1, -2,* and *-3* were strongly downregulated under strong light. The other *PPO* genes reacted with only minor transcript changes to the strong light treatment.

Interestingly, the observed changes in *PPO* gene expression in the light treated tissue were not reflected by significant changes in the overall PPO activity. So far it is not known precisely how *PPO* gene expression contributes to PPO regulation, since PPO protein in plants is known to exhibit certain persistence. For example, Chevalier *et al.* (1999) demonstrated that apricot PPO was still present and active at an advanced stage of fruit development, although its mRNA could

not be detected. Nevertheless, an early response of PPOs to stress conditions might be only detectable by analysing transcript levels and not by measuring PPO activity. Furthermore, a differentiation between different reactions of the 12 different *PPO* gene family members to modified conditions is only possible by analysing transcriptional changes.

Although transcription levels of some *PPO* genes were decreased under high light mediated stress, the overall *PPO* transcript level increased in strong light exposed tissue. Thus, regarding the overall *PPO* transcript level, a positive correlation to strong light irradiation was observed. So far, it is not possible to conclude, if the positively correlated response of *PPO* genes to strong light stress might have a protective effect for *Physcomitrella*.

No information regarding changes of *PPO* gene expression patterns after strong light irradiation in seed plants is available yet. However, PPO activity has been suggested to be involved in strong light protection. Mahdavian *et al.* (2008) observed increased PPO activities in leafs and roots of UV-B and UV-C treated *Capsicum annuum* tissue and proposed that PPO scavenges free radicals produced under stress conditions. Lavola *et al.* (2000) described an increased PPO activity in birch seedlings exposed to UV-B radiation in combination with elevated CO_2 exposure. In contrast, Balakumar *et al.* (1997) observed decreased PPO activities in leafs of UV-B treated tomato plants and proposed that the reduced PPO activities contribute to the maintenance of high levels of phenolic compounds acting as antioxidants.

Further experiments are needed, in order to elucidate a causal connection of transcriptional changes of *PPO* gene family members in *Physcomitrella* in response to stress caused by strong light exposure (perspectives 4.9).

PPO *expression pattern changes in the presence of caffeic acid*

The application of caffeic acid (CA) to the *Physcomitrella* culture medium inhibited protonema growth and caused browning of the culture medium (3.5.3). In contrast, CA-containing medium without tissue did not turn brown. Moreover, considerable extracellular CA consumption in protonema cultures was monitored spectrophotometrically within 3 days of cultivation (data not shown). These observations led to the assumption that CA applied to the culture medium, can be metabolised by certain PPOs produced (and secreted) by *Physcomitrella*.

Bollag *et al.* (1988) described that the exogenous applied growth inhibiting phenols 2,6-xylenol and *p*-cresol can be detoxified by an extracellular laccase of the fungus *Rhizoctonia praticola*. Moreover, transgenic *Arabidopsis* seedlings expressing a secreted laccase from *Gossypium arboreum* exhibited an enhanced resistance to certain growth inhibiting phenolic compounds, proposing an ecological role of laccase for transforming phenolic pollutants *ex planta* without uptake of the substance by the plant (Wang *et al.*, 2004).

So far, no studies have examined *PPO* expression levels in plants in the presence of extracellulary applied phenolic substances. However, it can be assumed that *PPO* expression is increased after addition of a phenolic compound due to substrate induction.

In this work, *PPO* expression was determined from *Physcomitrella* tissue cultivated in the presence of the putative PPO substrate caffeic acid (3.5.3). Real-time RT-PCR analysis revealed changes in *PPO* transcript levels. *PPO* genes reacted differently to the CA application, with increase of transcript levels of *PPO1* (and *-12*) and decrease of transcript levels of *PPO2, -3, -4, -5, -6, -9, and -11*; *PPO8* transcripts were only detected in CA treated tissue.

Taken together, changes in expression pattern of *PPO* genes suggested that only *PPO1, PPO8* (and eventually *PPO12*) might be involved in detoxification, as their transcript levels were found to be increased in the presence of CA.

Further experiments involving different phenolic compounds, are needed to elucidate the causal connection between substrate application and modulation of *PPO* gene expression (perspectives 4.9).

4.5. Phenolic compounds are inducible in *Physcomitrella*

So far, very little is known about phenolic compounds and flavonoids in *Physcomitrella* (see Asakawa, 1995). However, a large gene family encoding for putative chalcone synthases has been identified (Jiang *et al.*, 2006), suggesting the presence of flavonoids in *Physcomitrella*.

Phenolics are minor compounds in Physcomitrella *tissue cultivated under standard* in vitro *conditions*

In this work it was aimed to identify possible PPO substrates from *Physcomitrella* tissue (3.6.1). Astonishingly, no phenolic compounds were detectable and measurable by (LC-MS) HPLC analysis in extracts of *in vitro* cultivated protonema tissue. This leads to the conclusion, that polyphenols are not enriched in *Physcomitrella* standard *in vitro* cultures.

The fact that no polyphenols could be detected from *Physcomitrella* tissue, might be due to the *in vitro* cultivation conditions which included little light intensities (~50 µmol $m^{-2}s^{-1}$) and optimal supply with nutrients. It is possible that under natural growth conditions, field-grown *Physcomitrella* produces measurable amounts of phenolic substances.

As mentioned before, *Physcomitrella* possesses chalcone synthases, catalysing the first step in flavonoid biosynthesis (Jiang *et al.*, 2006). Further searches for phenylalanine ammonia-lyase (PAL) genes in genomic databases performed in this study revealed the presence of several putative *PAL* genes in the *Physcomitrella* genome (results not shown). Consequently, as PAL is a key enzyme in the polyphenol synthesis (Boudet, 2007), *Physcomitrella* possesses the general ability and a set of enzymes to synthesise simple phenolic compounds and flavonoids.

So far, nothing is known about possible functions of polyphenols in the bryophyte *Physcomitrella*. In seed plants, however, phenolic compounds have diverse functions such as protection from herbivores, protection from (UV) light, flower colouration and antibiotic effects against bacteria and fungi (reviewed by Waterman and Mole 1994). The production and enrichment of phenolic compounds is enhanced under certain stress conditions, and early extensive studies by Hahlbrock and colleagues demonstrated that PAL is induced under various conditions such as after mechanical wounding, fungal infections and light irradiation (reviewed by Hahlbrock and Scheel, 1989). Increased amounts of *PAL* mRNA were observed in potato leaves after infection with the fungal pathogen *Phytophtora infestans* (Fritzemeier *et al.*, 1987). Elevated levels of phenolic compounds under strong (UV) light were observed in various plant species. For example, Lavola *et al.* (2000) determined increased PAL activity and thereby elevated amount of phenolic compounds in birch seedlings exposed to UV-B light. Kondo and Kawashima (2000) determined elevated amounts of phenolic compounds in UV-B irradiated cucumber seedlings, and observed that UV-B treated plants possess an enhanced tolerance to free radicals formed under UV light.

Secretion of phenolic compounds to the Physcomitrella *culture medium is induced by glucose*

Further conditions inducing the accumulation of phenolics are described in the literature: Larronde *et al.* (1998) observed that cell suspension cultures of *Vitis vinifera* produced higher amounts of polyphenolic compounds (anthocyanins) secreted to the culture medium in the presence of different sugars namely sucrose and glucose.

Therefore, *Physcomitrella* was cultivated under standard conditions in medium supplemented with 0.45 % D-glucose. HPLC analysis of compounds extracted from concentrated culture medium revealed that a release of phenolic-like compounds was induced in the presence of glucose (3.6.2).

An induction of *PAL* gene expression by D-glucose was observed in suspension culture cells of *Chenopodium rubrum* by Ehness *et al.* (1997). Thus, the elevated production of phenolic compounds in *Physcomitrella* was most likely also provoked by an increased *PAL* gene expression induced by the glucose supplementation.

Only two compounds from *Physcomitrella* medium could be tentatively identified as 4-hydroxy benzoic acid and *p*-coumaric acid. All other detected substances could not be related to the reference compounds representing major seed plants phenolics, revealing that the composition of inducible phenolic compounds of the bryophyte strongly differs from the composition of phenolic compounds occurring in seed plants.

Elucidation of the structure of these phenolic compounds by HPLC and MS/MS analysis, as well as inducibility of polyphenol synthesis in *Physcomitrella* are subjects for further studies (perspectives 4.9).

4.6. *PPO1* knockout plants exhibit transcriptional, metabolic and morphological changes

In order to obtain information about potential roles of PPO in *Physcomitrella*, *PPO1* was chosen exemplary from the *PPO* gene family, and *PPO1* knockout lines were generated and analysed (3.7.1).

From a transformation with $4*10^6$ protoplasts 13 stable G418-resistant transformants were obtained, from which five lines were found to be haploid *PPO1* knockout lines with integration of

the transgene at the *PPO1* locus. *Physcomitrella* is well known for high frequencies of homologous recombination (Schaefer, 2001). The frequency of recombination events is positively correlated with the length of homologous DNA fragments; 1 kb overall homology is sufficient to achieve a 50 % yield of targeted transformants (Kamisugi *et al.*, 2005). For the generation of *PPO1* knockout lines, a construct consisting of the *nptII* sequence flanked by approx. 700 bp of *PPO1* sequence at each end was used for transformations. As these were proper conditions for homologous recombination, the determined frequency of gene replacement was comparable to the expected rate of homologous recombination described by Kamisugi *et al.* (2005).

Phenotypic changes of generated *PPO1* knockout plants were analysed (3.7.2) and are compared here to observations made for transgenically modified seed plants lacking *PPO* gene expression.

Previous studies have reported that the downregulation by antisense expression of potato *PPO* led to a reduction in overall PPO activity and reduced tuber browning, but not to significant phenotypical changes (Bachem *et al.*, 1994). The downregulation of all seven *PPO* gene family members in tomato by expression of a single potato *PPO* antisense construct resulted in a decreased PPO activity and in an enhanced susceptibility towards *Pseudomonas syringae* pv. *tomato*, but no changes in growth and development of the transgenic plants (Thipyapong *et al.*, 2004a). Moreover, when exposed to drought stress, these modified tomato plants with suppressed PPO activity exhibited less stress symptoms, delayed photoinhibition (i.e. higher F_v/F_m), and delayed photooxidative damage compared to wild type plants (Thipyapong *et al.*, 2004b).

In this study, several observations analysing the generated *Physcomitrella PPO1* knockout lines were made and will be discussed in the following:

- PPO1 *knockout lines possess a reduced extracellular PPO activity*
- PPO1 *knockout plants exhibit a decreased tolerance towards 4-methyl catechol*
- *Regulation of each* PPO *gene is to a great extent independent from* PPO1 *gene expression under standard conditions and strong light irradiation*
- PPO1 *knockout lines exhibit no differences in changes of photosynthetic activity under strong light irradiation compared to wild type*
- PPO1 *knockout lines exhibit abnormal protonema growth*
- PPO1 *knockout lines exhibit an enhanced differentiation*
- PPO1 *knockout plants possess reduced* in vivo *cytokinin degradation*

PPO1 *knockout lines possess a reduced extracellular PPO activity*

Determination of the *in vitro* PPO activity from *Physcomitrella* culture medium revealed that extracellular PPO activity of *PPO1*_ko lines was reduced approx. 60 % compared to that of wild type. As *Physcomitrella* plants lacking *PPO1*, exhibited a reduced PPO activity, this provides indirect functionality evidence for *PPO1* encoding for an *o*-diphenol oxidase. Moreover, these results clearly demonstrated that 4-methyl catechol (4-MC), already identified as a PPO11 substrate, is also a substrate for PPO1.

Additionally, these findings pointed towards the targeting of PPO1 with its *in silico* predicted secretion signal, as well as the contribution of PPO1 to the extracellular PPO activity. As mentioned above, 10 of the 12 PPO family members were predicted to possess an N-terminal signal sequences and to enter the secretory pathway. However, the strong reduction in overall extracellular PPO activity from *PPO1*_ko lines suggests, that the extracellular PPO activity mainly derived from *PPO1* secretion to the extracellular space. Hence, PPO1 can be assumed to be a major extracellular isoform contributing with ~60 % to the extracellular PPO activity secreted to the medium of 8 day old protonema cultures.

Yet, the intracellular PPO activity increased with the age of a *Physcomitrella* culture (Richter *et al.*, 2005), suggesting further production and/or a certain dynamic movement of PPOs. Thus, the portions of each PPO family member contributing to extra- or intracellular PPO activity might change during the time course of a *Physcomitrella* tissue culture.

PPO1 *knockout plants exhibit a decreased tolerance towards 4-methyl catechol*

Phenotypical changes of *PPO1*_ko protonema were observed, after incubation with 4-MC, which was shown to be a *Physcomitrella* PPO substrate. *PPO1* knockout lines exhibited an earlier die back after 4-MC application in comparison to wild type, suggesting that 4-MC is (more) toxic for *PPO1*_ko plants.

Further growth tests on medium containing caffeic acid, so far not identified as a substrate for *Physcomitrella* PPOs, revealed growth inhibition of *PPO1* knockout plants in the presence of caffeic acid (results not shown).

As already mentioned above, Wang *et al.* (2004) observed that transgenic *Arabidopsis* seedlings, expressing a secreted laccase from *Gossypium arboretum*, exhibited an enhanced resistance to certain phenolic compounds. HPLC analysis indicated that the growth inhibiting

phenols were detoxified *ex planta* by the secreted laccase, and the authors suggested an ecological role of laccase for transforming phenolic pollutants without uptake of the substance by the plant.

In summary, having demonstrated, that *PPO1*_ko lines exhibited a 60 % reduced extracellular PPO activity and a decreased tolerance towards 4-MC, it is proposed that that PPO1 is a major extracellular PPO with a potential role in detoxification of growth inhibiting phenolic compounds. Applied phenolic compounds, possibly toxic for *Physcomitrella* tissue, might be metabolised and removed by an extracellular PPO(1)-mediated oxidation.

Regulation of each PPO *gene is to a great extent independent from* PPO1 *gene expression*

PPO transcript determination under standard conditions and under strong light irradiation (~1000 µmol $m^{-2}s^{-1}$) revealed similar expression pattern of *PPO2* to *PPO12* in *PPO1*_ko lines and wild type. Thus, the absence of *PPO1* did not strongly influence the transcript levels of the other *PPO* gene family members under the tested conditions, and transcripts were mainly increased and decreased in strong light irradiated *PPO1*_ko lines as observed for wild type.

However, the increase of *PPO4* expression under strong light exposure was 2- to 3-fold higher in *PPO1*_ko plants than in wild type. A stronger increase of *PPO4* transcript in plants lacking *PPO1* did not match the data obtained for wild type, where a decrease in *PPO1* transcript level was measured in strong light irradiated tissue. Consequently, an increased *PPO4* transcription in plants lacking *PPO1* does not compensate the *PPO1* transcript decrease observed in wild type. So far, the enhanced increase of *PPO4* expression in *PPO1*_ko lines cannot be explained.

PPO1 *knockout lines exhibit no differences in changes of photosynthetic activity under strong light irradiation compared to wild type*

Determination of photosynthetic activity (F_v/F_m) during strong light exposure (~1000 µmol $m^{-2}s^{-1}$) was used to monitor the stress level of irradiated plants. As demonstrated by these measurements, both, wild type and *PPO1*_ko lines were stressed by strong light irradiation reflected in the decrease of activity of PSII. Tissue was not irreversible damaged, as reflected by the recovered activity of PSII after 4 h of regeneration under standard light conditions. Furthermore, plants lacking *PPO1* were not damaged any more or less than wild type; both genotypes reacted with a similar reduction of quantum yield of PSII electron transport under strong light irradiation.

Contrary to these observations, Thipyapong *et al.* (2004b) reported that tomato plants lacking expression of all seven *PPO* gene family members exhibited an enhanced stress tolerance and maintained higher dark adapted quantum yields of PSII electron transport (F_v/F_m) when exposed to drought stress. Hence, the authors concluded that tomato PPOs might be involved in development of water stress and photooxidative damage. Drought stress and stress caused by strong light irradiation are comparable to a certain extent, as both stresses can sequentially cause photooxidative damage. Thus, under the assumption that strong light irradiation applied in this work caused partly similar stress effects as the drought stress applied by Thipyapong and colleagues, *Physcomitrella PPO1*_ko plants reacted differently compared to the tomato plants lacking all seven PPOs.

Concluding from these results, the wild type like decrease in photosynthetic activity together with the wild type like *PPO* expression pattern in *PPO1*_ko lines under strong light exposure suggested that *PPO1* is not directly involved in a response towards stress caused by strong light exposure.

PPO1 *knockout lines exhibit abnormal protonema growth*

Protonema of *PPO1* knockout lines consisted of more roundly shaped and shorter chloronema cells. On one hand, this phenotype might be directly caused by the lack of *PPO1*, suggesting an involvement of PPO1 in cytoskeleton formation. On the other hand, an indirect involvement with PPO1 being part of a reaction cascade leading to this morphological abnormality can be assumed.

However, similar phenotypic alterations in cell shape were observed earlier in other transgenic *Physcomitrella* plants (Schween *et al.*, 2005b). Thus, atypical protonema growth might derive also from an unspecific stress reaction caused by unspecific metabolic interferences resulting from the *PPO1* absence.

PPO1 *knockout lines exhibit an enhanced differentiation*

*PPO1*_ko plants were found to produce significantly more gametophores than the wild type. So far, morphological changes were not observed in transgenically modified plants lacking *PPO*, and to date, no results have been published demonstrating a negative correlation between the amount of PPO protein or PPO activity and differentiation. In contrast, a positive correlation of PPO and the differentiation state was reported by Grotkass *et al.* (1995), who observed that PPO activity was higher in embryogenic cells of *Euphorbia pulcherrima* than in non-embryogenic cells.

The phenotypic observation found for *PPO1*_ko plants, can be connected to the hypothesis published by Galuszka *et al.* (2005), proposing that PPO could be involved in re-oxidation of cytokinin oxidase/dehydrogenase (CKX). The authors observed a co-localisation and co-expression of CKX and a laccase in the apoplast of maize kernels and in phloem cells of seedling shoots. Based on these findings, they proposed that the products of the PPO mediated reaction, the quinones, act as electron acceptors for the re-oxidation of the CKX enzyme, thus promoting cytokinin breakdown.

This implies that in the case of *Physcomitrella* plants lacking *PPO1*, lower PPO activities lead to less quinones and therefore to lower rates of CKX re-oxidation. Thereby, less cytokinin degradation occurs in plants having a reduced PPO activity, leading to an excess supply of active cytokinins and consequently causing an increased bud and gametophore production (Fig. 4.4).

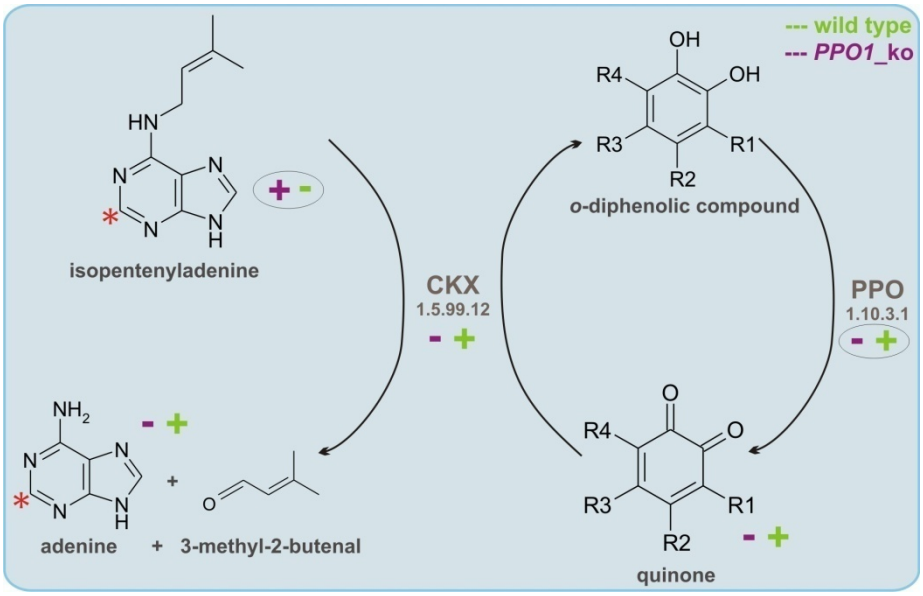

Fig. 4.4 Scheme of PPO-CKX cycling according to the hypothesis of Galuszka *et al.* (2005), suggesting that the reduction of the PPO-mediated reaction products leads to the re-oxidation and thereby re-activation of CKX enzyme. According to this hypothesis, theoretically expected differences between *PPO1*_ko and WT in enzyme, substrate and product amounts are schematically displayed with + and - (green for WT; purple for *PPO1*_ko plants). Differences in amounts experimentally shown in this work are encircled. The position of the tritiated hydrogen in the iP-molecule used for *in vivo* feeding experiments is marked by a red asterisk. Adenine resulting from the degradation of iP is rapidly incorporated by the cell; thus, CKX activity was determined indirectly by monitoring the depletion of radiolabelled iP in the culture medium.

PPO1 *knockout plants possess reduced* in vivo *cytokinin degradation*

In order to examine the above mentioned hypothesis of *PPO1* being involved in the maintenance of cytokinin breakdown, the depletion of applied radiolabelled isopentenyladenine of *PPO1*_ko plants was examined in comparison to wild type.

The amount of the applied tritiated iP (5 pmol/mL) is comparable to the amount of naturally occurring extracellular iP (~10 pmol/mL in 10 day old liquid cultures according to Schwartzenberg *et al.*, 2007), thus ensuring an appropriate breakdown capacity of additionally applied iP.

In *PPO1*_ko lines, the depletion of tritiated iP was significantly lower than in wild type. Indeed, these results support the hypothesis published by Galuszka and colleagues (Fig. 4.4). A slower metabolism of active cytokinins might result from a reduced PPO1 activity *in planta*, and accordingly, in *PPO1*_ko plants, a reduced CKX activity would be caused by a lower PPO activity.

4.7. Evidences for a different localisation of *Physcomitrella* PPOs compared to seed plant PPOs

Nearly all described PPOs from seed plants are found to be localised in plastids (reviewed by Steffens *et al.*, 1994; Mayer, 2006). Seed plant PPOs usually possess an N-terminal target peptide of approximately 60 to 100 amino acids. The transport of PPO by a two step mechanism leads to a processing of the prepro-protein to a mature form without the transit peptide, as demonstrated *in vitro* for a tomato PPO by Sommer *et al.* (1994).

Experiments carried out in this study gave several indications for a different localisation of PPOs (particularly PPO1) in *Physcomitrella* in comparison to PPO localisation in seed plant.

Evidences for secretion of several Physcomitrella PPOs

Ten of the 12 *Physcomitrella* PPOs were bioinformatically predicted to possess a short N-terminal signal peptide (19 – 29 amino acids) and to enter the secretory pathway. Targets were specified *in silico* to ER, Golgi, plasma membrane, or to the extracellular space.

In addition, a portion of the overall PPO activity was found to be secreted as demonstrated by *in vitro* PPO activity determinations, also indicating an extracellular targeting of several PPO family members. As the specific PPO activity in the medium was found to be 15-fold higher than the intracellular PPO activity, this might suggest a functional importance of PPO secretion.

Moreover, determination of PPO activity from culture medium of plants lacking *PPO1* revealed ca. 60 % lower extracellular PPO activities in these knockout lines than in wild type. This gave direct evidence that PPO1 in particular is secreted to the extracellular space. The remaining 40 % PPO activity in the culture medium of *PPO1*_ko plants suggests that other PPO family members are secreted as well.

PPO1 secretion was further suggested by transient expression of PPO1:GFP fusion constructs in *Physcomitrella* protoplasts. Transformations with a PPO1:GFP construct containing the complete *PPO1* coding sequence, led to no significant fluorescence, whereas a GFP signal was visible in protoplast transformed with a PPO1:GFP construct lacking the predicted signal sequence for PPO1 (data not shown).

Concluding from these observations, it is most likely, that other *Physcomitrella* PPOs are also targeted to the extracellular space, contrary to seed plant PPOs described so far. Bioinformatic analysis predicted several *Physcomitrella* PPOs to enter the secretory pathway and being targeted to organelles other than plastids.

Some Physcomitrella PPOs might be also localised in chloroplasts

In order to study the localisation of PPOs in *Physcomitrella*, not only extra- and intracellular protein extracts were analysed for PPO activity, but also protein extracts derived from isolated chloroplasts were used for *in vitro* PPO activity measurements (data not shown). Analysis revealed that chloroplast protein extracts possessed detectable PPO activity, suggesting that a portion of the overall PPO is also targeted to the *Physcomitrella* chloroplasts.

Detectable levels of PPO activity in chloroplast protein extracts in combination with the fact that the majority of *Physcomitrella* PPOs was predicted to possess a signal peptide to enter the secretory pathway, suggests a possible alternative targeting of some PPO family members to the chloroplast *via* the secretory pathway. This is known as "ER/Golgi to chloroplast targeting" reviewed by Radhamony and Theg (2006). Even a dual targeting might be possible, to transport the PPOs to the plasma membrane or extracellular lumen as well as to the chloroplasts *via* the ER and Golgi. It can be speculated, that targeting is dependent on abiotic and biotic environmental factors, such as nutrition supply, osmotic stress or light exposure, hence, also controlling even the function of *Physcomitrella* PPOs by its final destination.

Secretion signal and composition of Physcomitrella PPOs

Numerous laccases and tyrosinase from bacteria and fungi are known to possess an N-terminal signal peptide responsible for the secretion of the protein (e.g. Selinheimo *et al.*, 2006). But, as mentioned above, the identified *Physcomitrella* PPOs are *o*-diphenol oxidases, as demonstrated by sequence comparison, as well as experimentally for PPO1 and PPO11. Hence, the intermediate position of *Physcomitrella* within the evolutionary tree is reflected by the architecture of its PPO

family members possessing *o*-diphenol oxidase activity but a tyrosinase/laccase like targeting sequence. Mentioned earlier in the discussion, *o*-diphenol oxidases might have evolved from bacterial tyrosinases. Thus, the presence of a secretion signal within a *Physcomitrella o*-diphenol oxidase might point towards a more original PPO form in the basal land plant *Physcomitrella* compared to PPOs in seed plant.

Although some conclusions could be made on the localisation of *Physcomitrella* PPOs and in particular of PPO1 from the results of this work, yet information is incomplete, and further localisation experiments for selected PPO family members are aimed to be carried out (perspectives 4.9).

4.8. Conclusions on potential functions of *Physcomitrella* PPOs

In recent literature, different functions were suggested for seed plant PPOs. PPO-mediated reactions are proposed to take part for example, in pest and pathogen defence, in strong light stress response or in the inhibition of proteolysis. It was further hypothesised that PPOs might generate electron acceptors for the re-oxidation of cytokinin oxidase (CKX).

A general function for PPOs is not known. From the phylogenetic metagenome analysis performed in this study, it is assumed, that *o*-diphenol oxidases are likely to have evolved with the water to land transition of plants, and since then evolved to perform diverse functions in different plant species. Even within a single species, different functions for different *PPO* gene family members are most likely, such as reported by Thipyapong and colleagues who observed that different tomato *PPO* gene family members were upregulated under different stress conditions (Thipyapong *et al.*, 2004b; Thipyapong and Steffens, 1997).

Analysing PPOs and their substrates in the basal organism *Physcomitrella*, might give access to primal PPO involvements. With this aim, results obtained from this work are discussed with respect to functional aspects in the following sections.

4.8.1. Different functions of different *PPO* gene family members in *Physcomitrella*

** The basal land plant* Physcomitrella *possesses a large* PPO *gene family*

Physcomitrella possesses a large *PPO* gene family with 12 members, sharing structural similarities, but also exhibiting differences to seed plant PPOs. Nearly all *PPO* genes were found to be expressed; besides, they were differentially regulated under different culture conditions.

*PPO1 *knockout plants exhibit phenotypic changes*

PPO1 knockout lines exhibit significant phenotypic changes, although the very closely related paralogous gene *PPO2* is still present and transcribed.

Due to these findings, it is strongly assumed, that the different *PPO* gene family members hold different functions within the organism.

***>>> The different members of the Physcomitrella PPO multigene family are likely to be involved in different processes* (Fig. 4.5).**

4.8.2. Possible involvement in establishment of proper environmental conditions

** Portion of total PPO activity is detectable in the culture medium*

Physcomitrella possesses extracellular PPO activity. Analysis of *PPO1*_ko lines revealed that a large portion of the overall extracellular PPO activity was caused by PPO1 secretion.

*PPO1 *and* PPO8 *gene expression is increased after incubation with caffeic acid*

The gene expression level of *PPO1* was 3-fold increased in wild type tissue grown in the presence of caffeic acid. *PPO8,* not expressed under standard cultivation conditions, was transcribed after incubation with caffeic acid.

*PPO1 *knockout plants exhibit a decreased tolerance towards 4-methyl catechol*

Application of 4-methyl catechol to culture medium caused an enhanced susceptibility of plants lacking the secreted PPO1 protein.

Hence, the increased transcript level of *PPO1* in the presence of caffeic acid as well as the decreased tolerance towards 4-MC of *PPO1* knockout plants, suggests that PPO1 as a major extracellular PPO, is responsible for the conversion and detoxification of extracellulary occurring, growth inhibiting phenolic compounds.

***>>> Secretion of Physcomitrella PPOs, more specifically PPO1 (and PPO8), suggests a role in establishment of appropriate extracellular conditions, like the removal of (growth inhibiting) phenolic compounds* (Fig. 4.5).**

4.8.3. Possible involvement in light stress adaptation

** PPOs occurred with the conquest of land*

PPOs presumably occurred with the water to land transition, that was accompanied by the adaptation to harsh environmental conditions such as exposure to strong (UV) light.

** Upregulation of several* PPO *gene family members under strong light exposure*

Irradiation with strong light caused an upregulation of *PPO4* and *PPO12* gene expression. *PPO10*, not expressed under standard cultivation conditions, was transcribed under strong light exposure.

***>>> Transcriptional upregulation of Physcomitrella PPOs, more specifically PPO4, PPO12 (and PPO10), under strong light irradiation, suggests a role in adaptation mechanisms under strong light exposure* (Fig. 4.5).**

***PPO1 *might not be involved in light stress adaptation*

As *PPO1* gene expression was decreased in wild type tissue irradiated with strong light, and *PPO1*_ko lines exposed to strong light exhibited only slight changes in *PPO2* to *PPO12* expression, as well as no differences in changes of photosynthetic activity compared to wild type, it can be assumed that *PPO1* is not involved in light stress response.

4.8.4. Possible involvement in promotion of cytokinin degradation

***PPO1 *knockout lines exhibit an enhanced differentiation*

*PPO1*_ko plant produced significantly more gametophores than wild type under standard *in vitro* cultivation condition.

***PPO1 *knockout plants possess reduced* in vivo *cytokinin degradation*

Cytokinin feeding experiments revealed that plants lacking *PPO1* had a reduced *in vivo* CKX activity. Consistent with the hypothesis of Galuszka *et al.* (2005), a correlation between the PPO-mediated oxidation of phenolic compounds promoting the re-oxidation of CKX enzyme can be explained with these results (Fig. 4.4).

** Putative phenolic compounds are secreted to the* Physcomitrella *culture medium*

Physcomitrella secreted few putative phenolic-like compounds into the culture medium. *In vivo* these compounds might serve as substrates for an extracellular PPO(1)-mediated oxidation promoting the re-oxidation of extracellular CKX enzyme.

***>>> Physcomitrella PPOs, more specifically PPO1, are likely to be involved in regulation or tuning of differentiation processes* (Fig. 4.5).**

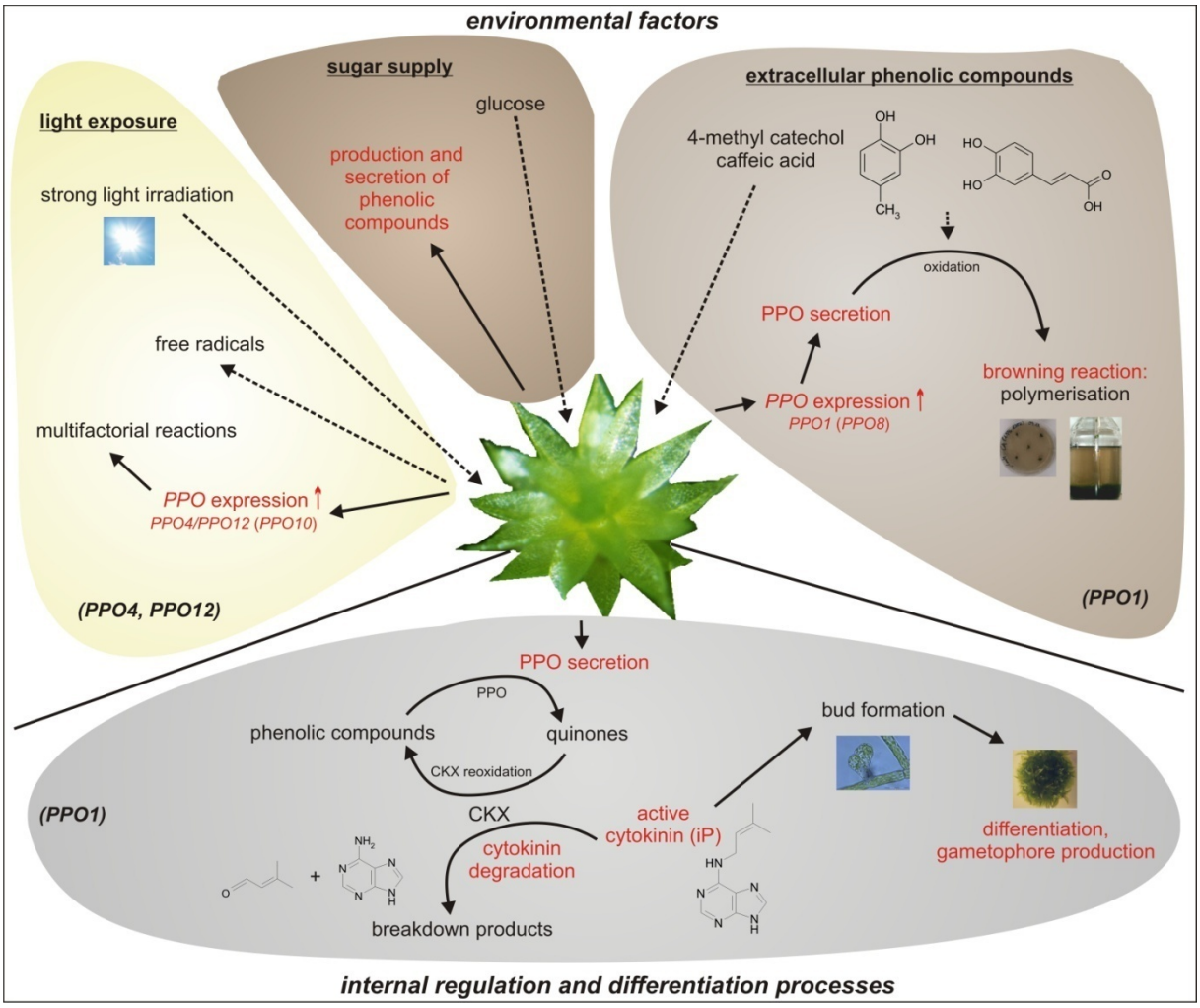

Fig. 4.5 Schematic overview of hypothetical involvements of *Physcomitrella* PPOs concluded from the results of this work. Results obtained from this research propose *Physcomitrella* PPOs being involved in multiple processes, such as coping with strong light exposure (mainly *PPO4* and *PPO12*) and metabolism of extracellular occurring phenolics (mainly *PPO1*) as well as involvement in differentiation processes (*PPO1*). Elements marked in red are supported by results from this work and are discussed in section 4.4 to 4.6.

4.9. Perspectives

Within this research, a bryophyte *PPO* gene family was identified and characterised. *Physcomitrella* PPO activity and *PPO* gene expression profiles were analysed under different cultivation conditions. Putative PPO substrates and plants lacking one *PPO* gene family member were analysed. Further experimental approaches could deepen the understanding on PPOs under various aspects:

* Expression profiles of the *Physcomitrella PPO* gene family under further (stress) conditions are aimed to be analysed. Promoter characterisations can be carried out *in silico* for each *PPO* gene and e.g. by promoter::GFP-fusions.
* To confirm the reduced degradation of cytokinins in *PPO1*_ko plants, the cytokinin profile of these plants in comparison to wild type is currently analysed by HPLC LC-MS.
* *Physcomitrella* plants lacking the complete *PPO* gene family are aimed to be generated by down-regulation of the *PPO* genes using artificial micro-RNAs.
* More information on localisation of *Physcomitrella* PPOs could be obtained e.g. by PPO:GFP-fusions.
* Substrate specificities of *Physcomitrella* PPOs could be analysed with purified recombinant PPO proteins, expressed in a eukaryotic expression system, e.g., *Pichia pastoris*, ensuring higher protein yields and proper posttranslational modifications.
* Phenolic substances of *Physcomitrella*, inducible by glucose are aimed to be identified by LC-MS analysis. Other culture conditions including strong light irradiation can be further tested for the ability to induce the polyphenol production.

To conclude, in this work, the field of PPO research has been extended to a basal land plant, and further experiments should therefore unravel more information on evolution and functions of PPOs.

5. REFERENCES

Abascal F., Zardoya R., Posada D. (2005) ProtTest: selection of best-fit models of protein evolution. Bioinformatics 21: 2104 – 2105

Asakawa Y. (1995) Chemical constituents of the bryophytes. In: Progress in the Chemistry of Organic Natural products (Herz W. *et al.*, eds.), Vol. 65, Vienna, Springer: pp. 1 – 618

Ashton N.W., Cove D.J. (1977) The isolation and preliminary characterisation of auxotrophic and analogue resistant mutants of the moss, *Physcomitrella patens*. Molecular and general Genetics 154: 87 – 95

Ashton N.W., Grimsley N.H., Cove D.J. (1979) Analysis of gametophytic development in the moss, *Physcomitrella patens,* using auxin and cytokinin resistant mutants. Planta 144, 427 - 435

Bachem C.W.B., Speckman G.J., van der Line P.C.G., Verheggen F.T.M., Hunt M.D., Steffens J.C., Zabeau M. (1994) Antisense expression of polyphenol oxidase genes inhibits enzymatic browning in potato tubers. Bio/Technology 12: 1101 - 1105

Balakumar T., Gayathri B., Anbudurai P.R. (1997) Oxidative stress injury in tomato plants induced by supplemental UV-B radiation. Biologia Plantarum 39 (2): 215 – 221

Bezanilla M., Perroud P.-F., Pan A., Klueh P., Quatrano. R. (2005) An RNAi system in *Physcomitrella patens* with an internal marker for silencing allows for rapid identification of loss of function phenotypes. Plant Biology 7: 251 - 257.

Bollag J.M., Shuttleworth K.L., Anderson D.H. (1988) Laccase-mediated detoxification of phenolic compounds. Applied and Environmental Microbiology 54 (12): 3086 – 3091

Bopp M., Brandes H. (1964) Versuche zur Analyse der Protonemaentwicklung der Laubmoose. Planta 62: 116 – 136

Boudet A.M. (2007) Evolution and current status of research in phenolic compounds. Phytochemistry 68: 2722 – 2735

Bradford M. (1976) A rapid and sensitive method for the quantitation of microgram quantities of protein utilizing the principle of protein-dye binding. Analytical Biochemistry 72: 248 – 254

Cary J.W., Lax A.R., Flurkey W.H. (1992) Cloning and characterisation of cDNAs coding for *Vicia faba* polyphenol oxidase. Plant Molecular Biology 20: 245 – 253

Chevalier T., Rigal D., Mbéguié-A-Mbéguié D., Gauillard F., Richard-Forget F., Fils-Lycaon B. (1999) Molecular cloning and characterization of apricot fruit polyphenol oxidase. Plant Physiology 11: 1261 - 1269

Clamp M., Cuff J., Searle S. M., Barton G. J. (2004) The Jalview Java Alignment Editor. Bioinformatics 20: 426 – 427

Constabel C.P, Yip L., Patton J.J., Christopher M.E. (2000) Polyphenol oxidase from hybrid poplar. Cloning and expression in response to wounding and herbivory. Plant Physiology 124 (1): 285 – 295

Cove D. (2000) The Moss, *Physcomitrella patens*. Journal of Plant Growth Regulation 19: 275 – 283

Cove D. (2005) The moss *Physcomitrella patens*. Annual Review of Genetics 39: 339 – 358

Demeke T., Morris C.F. (2002) Molecular characterization of wheat polyphenol oxidase (PPO). Theoretical and Applied Genetics 104: 813 – 818

Dry I.B., Robinson S.P. (1994) Molecular cloning and characterisation of grape berry polyphenol oxidase. Plant Molecular Biology 26: 495 – 502

Ehness R., Ecker M., Godt D.E., Roitsch T. (1997) Glucose and Stress Independently Regulate Source and Sink Metabolism and Defense Mechanisms via Signal Transduction Pathways lnvolving Protein Phosphorylation. The Plant Cell 9: 1825 – 1841

Emanuelsson O., Brunak S., von Heijne G., Nielsen H. (2007) Locating proteins in the cell using TargetP, SignalP, and related tools. Nature Protocols 2: 953 – 971

Flurkey W.H. (1989) Polypeptide Composition and Amino-Terminal Sequence of Broad Bean Polyphenoloxidase Plant Physiology 91: 481 – 483

Flurkey W.H., Inlow J.K. (2008) Proteolytic processing of polyphenol oxidase from plants and fungi. Journal of Inorganic Biochemistry 102 (12): 2160 – 2170

Frank W., Ratnadewi D., Reski R. (2005) *Physcomitrella patens* is highly tolerant against drought, salt and osmotic stress. Planta 220 (3): 384 – 394

Frébortová J., Fraaije M.W., Galuszka P., Sebela M., Pec P., Hrbác J., Novák O., Bilyeu K.D., English J.T., Frébort I. (2004) Catalytic reaction of cytokinin dehydrogenase: preference for quinones as electron acceptors. Biochemical Journal 380: 121 – 130

Fritzemeier K.-H., Cretin C., Kombrink E., Rohwer F., Taylor J., Scheel D., Hahlbrock K. (1987) Transient induction of phenylalanine ammonia-lyase and 4-coumarate: CoA ligase mRNAs in potato leaves infected with virulent or avirulent races of *Phytophthora infestans*. Plant Physiology 85: 34 - 41

Galuszka P., Frébortová J., Luhová L., Bilyeu K.D., English J.T., Frébort I. (2005) Tissue localization of cytokinin dehydrogenase in maize: possible involvement of quinone species generated from plant phenolics by other enzymatic systems in the catalytic reaction. Plant Cell Physiology 46: 716 – 728

Gerdemann C., Eicken C., Krebs B. (2002) The crystal structure of catechol oxidase: new insight into the function of type-3 copper proteins. Accounts of Chemical Research 35: 183 – 191

Gooding P.S., Bird C., Robinson S.P. (2001) Molecular cloning and characterisation of banana fruit polyphenol oxidase. Planta 213: 748 – 757

Grotkass C., Lieberei R., Preil W. (1995) Polyphenoloxidase-activity and -activation in embryogenic and non-embryogenic suspension cultures of *Euphorbia pulcherrima*. Plant Cell Reports 14: 428 – 431

Hahlbrock K., Scheel D. (1989) Physiology and molecular biology of phenylpropanoid metabolism. Annual Review of Plant Physiology and Plant Molecular Biology 40: 347 – 369

Halaouli S., Record E., Casalot L., Hamdi M., Sigoillot J.-C., Asther M., Lomascolo A. (2006) Cloning and characterization of a tyrosinase gene from the white-rot fungus *Pycnoporus sanguineus*, and overproduction of the recombinant protein in *Aspergillus niger*. Applied Microbiology and Biotechnology 70 (5): 580 – 589

Hanelt D., Uhrmacher S., Nultsch W. (1995) The effect of photoinhibition on photosynthetic oxygen production in the brown alga *Dictyota dichotoma*. Botanica Acta 108: 99 – 105

Hanelt D., Hawes I., Rae R. (2006) Reduction of UV-B radiation causes an enhancement of photoinhibition in high light stressed aquatic plants from New Zealand lakes. Journal of photochemistry and photobiology biology 84 (2): 89 – 102

Haruta M., Murata M., Hiraide A., Kadokura H., Yamasaki M., Sakuta M., Shimizu S., Homma S. (1998) Cloning genomic DNA encoding apple polyphenol oxidase and comparison of the gene product in *Escherichia coli* and in apple. Bioscience, Biotechnology and Biochemistry 62 (2): 358 – 362

He X.Y., He Z.H., Zhang L.P., Sun D.J., Morris C.F., Fuerst E.P., Xia X.C. (2007) Allelic variation of polyphenol oxidase (PPO) genes located on chromosomes 2A and 2D and development of functional markers for the PPO genes in common wheat. Theoretical and Applied Genetics 115 (1): 47 – 58

Hernández-Romero D., Solano F., Sanchez-Amat A. (2005) Polyphenol Oxidase Activity Expression in *Ralstonia solanacearum*. Applied and Environmental Microbiology 71 (11): 6808 – 6815

Hind G., Marshak D. R., Coughlan S. J. (1995) Spinach Thylakoid Polyphenol Oxidase: Cloning, Characterization, and Relation to a Putative Protein Kinase. Biochemistry 34: 8157 – 8164

Hoeglund A., Doennes P., Blum T., Adolph H.-W., Kohlbacher O. (2006) MultiLoc: prediction of protein subcellular localization using N-terminal targeting sequences, sequence motifs, and amino acid composition. Bioinformatics 22 (10): 1158 – 1165

Hofmann A.H., Codón A.C., Ivascu C., Russo V.E., Knight C., Cove D., Schaefer D.G., Chakhparonian M., Zryd J.P. (1999) A specific member of the Cab multigene family can be efficiently targeted and disrupted in the moss *Physcomitrella patens*. Molecular and general Genetics 261 (1): 92 – 99

Howe K, Bateman A, Durbin R (2002) QuickTree: building huge Neighbour-Joining trees of protein sequences. Bioinformatics 18: 1546 – 1547

Hunt M.D., Eannetta N.T., Yu H., Newman S.M., Steffens J.C. (1993) cDNA cloning and expression of potato polyphenol oxidase. Plant Molecular Biology 21: 59 – 68

Jiang C., Schommer C.K., Kim S.Y., Suh D.-Y. (2006) Cloning and characterization of chalcone synthase from the moss, *Physcomitrella patens*. Phytochemistry 67: 2531 – 2540

Kamisugi Y., Cuming A.C., Cove D.J. (2005) Parameters determining the efficiency of gene targeting in the moss *Physcomitrella* patens. Nucleic Acids Research 33 (19): e173

Kanade S.R., Paul B., Rao A.G.A., Gowda L.R. (2006) The conformational state of polyphenol oxidase from field bean (*Dolichos lablab*) upon SDS and acid-pH activation Biochemical Journal 395: 551 – 562

Kapoor S., Bhatla S.C. (1999) Auxin dependent changes in peroxidase and polyphenol oxidase activities accompanying cell differentiation in protonema of wild strain and auxin mutants of *Funaria hygrometrica*. Indian Journal of Experimental Biology 37: 1017 – 1021

Katoh K., Kuma K., Toh H., Miyata T. (2005) MAFFT version 5: improvement in accuracy of multiple sequence alignment. Nucleic Acids Research 33 (2): 511 – 518

Kavrayan D., Aydemir T. (2001) Partial purification and characterization of polyphenoloxidase from peppermint (*Mentha piperita*). Food Chemistry 74: 147 – 154

Khraiwesh B., Ossowski S., Weigel D., Reski R., Frank W. (2008) Specific gene silencing by artificial microRNAs in *Physcomitrella patens*: An alternative to targeted gene knockouts. Plant Physiology 148: 684 – 693

Klabunde T., Eicken C., Sacchettini J.C., Krebs B. (1998) Crystal structure of a plant catechol oxidase containing a dicopper center. Nature Structural Biology 5 (12): 1084 – 1090

Knight C.D., Cove D.J., Boyd P.J, Ashton N.W. (1988) The isolation of biochemical and developmental mutants in *Physcomitrella patens*. In: Methods in Bryology (Glime J.M., ed.,). The Hattori Botanical Laboratory, Nichinan, Miyazaki, Japan: pp 47 – 58

Kondo N., Kawashima M. (2000) Enhancement of the Tolerance to Oxidative Stress in Cucumber (*Cucumis sativus* L.) Seedlings by UV-B Irradiation: Possible Involvement of Phenolic Compounds and Antioxidative Enzymes. Journal of Plant Research 113: 311 – 317

Koprivova A., Meyer A.J., Schween G., Herschbach C., Reski R., Kopriva S. (2002) Functional knockout of the adenosine 5'-phosphosulfate reductase gene in *Physcomitrella patens* revives an old route of sulfate assimilation. The Journal of biological Chemistry 277 (35): 32195 – 32201

Krause G.H., Weis E. (1991) Chlorophyll fluorescence and photosynthesis: the basics. Annual Review of Plant Physiology and Plant Molecular Biology 42: 313 – 349

Kroemer K., Reski R., Frank W. (2004) Abiotic stress response in the moss *Physcomitrella patens*: evidence for an evolutionary alteration in signaling pathways in land plants. Plant Cell Reports 22: 864 – 870

Kyle J., Doolittle R.F. (1982) A simple method for displaying the hydropathic character of a protein. Journal of Molecular Biology 157: 105 – 132

Lang D., Eisinger J., Reski R., Rensing S. (2005) Representation and high-quality annotation of the *Physcomitrella patens* transcriptome demonstrates a high proportion of proteins involved in metabolism among mosses. Plant Biology 7: 228 – 237

Lang D., Zimmer A.D., Rensing S.A., Reski R. (2008) Exploring plant biodiversity: the *Physcomitrella* genome and beyond. Trends in Plant Science 13 (10): 542 – 549

Larronde F., Krisa S., Decendit A., Chèze C., Deffieux G., Mérillon J.M. (1998) Regulation of polyphenol production in *Vitis vinifera* cell suspension cultures by sugars. Plant Cell Reports 17: 946 – 950

Lavola A., Julkunen-Tiitto R., de la Rosa T.M., Lehto T., Aphalo P.J. (2000) Allocation of carbon to growth and secondary metabolites in birch seedlings under UV-B radiation and CO2 exposure. Physiologia Plantarum 109: 260 – 267

Lax A.R., Vaughn K.C., Templeton G.E. (1984) Nuclear inheritance of polyphenol oxidase in *Nicotiana*. The Journal of Heredity 75: 285 – 287

Li L., Steffens J.C. (2002) Overexpression of polyphenol oxidase in transgenic tomato plants results in enhanced bacterial disease resistance. Planta 215: 239 – 247

Livak K.J., Schmittgen T.D. (2001) Analysis of relative gene expression data using real-time quantitative PCR and the $2^{-\Delta\Delta CT}$ method. Methods 25 (4): 402 – 408

Mahdavian K., Ghorbanli M., Kalantari K.M. (2008) The Effects of Ultraviolet Radiation on Some Antioxidant Compounds and Enzymes in *Capsicum annuum* L. Turkish Journal of Botany 32: 129 – 134

Massa A.N., Beecher B., Morris C.F. (2007) Polyphenol oxidase (PPO) in wheat and wild relatives: molecular evidence for a multigene family. Theoretical and Applied Genetics 114: 1239 – 1247

Mayer A.M. (2006) Polyphenol oxidases in plants and fungi: Going places? A review. Phytochemistry 67 2318 – 2331

Mazzafera P., Robinson S.P. (2000) Characterization of polyphenol oxidase in coffee. Phytochemistry 55: 285 – 296

McCaig B.C., Meagher R.B., Dean J.F.D. (2005) Gene structure and molecular analysis of the laccase-like multicopperoxidase (LMCO) gene family in *Arabidopsis thaliana*. Planta 221: 619 – 636

Mittmann F., Brucker G., Zeidler M., Repp A., Abts T., Hartmann E., Hughes J. (2004) Targeted knockout in *Physcomitrella* reveals direct actions of phytochrome in the cytoplasm. PNAS 101 (38): 13939 – 13944

Nakamura T., Sugiura C., Kobayashi Y., Sugita M. (2005) Transcript Profiling in Plastid Arginine tRNA-CCG Gene Knockout Moss: Construction of *Physcomitrella patens* Plastid DNA Microarray. Plant Biology 7 (3): 258 – 265

Nakayama T., Yonekura-Sakakibara K., Sato T., Kikuchi S., Fukui Y., Fukuchi-Mizutani M., Ueda T., Nakao M., Tanaka Y., Kusumi T., Nishino T. (2000) Aureusidin Synthase: A Polyphenol Oxidase Homolog Responsible for Flower Coloration. Science 290: 1163 – 1166

Newman S.M., Eannetta N.T., Yu H., Prince J.P., de Vicente M.C., Tanksley S.D., Steffens J.C. (1993) Organisation of the tomato polyphenol oxidase gene family. Plant Molecular Biology 21: 1035 – 1051

Nishiyama T., Fujita T., Shin-I T., Seki M., Nishide H., Uchiyama I., Kamiya A., Carnici P., Hayashizaki Y., Shinozaki K., Kohara Y., Hasebe M. (2003) Comparative genomics of *Physcomitrella patens* gametophytic transcriptome and *Arabidopsis thaliana*: Implication for land plant evolution. PNAS 100 (13): 8007 – 8012

Ono E., Hatayama M., Isono Y., Sato T., Watanabe R., Yonekura-Sakakibara K., Fukuchi-Mizutani M., Tanaka Y., Kusumi T., Nishino T., Nakayama T. (2006) Localization of a flavonoid biosynthetic polyphenol oxidase in vacuoles. The Plant Journal 45: 133 – 143

Paszkowski J., Baur M., Bogucki A., Potrykus I. (1988) Gene targeting in plants. The EMBO Journal 7(13): 4021 – 4026

Radhamony R.N., Theg S.M. (2006) Evidence for an ER to Golgi to chloroplast protein transport pathway. Trends in Cell Biology 16 (8): 385 – 387

Rensing S.A., Rombauts S., Hohe A., Lang D., Duwenig E., Rouze P., van de Peer Y., Reski R. (2002) The transcriptome of the moss *Physcomitrella patens*: comparative analysis reveals a rich source of new genes. http://www.plant-biotech.net/Rensing_et_al_transcriptome2002.pdf.

Rensing S.A., Fritzowsky D., Lang D., Reski R. (2005) Protein encoding genes in an ancient plant: analysis of codon usage, retained genes and splice sites in a moss, *Physcomitrella patens*. BMC Genomics 6: 43

Rensing S.A, Ick J., Fawcett J.A, Lang D., Zimmer A., van de Peer Y., Reski R. (2007) An ancient genome duplication contributed to the abundance of metabolic genes in the moss *Physcomitrella patens*. BMC Evolutionary Biology 7: 130

Rensing S.A., Lang D., Zimmer A.D., Terry A., Salamov A., Shapiro H., Nishiyama T., Perroud P.F., Lindquist E.A., Kamisugi Y., Tanahashi T., Sakakibara K., Fujita T., Oishi K., Shin-I T., Kuroki Y., Toyoda A., Suzuki Y., Hashimoto S., Yamaguchi K., Sugano S., Kohara Y., Fujiyama A., Anterola A., Aoki S., Ashton N., Barbazuk W.B., Barker E., Bennetzen J.L., Blankenship R., Cho S.H., Dutcher S.K., Estelle M., Fawcett J.A., Gundlach H., Hanada K., Heyl A., Hicks K.A., Hughes J., Lohr M., Mayer K., Melkozernov A., Murata T., Nelson D.R., Pils B., Prigge M., Reiss B., Renner T., Rombauts S., Rushton P.J., Sanderfoot A., Schween G., Shiu S.H., Stueber K., Theodoulou F.L., Tu H., Van de Peer Y., Verrier P.J., Waters E., Wood A., Yang L., Cove D., Cuming A.C., Hasebe M., Lucas S., Mishler B.D., Reski R., Grigoriev I.V., Quatrano R.S., Boore J.L. (2008) The *Physcomitrella* genome reveals evolutionary insights into the conquest of land by plants. Science 319 (5859): 64 - 69

Reski R., Abel W.O. (1985) Induction of budding on chloronemata and caulonemata of the moss, *Physcomitrella patens*, using isopentenyladenine. Planta 165: 354 – 358

Reski R., Reutter K., Karsten B., Faust M., Kruse S., Gorr G., Strepp R., Abel W.O. (1995) Molecular analysis of chloroplast division. In: Current Issues in Plant Molecular and Cellular Biology (Terzi M. *et al.*, eds.), Dordrecht, Kluwer Academic Publishers: pp. 291 – 296

Reski R. (1998) Development, genetics and molecular biology of mosses. Botanica Acta 111: 1 – 15

Reski R., Frank W. (2005) Moss (*Physcomitrella patens*) functional genomics - Gene discovery and tool development with implications for crop plants and human health. Briefings in Functional Genomics & Proteomics 4: 48 – 57

Rice-Evans C.A., Miller N.J., Bolwell P.G., Bramley P.M., Pridham J.B. (1995) The relative antioxidant activities of plant-derived polyphenolic flavonoids. Free Radical Research 22 (4): 375 – 383

Richter H. (2003) Molekulare und physiologische Studien zur Polyphenoloxidase bei *Physcomitrella patens* (Hedw.) B.S.G. Diploma thesis at the University of Hamburg

Richter H., Lieberei R., von Schwartzenberg K. (2005) Identification and characterisation of a bryophyte polyphenol oxidase encoding gene from *Physcomitrella patens*. Plant Biology 7 (3): 283 - 291

Robinson S.P., Dry I.B. (1992) Broad bean leaf polyphenol oxidase is a 60-kilodalton protein susceptible to proteolytic cleavage. Plant Physiology 99: 317 – 323

Ronquist F., Huelsenbeck J.P. (2003) MrBayes 3: Bayesian phylogenetic inference under mixed models. Bioinformatics 19: 1572 – 1574

Sanchez-Amat A., Lucas-Elío P., Fernández E., García-Borrón J.C., Solano F. (2001) Molecular cloning and functional characterization of a unique multipotent polyphenol oxidase from *Marinomonas mediterranea*. Biochimica et Biophysica Acta 1547: 104 – 116

Sawahel W., Onde S., Knight C.D., Cove D.J. (1992) Transfer of foreign DNA into *Physcomitrella patens* Protonemal Tissue by Using the Gene Gun. Plant Molecular Biology Reporter 10 (4): 314 – 315

Schaefer D.G., Zryd J.-P., Knight C.D., Cove D.J. (1991) Stable transformation of the moss *Physcomitrella patens*. Molecular Genetics and Genomics 226: 418 – 424

Schaefer D.G., Zryd J.P. (1997) Efficient gene targeting in the moss *Physcomitrella patens*. The Plant Journal 11: 1195 – 1206

Schaefer D.G. (2001) Gene targeting in *Physcomitrella patens*. Current Opinion in Plant Biology 4: 143 – 150

Schaefer D.G. (2002) A new Moss Genetics: Targeted Mutagenesis in *Physcomitrella patens*. Annual Review of Plant Biology 53: 477 – 501

Schwartzenberg v. K., Pethe C., Laloue M. (2003) Cytokinin metabolism in *Physcomitrella patens* – differences and similarities to higher plants. Plant Growth Regulation 39: 99 – 106

Schwartzenberg v. K., Fernández Núñez M., Blaschke H., Dobrev P.I., Novák O., Motyka V., Strnad M. (2007) Cytokinins in the Bryophyte *Physcomitrella patens*: Analyses of Activity, Distribution, and Cytokinin Oxidase/Dehydrogenase Overexpression Reveal the Role of Extracellular Cytokinins. Plant Physiology 145: 786 – 800

Schween G., Gorr G., Hohe A., Reski R. (2003) Unique tissue-specific cell cycle in *Physcomitrella*. Plant Biology 5: 50 – 58

Schween G, Hohe A., Schulte J., Reski R. (2005a) Effect of ploidy level on growth, differentiation and phenotype in *Physcomitrella patens*. The Bryologist 108: 27 – 35

Schween G., Egener T., Fritzowsky D., Granado J., Guitton M.-C., Hartmann N., Hohe A., Holtorf H., Lang D., Lucht J.M., Reinhard C., Rensing S.A., Schlink K., Schulte J., Reski R. (2005b) Large-scale analysis of 73329 *Physcomitrella* plants transformed with different gene disruption libraries: production parameters and mutant phenotypes. Plant Biology 7: 228 – 237

Selinheimo E., Saloheimo M., Ahola E., Westerholm-Parvinen A., Kalkkinen N., Buchert J., Kruus K. (2006) Production and characterization of a secreted, C-terminally processed tyrosinase from the filamentous fungus *Trichoderma reesei*. FEBS Journal 273: 4322 – 4335

Sherman T.D., Vaughn K.C., Duke S.O. (1991) A limited survey of the phylogenetic distribution of polyphenol oxidase. Phytochemistry 30 (8): 2499 – 2506

Sommer A., Ne´eman E., Steffens J.C., Mayer A.M., Harel E. (1994) Import, targeting and processing of a plant polyphenol oxidase. Plant Physiology 105 (4): 1301 – 1311

Steffens J.C., Harel E., Hunt M.D. (1994) Polyphenol oxidase. In: Recent Advances in Phytochemistry, Genetic Engineering of Plant Secondary Metabolism (Ellis B.E. *et al.*, eds.), Vol. 28, New York, Plenum Press: pp. 275 – 312

Stenøien H. K. (2008) Slow molecular evolution in 18S rDNA, rbcL and nad5 genes of mosses compared with higher plants. Journal of Evolutionary Biology 21: 566 – 571

Sullivan M.L., Hatfield R.D., Thoma S.L., Samac D.A. (2004) Cloning and characterisation of red clover polyphenol oxidase cDNAs and expression of active protein in *Escherichia coli* and transgenic alfalfa. Plant Physiology 136 (2): 3234 – 3244

Sun D.J., He Z.H., Xia X.C., Zhang L.P., Morris C.F., Appels R., Ma W.J., Wang H. (2005) A novel STS marker for polyphenol oxidase activity in bread wheat. Molecular Breeding 16: 209 – 218

Thipyapong P., Steffens J.C. (1997) Tomato Polyphenol Oxidase: Differential Response of the Polyphenol Oxidase F Promoter to Injuries and Wound Signals. Plant Physiology 115: 409 – 418

Thipyapong P., Joel D.M., Steffens J.C. (1997) Differential Expression and Turnover of the Tomato Polyphenol Oxidase Gene Family during Vegetative and Reproductive Development. Plant Physiology 113 (3): 707 – 718

Thipyapong P., Hunt M.D., Steffens J.C. (2004a) Antisense downregulation of polyphenol oxidase results in enhanced disease susceptibility. Planta 220: 105- 117

Thipyapong P., Melkonian J., Wolfe D.W., Steffens J.C. (2004b) Suppression of polyphenol oxidases increases stress tolerance in tomato. Plant Science 167: 693 – 703

Thipyapong P., Stout M.J., Attajarusit J. (2007) Functional Analysis of Polyphenol Oxidases by Antisense/Sense Technology. Molecules 12: 1569 – 1595

Thygesen P.W., Dry I.B., Robinson S.P. (1995) Polyphenol oxidase in potato (A multigene family that exhibits differential expression patterns). Plant Physiology 109 (2): 525 – 531

Vaughn K.C., Lax A.R., Duke S.O. (1988) Polyphenol oxidase: the chloroplast oxidase with no established function. Physiologia Plantarum 72: 659 – 665

Wang G.-D., Li Q.-J., Luo B., Chen X.-Y. (2004) *Ex planta* phytoremediation of trichlorophenol and phenolic allelochemicals via an engineered secretory laccase. Nature Biotechnology 22 (7): 893 – 897

Wang J., Constabel C.P. (2004) Polyphenol oxidase overexpression in transgenic *Populus* enhances resistance to herbivory by forst tent caterpillar (*Malacosoma disstria*). Planta 220: 87 – 96

Wang T.L., Cove D.J., Beutelmann P., Hartmann E. (1980) Isopentenyladenine from mutants of the moss *Physcomitrella patens*. Phytochemistry 19: 1103 – 1105

Waterman P.G., Mole S. (1994) Analysis of phenolic plant metabolites. Oxford: Blackwell Scientific Publications

Whelan S., Goldman N. (2001) A general empirical model of protein evolution derived from multiple protein families using a maximum-likelihood approach. Molecular Biology and Evolution 18: 691 – 699

Wichard T., Göbel C., Feussner I., Pohnert G. (2005) Unprecedented Liopoxygenase/ Hydroperoxide Lyase Pathways in the Moss *Physcomitrella patens*. Angewandte Chemie International Edition 44: 158 – 161

Zhou Y., O'Hare T.J., Jobin-Décor M., Underhill S.J.R., Wills R.B.H., Graham M.W. (2003) Transcriptional regulation of a pineapple polyphenol oxidase gene and its relationship to blackheart. Plant Biotechnol Journal 1: 463 – 478

6. APPENDIX

6.1. List of abbreviations

Chemical symbols and international SI units are not listed separately.

^{3}H-iP	tritiated isopentenyladenine
4-MC	4-methyl catechol
aa	amino acid(s)
ACT	actin
BI	Bayesian inference
BLAST	Basic Local Alignment Search Tools
bp	base pair(s)
BSA	bovine serum albumin
CA	caffeic acid
cDNA	complementary DNA
CDS	coding sequence
CIAP	calf intestine alkaline phosphatase
CKX	cytokinin oxidase/dehydrogenase
CT	cycle threshold
CTAB	cetyl trimethyl ammonium bromide
CuA / CuB	copper-binding domain A / B
DAPI	4',6-diamidino-2-phenylindole
DEPC	diethylpyrocarbonate
DMSO	dimethyl sulfoxide
dNTP	desoxyribonucleosid triphosphate
dpm	disintegrations per minute
DTT	dithiothreitol
EDTA	ethylenediamine tetraacetic acid
ER	endoplasmatic reticulum
EST	expressed sequence tag
FDA	fluorescein diacetate
G418	geniticin
GFP	green fluorescent protein
HPLC	high performance liquid chromatography
iP	isopentenyladenine
JGI	Joint Genome Institute
kb	kilo base pair(s)
kDa	kilo Dalton
ko	knockout
LAC	laccase
LSC	liquid scintillation counting
MES	2-(N-morpholino)ethanesulfonic acid
NCBI	National Center for Biotechnology Information
NJ	Neighbour-joining
nptII	neomycin phosphotransferase II
nt	nucleotide
OD	optical density
ORF	open reading frame

PAGE	polyacrylamid gel electrophoresis
PAM	pulse-amplitude modulation
PBS	phosphate buffered saline
PCR	polymerase chain reaction
PDA	photodiode array
PEG	polyethylene glycol
PPO	polyphenol oxidase
PS	photosynthetic
PSII	photosystem II
PVA	polyvinyl alcohol
rpm	rounds per minute
RT	reverse transcriptase/transcription
SDS	sodium dodecyl sulphate
TAE	Tris/acetic acid/EDTA
TE	Tris/EDTA
TEA	triethylamine
TEMED	N,N,N',N'-tetramethylethylenediamine
TES	trace element solution
Tris	Tris(hydroxymethyl)aminomethan
TYR	tyrosinase
U	unit
UTR	untranslated region
v/v	volume per volume
w/v	weight per volume
WT	wild type

6.2. Supplementary data

6.2.1. Further detailed information on analysis and evaluation of *PPO* gene models

EST evidences for *PPO5, PPO9,* and *PPO12* were inconsistent with the exon/intron structure of the server-proposed gene models. One EST (*BJ960568*) allocated to the *PPO5* locus does not confirm the predicted intron adjacent to the CuB encoding region. The absence of the intron predicted by the gene model would lead to a C-terminal truncated PPO sequence due to an *in frame* stop codon in this part of the genomic sequence. An intron at another position within the sequence of *PPO5* was suggested by an appropriate EST match, but was not taken into account based on homology analysis of the derived amino acid sequence with other PPOs. All available gene models for *PPO5* predicted the same intron/exon structure disregarding the intron/exon structure given by the EST *BJ960568*. Based on homology analysis, another gene model (*all_Phypa_156596*) was selected for *PPO5* with a longer ORF leading to an N-terminal prolonged amino acid sequence.

ESTs present for *PPO9* supported the absence of the intron predicted by the *Phypa* gene model. According to these findings and based on homology analysis of the derived amino acid sequence of *PPO9* with other *Physcomitrella* PPOs, another intronless gene model (*all_Phypa_173397*) was selected.

The gene model of *PPO12* was found to be nearly completely covered by five ESTs, although one EST (*PP015007132R*) proposed the presence of a second intron in addition to the intron predicted by the selected *Phypa* gene model. But according to homology analysis with other plant PPOs, this second intron was not taken into account.

6.2.2. Relative transcript levels of *PPO* genes in WT and *PPO1*_ko lines #1 and #5

Tab. 6.1 Relative expression level of *PPO1* to *PPO12* under strong light conditions of wild type (A.) and *PPO1* knockout lines #1 and #5 (B. and C.) resulting from two different experiments 1 and 2. Adjustment of CT values and relative expression for each *PPO* gene was determined according to equation 3 and 4 as described in 2.3.4.3.

A. Wild type

1.	WT (standard light conditions)	WT (strong light irradiation)	2.	WT (standard light conditions)	WT (strong light irradiation)
PPO1	181.0	4.6	***PPO1***	194.0	10.6
PPO2	64.0	9.8	***PPO2***	104.0	26.0
PPO3	84.4	2.6	***PPO3***	147.0	2.8
PPO4	18.4	168.9	***PPO4***	78.8	415.9
PPO5	3.2	2.3	***PPO5***	9.8	7.0
PPO6	7.5	8.0	***PPO6***	36.8	17.1
PPO7	-	-	***PPO7***	-	-
PPO8	-	-	***PPO8***	-	-
PPO9	16.0	55.7	***PPO9***	119.4	194.0
PPO10	-	1.3	***PPO10***	-	3.2
PPO11	128.0	194.0	***PPO11***	337.8	388.0
PPO12	90.5	548.7	***PPO12***	157.6	1782.9

B. *PPO1* knockout line #1

1.	*PPO1*_ko #1 (standard light conditions)	*PPO1*_ko #1 (strong light irradiation)	2.	*PPO1*_ko #1 (standard light conditions)	*PPO1*_ko #1 (strong light irradiation)
PPO1	-	-	***PPO1***	-	-
PPO2	64.0	4.9	***PPO2***	73.5	9.2
PPO3	52.0	2.1	***PPO3***	73.5	2.0
PPO4	6.5	194.0	***PPO4***	22.6	548.7
PPO5	3.7	2.0	***PPO5***	8.0	5.3
PPO6	8.6	4.3	***PPO6***	14.9	6.1
PPO7	-	-	***PPO7***	-	-
PPO8	-	-	***PPO8***	-	-
PPO9	48.5	45.3	***PPO9***	111.4	168.9
PPO10	-	2.8	***PPO10***	-	4.3
PPO11	181.0	48.5	***PPO11***	415.9	119.4
PPO12	128.0	315.2	***PPO12***	84.4	630.3

C. *PPO1* knockout line #5

1.	*PPO1*_ko #5 (standard light conditions)	*PPO1*_ko #5 (strong light irradiation)	2.	*PPO1*_ko #5 (standard light conditions)	*PPO1*_ko #5 (strong light irradiation)
PPO1	-	-	***PPO1***	-	-
PPO2	39.4	16.0	***PPO2***	55.7	27.9
PPO3	194.0	16.0	***PPO3***	194.0	19.7
PPO4	42.2	675.6	***PPO4***	78.8	1097.5
PPO5	3.5	3.2	***PPO5***	8.0	11.3
PPO6	14.9	10.6	***PPO6***	24.3	24.3
PPO7	-	-	***PPO7***	-	-
PPO8	-	-	***PPO8***	-	-
PPO9	55.7	78.8	***PPO9***	128.0	147.0
PPO10	-	8.6	***PPO10***	-	13.0
PPO11	104.0	315.2	***PPO11***	194.0	445.7
PPO12	147.0	1260.7	***PPO12***	181.0	1910.9

6.3. Posters, talks and publication

Publication

Richter, H., Lieberei, R., and von Schwartzenberg, K. (2005): Identification and Characterisation of a Bryophyte Polyphenol Oxidase Encoding Gene from *Physcomitrella*.
Plant Biology 7 (3), 283-292

Talks

Richter, H., Lieberei, R., and von Schwartzenberg, K. (2005):
Polyphenol oxidase in *Physcomitrella*. at MOSS 2005 in Brno, Czech Republic

Richter, H., Lieberei, R., Rensing, S., and von Schwartzenberg, K. (2008):
The polyphenol oxidase multigene family of *Physcomitrella*. at MOSS 2008 in Tampere, Finland

Posters

Richter, H., Lieberei, R., and von Schwartzenberg, K. (2004): Identification, molecular Cloning and Characterisation of a Polyphenoloxidase-encoding gene *Pp_ppo1* from *Physcomitrella patens* at Botanical Congress of the German Botanical Society 2004 in Braunschweig, Germany

Richter, H., Lieberei, R., and von Schwartzenberg, K. (2007): Characterisation of the polyphenol oxidase multigene family from *Physcomitrella patens*
at Botanical Congress of the German Botanical Society 2007 in Hamburg, Germany

Danksagung

Bei meinen Betreuern, Prof. Dr. Reinhard Lieberei und PD Dr. Klaus von Schwartzenberg, möchte ich mich recht herzlich für die tolle wissenschaftliche Anleitung und Diskussion sowie für Anregungen und konstruktive Kritik bedanken.

PD Dr. Klaus von Schwartzenberg danke ich für seine hilfreichen Ratschläge fachlicher und privater Art, für seinen Optimismus und seine Aufmunterungen sowie für sein Vertrauen.

Bei Andreas Zimmer, Daniel Lang und PD Dr. Stefan Rensing (Universität Freiburg) bedanke ich mich für die Einführung in die Benutzung des *cosmoss genome browsers*. Insbesondere PD Dr. Stefan Rensing danke ich für die Hilfe bei den phylogenetischen Analysen und der Erstellung der Stammbäume sowie für die spannenden und hilfreichen Diskussionen dieser Daten.

Für die Bestrahlungsversuche wurden der Sonnensimulator und das PAM-Fluorometer von Prof. Dr. Dieter Hanelt (Universität Hamburg) zur Verfügung gestellt. Vielen Dank für die Einführung in die Gerätebedienung und Beantwortung aller hierzu entstandenen Fragen.

Die LC-MS-Analysen wurden in Kooperation mit Dr. Stefan Franke (Universität Hamburg) durchgeführt. Vielen Dank für die Probenanalysen und die Diskussionen zur Strukturaufklärung.

Allen Mitarbeitern der Nutzpflanzenbiologie danke ich für die schöne Arbeitsatmosphäre und Hilfsbereitschaft. Vor allem Susanne Bringe und Vera Schwekendiek für die Erhaltung des Laborbetriebes sowie Thomas Tumforde für die Hilfe rund um die HPLC-Analytik sei gedankt. Hanna Turčinov danke ich für wichtige freundschaftliche und fachliche Ratschläge und die tolle Zeit im Labor und außerhalb.

Prof. Dr. Barbara Moffatt (University of Waterloo, Kanada) möchte ich für die schöne Zeit bei ihr im Labor, für ihre Gastfreundschaft und für ihr Interesse am Fortgang meiner Arbeit danken.

Dr. Gilbert Gorr (greenovation Biotech GmbH) danke ich für die interessanten Diskussionen rund um *Physcomitrella* Transformation und Expression.

Ferner danke ich dem DAAD und der Universität Hamburg für die finanzielle Unterstützung in Form von Stipendien sowie der DFG für die Förderung des Projektes SCHW 687/5-1.

Bei Freunden und Familie möchte ich mich von ganzem Herzen dafür bedanken, dass sie immer für mich da sind - für ihre Stärkung, ihre Ablenkung und unendliche Geduld.